

AD-A119 764

PISA UNIV (ITALY) INST OF AERONAUTICS

F/G 1/3

THE FATIGUE CRACK GROWTH UNDER VARIABLE AMPLITUDE LOADING IN BU--ETC(U)

APR 82 A SALVETTI, G CAVALLINI, L LAZZERI

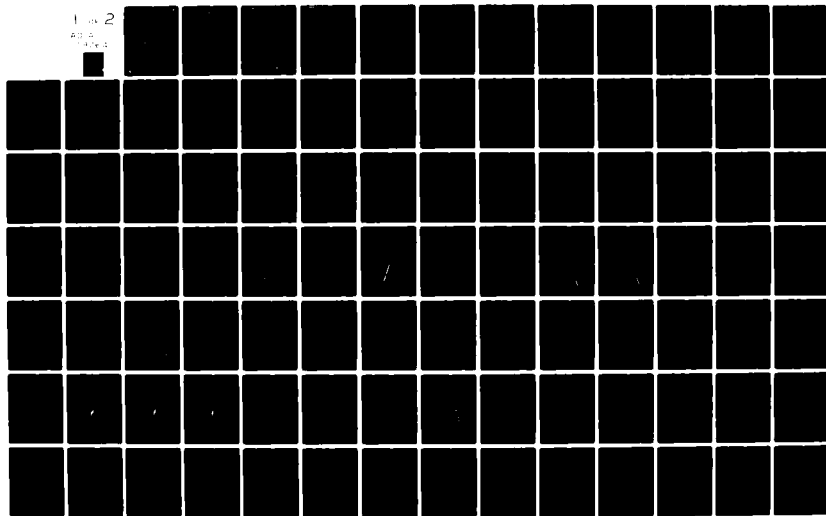
DA-ERO-78-G-107

NL

UNCLASSIFIED

1 of 2

AD-A119 764



AD A119764

AD



# THE FATIGUE CRACK GROWTH UNDER VARIABLE AMPLITUDE LOADING IN BUILT-UP STRUCTURES

Final Technical Report

by

A. SALVETTI - Principal Investigator  
G. CAVALLINI and L. LAZZERI

April 1982

## EUROPEAN RESEARCH OFFICE

United States Army  
London England

GRANT NUMBER DA ERO - 78 - G - 107



Istituto di Aeronautica  
Università di Pisa  
Italy

Approved for Public Release ; distribution unlimited

82 09 29 004

DTIC FILE COPY

# **THE FATIGUE CRACK GROWTH UNDER VARIABLE AMPLITUDE LOADING IN BUILT-UP STRUCTURES**

**Final Technical Report**

by

**A. SALVETTI - Principal Investigator  
G. CAVALLINI and L. LAZZERI**

**April 1982**

**EUROPEAN RESEARCH OFFICE**

**United States Army  
London                      England**

**GRANT NUMBER DA ERO - 78 - G - 107**

**Istituto di Aeronautica  
Università di Pisa  
Italy**

**Approved for Public Release ; distribution unlimited**

UNCLASSIFIED

REF 2600-AN

SECURITY CLASSIFICATION OF THIS PAGE (When Data Entered)

REPORT DOCUMENTATION PAGE		READ INSTRUCTIONS BEFORE COMPLETING FORM
1. REPORT NUMBER	2. GOVT ACCESSION NO. <b>AD A119764</b>	3. RECIPIENT'S CATALOG NUMBER
4. TITLE (and Subtitle) <b>The Fatigue Crack Growth Under Variable Amplitude Loading in Built-up Structures</b>		5. TYPE OF REPORT & PERIOD COVERED <b>Final Technical Report Sept 78 - Feb 82</b>
		6. PERFORMING ORG. REPORT NUMBER
7. AUTHOR(s) <b>A. Salvetti, G. Cavallini, L. Lazzeri</b>		8. CONTRACT OR GRANT NUMBER(s) <b>DA-ERO-78-G-107</b>
9. PERFORMING ORGANIZATION NAME AND ADDRESS <b>Istituto di Aeronautica Universita di Pisa</b>		10. PROGRAM ELEMENT, PROJECT, TASK AREA & WORK UNIT NUMBERS <b>6.11.02A 1T161102BH57-06</b>
11. CONTROLLING OFFICE NAME AND ADDRESS <b>USARDCG-UK Box 65, FPO NY 09510</b>		12. REPORT DATE <b>April 1982</b>
		13. NUMBER OF PAGES <b>110</b>
14. MONITORING AGENCY NAME & ADDRESS (if different from Controlling Office)		15. SECURITY CLASS. (of this report) <b>Unclassified</b>
		15a. DECLASSIFICATION/DOWNGRADING SCHEDULE
16. DISTRIBUTION STATEMENT (of this Report) <b>Approved for Public Release; distribution unlimited</b>		
17. DISTRIBUTION STATEMENT (of the abstract entered in Block 20, if different from Report)		
18. SUPPLEMENTARY NOTES		
19. KEY WORDS (Continue on reverse side if necessary and identify by block number) <b>Fatigue crack growth in built-up structures for various load spectra</b>		
20. ABSTRACT (Continue on reverse side if necessary and identify by block number) <b>A research activity aimed at developing reliable methods for predicting the growth of a crack in built-up aircraft structures under realistic load conditions has been carried out at the Institute of Aeronautics of the University of Pisa under a three-year research contract DA-ERO-78-G-107.</b>  <b>This paper presents the results obtained in the course of the third year during which, altogether, 74 specimens, made of 2024-T3 aluminium alloy,</b>		

DD FORM 1 JAN 73 1473

EDITION OF 1 NOV 68 IS OBSOLETE  
S/N 0102-LF-014-6601

UNCLASSIFIED

SECURITY CLASSIFICATION OF THIS PAGE (When Data Entered)

**UNCLASSIFIED**

SECURITY CLASSIFICATION OF THIS PAGE (When Data Entered)

20. Contd.

were tested both at constant and variable amplitude loading. The specimens were both simple sheets and riveted stiffened panels.

The constant amplitude tests on simple sheet specimens were conducted in order to obtain the average K-rate relationship and the relevant scatter of the batch of sheets. The constant amplitude tests of stiffened panels were aimed at obtaining information on the overall junction flexibility.

Variable amplitude tests were performed utilizing three standard fatigue spectra, like FALSTAFF, MINITWIST and Gaussian random. The data from sheet specimens was used to assess the reliability of prediction methods such as those devised by Wheeler and Willenborg, and the stiffened panels test data to evaluate how these methods work in the case of built-up structures.

Some general conclusions on the reliability of the crack growth prediction methods have been obtained treating on statistical basis the data collected in the current year, as well as in the previous year's research activity.

To this end, data from variable amplitude tests, irrespective of the type of spectrum and of the material, has been collected and analyzed in order to evaluate in this respect the methods proposed by Willenborg and by Wheeler. The results are quite interesting, because they allow to evaluate the scatter associated with most of the parameters involved in crack growth predictions.

Accession For	
DTIS G-31	<input checked="checked" type="checkbox"/>
DTIC T. 3	<input type="checkbox"/>
Unannounced	<input type="checkbox"/>
Justification	<input type="checkbox"/>
By _____	
Distribution/ _____	
Availability Codes _____	
Dist	Avail and/or Special



**UNCLASSIFIED**

SECURITY CLASSIFICATION OF THIS PAGE(When Data Entered)

## SUMMARY

*A research activity aimed at developing reliable methods for predicting the growth of a crack in built-up aircraft structures under realistic load conditions has been carried out at the Institute of Aeronautics of the University of Pisa under a three-year research contract DA ERO-78-G-107.*

*This paper presents the results obtained in the course of the third year during which, altogether, 74 specimens, made of 2024-T3 aluminium alloy, were tested both at constant and variable amplitude loading. The specimens were both simple sheets and riveted stiffened panels.*

*The constant amplitude tests on simple sheet specimens were conducted in order to obtain the average K-rate relationship and the relevant scatter of the batch of sheets. The constant amplitude tests on stiffened panels were aimed at obtaining information on the overall junction flexibility.*

*Variable amplitude tests were performed utilizing three standard fatigue spectra, viz. FALSTAFF, MINITWIST and Gaussian random. The data from sheet specimens was used to assess the reliability of prediction methods such as those devised by Wheeler and Willenborg, and the stiffened panels test data to evaluate how these methods work in the case of built-up structures.*

*Some general conclusions on the reliability of the crack growth prediction methods have been drawn by treating on a statistical basis the data collected in the current year, as well as in the previous year's research activity.*

*To this end data from variable amplitude tests, irrespective of the type of spectrum and of the material, has been collected and analysed in order to evaluate in this respect the methods proposed by Willenborg and by Wheeler. The results are quite interesting, because they allow us to evaluate the scatter associated with most of the parameters involved in crack growth predictions.*

## TABLE OF CONTENTS

SUMMARY .....	Page	III
LIST OF ILLUSTRATIONS .....	"	V
LIST OF TABLES .....	"	X
LIST OF SYMBOLS .....	"	XII
1 - INTRODUCTION .....	"	1
2 - TEST PROGRAM AND OBJECTIVES .....	"	3
3 - TEST PROCEDURE AND DATA EVALUATION .....	"	5
4 - ANALYSIS OF RESULTS .....	"	9
4.1 - SIMPLE SHEET-CONSTANT AMPLITUDE TESTS .....	"	9
4.2 - SIMPLE SHEET-VARIABLE AMPLITUDE TESTS .....	"	11
4.3 - STIFFENED PANEL-CONSTANT AMPLITUDE TESTS ..	"	14
4.4 - STIFFENED PANEL-VARIABLE AMPLITUDE TESTS ..	"	15
5 - CRACK GROWTH PREDICTION RELIABILITY .....	"	17
6 - CONCLUSIONS .....	"	19
REFERENCES .....	"	22
APPENDIX 1 .....	"	25
APPENDIX 2 .....	"	27
FIGURES .....	"	30
TABLES .....	"	75

# LIST OF ILLUSTRATIONS

## Figures

Fig. 1	- Regression analysis on experimental data for evaluating Forman's law. The best-fit values are: $C=0.22686 \times 10^{-5}$ , $n=2.6027$ .....	Page 30
Fig. 2a	- Regression analysis on experimental data for evaluating the Elnes law .....	" 31
Fig. 2b	- Regression analysis on a reduced set of experimental data for evaluating the Elnes law. The best-fit values are: $\alpha=0.12$ , $C=0.2019 \times 10^{-7}$ , $n=2.87$ .....	" 32
Fig. 2c	- Regression analysis on a wider set of experimental data for evaluating the Elnes law ..	" 33
Fig. 3	- Lognormal cumulative distributions of the variable $\Delta N_{ex}/\Delta N_c$ for two ranges of damage growth .....	" 34
Fig. 4	- Lognormal cumulative distributions of the variable $\Delta N_{ex}/\Delta N_c$ for two ranges of damage growth .....	" 35
Fig. 5a	- Experimental results of flat panels tests under FALSTAFF spectrum loading with $S_{max}=20.0 \text{ Kg/mm}^2$ .....	" 36
Fig. 5b	- Comparison of experimental results with predictions obtained with Elnes law for flat panels tests under FALSTAFF spectrum loading with $S_{max}=20.0 \text{ Kg/mm}^2$ .....	" 37
Fig. 5c	- Lognormal cumulative distributions of the variable $\Delta F_{ex}/\Delta F_c$ for the first series of flat panels tests under FALSTAFF spectrum loading with $S_{max}=20.0 \text{ Kg/mm}^2$ . $F_c$ has been calculated using the Elnes law .....	" 38
Fig. 5c	- Concluded .....	" 39
Fig. 5d	- Lognormal cumulative distributions of the variable $\Delta F_{ex}/\Delta F_c$ for the complete series of flat panels tests under FALSTAFF spectrum loading with $S_{max}=20.0 \text{ Kg/mm}^2$ . $F_c$ has been calculated using the Elnes law .....	" 40

Fig. 5d	- Concluded .....	Page 41
Fig. 6a	- Experimental results of flat panels tests under FALSTAFF spectrum loading with $S_{max}=24.0 \text{ Kg/mm}^2$ .....	" 42
Fig. 6b	- Comparison of experimental results with predictions obtained with Elnes law for flat panels tests under FALSTAFF spectrum loading with $S_{max}=24.0 \text{ Kg/mm}^2$ .....	" 43
Fig. 6c	- Lognormal cumulative distributions of the variable $\Delta F_{ex}/\Delta F_c$ for flat panels tests under FALSTAFF spectrum loading with $S_{max}=24.0 \text{ Kg/mm}^2$ . $F_c$ has been calculated using Elnes law .....	" 44
Fig. 6c	- Concluded .....	" 45
Fig. 7a	- Experimental results of flat panels tests under MINITWIST spectrum loading with $S_{1g}=7.0 \text{ Kg/mm}^2$ .....	" 46
Fig. 7b	- Comparison of experimental data with predictions obtained with Elnes law for flat panels tests under MINITWIST spectrum loading with $S_{1g}=7.0 \text{ Kg/mm}^2$ ..	" 47
Fig. 7c	- Lognormal cumulative distributions of the variable $\Delta F_{ex}/\Delta F_c$ for flat panels tests under MINITWIST spectrum loading with $S_{1g}=7.0 \text{ Kg/mm}^2$ . $F_c$ has been calculated using the Elnes law .....	" 48
Fig. 7c	- Concluded .....	" 49
Fig. 8a	- Experimental results of flat panels tests under MINITWIST spectrum loading with $S_{1g}=10.0 \text{ Kg/mm}^2$ .....	" 50
Fig. 8b	- Comparison of experimental data with predictions obtained with Elnes law for flat panels tests under MINITWIST spectrum loading with $S_{1g}=10.0 \text{ Kg/mm}^2$ ..	" 51
Fig. 8c	- Lognormal cumulative distributions of the variable $\Delta F_{ex}/\Delta F_c$ for flat panels tests under MINITWIST spectrum loading with $S_{1g}=10.0 \text{ Kg/mm}^2$ . $F_c$ has been calculated using Elnes law .....	" 52
Fig. 9a	- Experimental results of flat panels tests under Gaussian random spectrum loading with $S_{rms}=2.5 \text{ Kg/mm}^2$ .....	" 53

Fig. 9b	- Comparison of experimental data with predictions obtained with Elnes law for flat panels tests under Gaussian random spectrum loading with $S_{rms}=2.5 \text{ Kg/mm}^2$ .....	Page 54
Fig. 9c	- Lognormal cumulative distributions of the variable $\Delta N_{ex}/\Delta N_c$ for flat panels tests under Gaussian random spectrum loading with $S_{rms}=2.5 \text{ Kg/mm}^2$ . $N_c$ has been calculated using Elnes law .....	" 55
Fig. 10a	- Regression analysis of experimental data from constant amplitude tests on stiffened panels. $\Delta K$ has been evaluated disregarding friction forces and assuming for the rivet flexibility parameter the value $\xi=0.10$ .....	" 56
Fig. 10b	- Regression analysis of experimental data from constant amplitude tests on stiffened panels. $\Delta K$ has been evaluated disregarding friction forces and assuming the optimum value $\xi=0.30$ . The best-fit Forman's law is defined by $C=0.1532 \times 10^{-5}$ , $n=2.774$ .....	" 57
Fig. 10c	- Regression analysis of experimental data from constant amplitude tests on stiffened panels. $\Delta K$ has been evaluated disregarding friction forces and assuming $\xi=0.70$ .....	" 58
Fig. 11	- FDATA versus flexibility parameter $\xi$ for some constant amplitude-stiffened panels tests .....	" 59
Fig. 12	- Lognormal cumulative distributions of the variable $\Delta N_{ex}/\Delta N_c$ for stiffened panels tests under constant amplitude loading. $N_c$ has been calculated using Forman's law and assuming different values of the rivet flexibility .....	" 60
Fig. 13a	- Experimental results of built-up panels tests under FALSTAFF spectrum loading with $S_{max}=20.0 \text{ Kg/mm}^2$ .....	" 61
Fig. 13b	- Comparison of experimental results with predictions obtained with Forman's law for built-up panels tests under FALSTAFF spectrum loading with $S_{max}=20.0 \text{ Kg/mm}^2$ ..	" 62

Fig. 13c -	Lognormal cumulative distributions of the variable $\Delta F_{ex}/\Delta F_c$ for built-up panels tests under FALSTAFF spectrum loading with $S_{max}=20.0 \text{ Kg/mm}^2$ . $F_c$ has been calculated using the Forman's law of built-up panels .....	Page 63
Fig. 14a -	Experimental results of built-up panels tests under MINITWIST spectrum loading with $S_{1g}=7.0 \text{ Kg/mm}^2$ .....	" 64
Fig. 14b -	Comparison of experimental results with predictions obtained with Forman's law for stiffened panels tests under MINITWIST spectrum loading with $S_{1g}=7.0 \text{ Kg/mm}^2$ .....	" 65
Fig. 14c -	Lognormal cumulative distributions of the variable $\Delta F_{ex}/\Delta F_c$ for stiffened panels tests under MINITWIST spectrum loading with $S_{1g}=7.0 \text{ Kg/mm}^2$ . $F_c$ has been calculated using the Forman's law of stiffened panels .....	" 66
Fig. 14c -	Concluded .....	" 67
Fig. 15a -	Experimental results of built-up panels tests under Gaussian random spectrum loading with $S_{rms}=2.5 \text{ Kg/mm}^2$ .....	" 68
Fig. 15b -	Comparison of experimental results with predictions obtained with Forman's law for stiffened panels tests under Gaussian random spectrum loading with $S_{rms}=2.5 \text{ Kg/mm}^2$ .....	" 69
Fig. 15c -	Lognormal cumulative distributions of the variable $\Delta N_{ex}/\Delta N_c$ for stiffened panels tests under Gaussian random spectrum loading with $S_{rms}=2.5 \text{ Kg/mm}^2$ . $N_c$ has been calculated using the Forman's law of stiffened panels .....	" 70
Fig. 16 -	Comparison of variable amplitude tests results with predictions obtained according to various retardation methods. Lognormal distributions of the variable $\Delta F_{ex}/\Delta F_c$ .....	" 71
Fig. 17 -	Predictions sensibility to the Wheeler's plastic zone parameter. The curves are relevant to flat panels subjected to FALSTAFF spectrum loading with $S_{max}=24.0 \text{ Kg/mm}^2$ .....	" 72

- Fig. 18 - A sample histogram of error occurrences  
in the fatigue machine setting up phase  
for variable amplitude loading tests ... Page 73
- Fig. 19 - The model adopted for the description  
of the rivet elasto-plastic behaviour .. " 74

# LIST OF TABLES

## Tables

Tab.1a	- Main characteristics of the constant amplitude-flat panels tests .....	Page	75
Tab.1b	- Main characteristics of FALSTAFF spectrum tests on flat panels.....	"	76
Tab.1c	- Main characteristics of MINITWIST spectrum tests on flat panels .....	"	77
Tab.1d	- Main characteristics of Gaussian random spectrum tests on sheet specimens. $S_{ref}$ stands for $S_{rms}$ and the spectrum is superposed to an average stress equal to $7.0 \text{ Kg/mm}^2$ .....	"	78
Tab.1e	- Main characteristics of the constant amplitude-stiffened panels tests .....	"	79
Tab.1f	- Main characteristics of the variable amplitude-stiffened panels tests .....	"	80
Tab.1g	- Dimensions of the specimens used for evaluating the yield stress and tensile strength .....	"	81
Tab.2a	- Results of constant amplitude-flat specimens tests .....	"	82
Tab.2a	- Continued .....	"	83
Tab.2a	- Continued .....	"	84
Tab.2a	- Concluded .....	"	85
Tab.2b	- Results of flat panels tests under FALSTAFF spectrum loading .....	"	86
Tab.2b	- Continued .....	"	87
Tab.2b	- Continued .....	"	88
Tab.2b	- Continued .....	"	89
Tab.2b	- Continued .....	"	90
Tab.2b	- Continued .....	"	91
Tab.2b	- Concluded .....	"	92
Tab.2c	- Results of flat panels tests under MINITWIST spectrum loading .....	"	93
Tab.2c	- Continued .....	"	94
Tab.2c	- Continued .....	"	95
Tab.2c	- Concluded .....	"	96

Tab.2d	- Results of flat panels tests under Gaussian random spectrum loading .....	Page 97
Tab.2d	- Concluded .....	" 98
Tab.2e	- Results of constant amplitude-stiffened panels tests .....	" 99
Tab.2e	- Continued .....	" 100
Tab.2e	- Continued .....	" 101
Tab.2e	- Concluded .....	" 102
Tab.2f	- Results of variable amplitude-stiffened panels tests .....	" 103
Tab.2f	- Continued .....	" 104
Tab.2f	- Continued .....	" 105
Tab.2f	- Continued .....	" 106
Tab.2f	- Continued .....	" 107
Tab.2f	- Continued .....	" 108
Tab.2f	- Concluded .....	" 109
Tab.2g	- Some mechanical properties of a few flat panels utilized in the tests .....	" 110

## LIST OF SYMBOLS

- a - Half-crack length, mm.
- da/dn - Crack growth rate, mm/cycle
- F<sub>DATA</sub> - Statistical parameter of regression
- K - Stress intensity factor, Kg/mm<sup>3/2</sup>
- K<sub>c</sub> - Critical stress intensity factor, Kg/mm<sup>3/2</sup>
- K<sub>th</sub> - Threshold value of the stress intensity factor, Kg/mm<sup>3/2</sup>
- n - Number of load cycles
- R - Stress ratio, S<sub>min</sub>/S<sub>max</sub>
- S<sub>y</sub> - Yielding stress, Kg/mm<sup>2</sup>
- ΔK - Stress intensity factor range, Kg/mm<sup>3/2</sup>
- ξ - Flexibility parameter

## 1 - INTRODUCTION

This paper presents the third year's results of an investigation carried out at the Institute of Aeronautics, Pisa University, under the contract DA ERO-78-G-107.

The objective of this investigation is the evaluation of the reliability of available methods to predict the growth of a crack in riveted built-up structures under loading conditions representative of aircraft operational environment.

At present the available methods for computing the growth of a crack under variable amplitude loading are cycle-by-cycle procedures based on constant amplitude "K-rate" relationships suitably modified to allow for the reduced propagation rate of a crack growing in the plastic wake created by previous peak loads,/1/,/2/,/3/. Such modifications are carried out in essentially empirical ways and derive their substantiation mainly on tests performed on sheet specimens.

To increase confidence in these methods as design tools, it is worthwhile to evaluate them further, by utilizing test data on more representative aircraft structures and load environments.

To this end, in this investigation, crack propagation tests were carried out on built-up structures as well as on simple sheets utilizing three types of spectrum loading, namely FALSTAFF,/4/, MINITWIST,/5/, and Gaussian random,/6/. Ancillary tests at constant amplitude both on sheets and stiffened panels were also carried out. At the same time an effective method to treat the test data was developed. It allows an evaluation of the reliability of the various approaches for crack growth computation taking into account different structure configurations and load conditions.

The previous two years research activity was mainly devoted to the implementation of such a method by means of computer programs and to its substantiation by means of test

data,/7/,/8/.

As far as the crack growth computational approaches are concerned, attention was focused on the following ones:

- Wheeler's method,
- Willenborg's method,
- Linear-cumulative non interactive method.

All these approaches are implemented in the computer program, CDAV,/7/, which computes the number of flights necessary to reach a given crack length in a certain structure undergoing a given spectrum loading.

The assessment of the reliability of such computational procedures was carried out on the basis of a sequence of tests performed on specimens drawn from the same batch of sheet, namely

- simple sheet-constant amplitude tests
- simple sheet-variable amplitude tests
- stiffened panels-constant amplitude tests
- stiffened panels-variable amplitude tests.

In particular during the second year's research activity tests were carried out with specimens made of 7075-T6 aluminum alloy, utilizing, for variable amplitude tests, the FALSTAFF spectrum. Test data, treated on a statistical basis, was utilized to evaluate the accuracy of the different computational approaches, and in the case of the Wheeler's method, to find the best value of the plastic zone parameter.

The entire process of evaluation strongly depends on the accuracy with which the stress intensity factor is computed.

The problem is particularly involved in the case of built-up structures where the fastener flexibility and the friction between faying surfaces can have a significant influence on the K values. Consequently, a procedure was envisaged and implemented in the computer program SKESA,/8/, which furnishes the fastener flexibility and friction forces by suitably

treating crack propagation data from tests on stiffened panels under constant amplitude loading.

The general conclusion of the first two years research activity is that the approach, proposed to assess the reliability of crack growth prediction, apart from minor improvement, works satisfactorily.

As a consequence the third year's activity, described in the present report, was prevailingly devoted to obtain systematic test data.

To this end, according to the test sequence previously outlined, crack propagation tests both under constant and variable amplitude loading, were carried out on simple sheets and stiffened panels.

Three types of spectra, FALSTAFF, MINITWIST and Gaussian Random, and one material were investigated.

Test data and relevant treatment allow us to draw sufficiently general conclusions on the current capability of predicting crack growth in a built-up aircraft structure under realistic loading conditions.

## 2 - TEST PROGRAM AND OBJECTIVES

To reach the objectives of the research a rational sequence of tests was devised.

Two types of specimens were selected, namely simple sheets and riveted stiffened panels. Both types of specimens were prepared utilizing the aluminum alloy 2024-T3 cut from the same stock of sheets. Certain of these specimens were tested at constant amplitude loading, the others at variable amplitude loading on the basis of three standard load sequences, namely FALSTAFF, MINITWIST and Gaussian Random, /4/, /5/, /6/.

Tabs. 1a to 1f show the geometric shape and dimensions of the specimens together with initial crack lengths and the

relevant load conditions.

The tables give the maximum stress and the stress ratio for constant amplitude tests; in the case of variable amplitude loading, the reference stress in the spectrum is given.

All the stiffened panels were fastened with countersunk head rivets. The rivets were hand riveted by a skilled operator in such a way that the driven head had a diameter approximately equal to  $1.4 \div 1.5$  the shank diameter.

Altogether 74 specimens were tested, of which 54 under variable amplitude loading<sup>(°)</sup>.

The test program was completed by static tests to obtain the  $\sigma$ - $\epsilon$  relationship with a view to a better characterization of the material used to construct the specimens. The results are shown in Tab.2g. The specimens used in this last type of test, whose dimensions are shown in Tab.1g, were cut from the specimens utilized for the crack propagation tests after the completion of the tests.

These different types of tests were devised to obtain all the significant information necessary to interpret the data obtained by testing stiffened panels under variable amplitude loading.

In particular, the constant amplitude loading tests on simple sheets were devised to obtain average crack growth data and the relevant scatter for the material.

The spectrum loading tests on simple sheets were planned to obtain a comparison between different methods suitable for predicting the crack growth under variable amplitude loading.

---

(°) *This test program is somewhat reduced version of the fairly preliminary test program outlined in /8/. This reduction was felt consistent with the fulfilment of the research objectives and, at the same time, compatible with time and budget restraints.*

The methods considered in the present investigation are those already considered in the course of the first two year's activity, /7/, /8/, namely: non-interactive, Willenborg and Wheeler plus a relatively new method, developed by ONERA, /3/, which is restricted to FALSTAFF spectrum.

The purpose of the comparison is to select a sufficiently accurate method to be used in the evaluation of crack growth data in stiffened panels under spectrum loading.

The constant amplitude tests on stiffened panels were devised to obtain a quantitative assessment of fastener flexibility and friction forces, together with the "best" average  $\Delta K$ -rate relationship and the relevant scatter.

The results of all the tests previously outlined, besides being significant in themselves, give us the necessary background for adequately interpreting the crack growth data obtained from variable amplitude tests on stiffened panels.

All the results, namely constant and variable amplitude loading-sheet and stiffened panel test data, are then utilized to assess the capability of the computational approaches to predict reliably the crack growth in typical low-gage aircraft structures.

### 3 - TEST PROCEDURE AND DATA EVALUATION

The specimens were tested in two load apparatuses, capable respectively of  $\pm 500$  KN and  $\pm 250$  KN, each one composed of a rig, plates for clamping the specimen by friction, a servo-controlled hydraulic actuator, and an optical device for crack length measurement, capable of an accuracy of 0.1 mm. The actuators are driven by an electrical signal, which is supplied for constant amplitude tests by the machine internal waveform generator and for spectrum loading tests by a process computer, Digital PDP 11/34.

The load spectra utilized in the variable amplitude tests are three standard sequences: FALSTAFF, MINITWIST and GAUSSIAN Random. The first one is a well-known spectrum for fatigue evaluation deduced from load factor histories recorded in flight of a typical fighter aircraft. The sequence is composed by a block of 200 flights of different length and severity, which is periodically repeated. In the spectrum 32 different load levels are defined and usually the maximum stress level is assumed as a reference to characterize the severity of the spectrum, as all the other levels are scaled linearly. More details can be found in /4/.

MINITWIST is a standard spectrum representative of the load history of the wing root of a transport aircraft. The load sequence simulates mainly the gust loads and the complete spectrum of 4000 flights contains 10 different types of flights of different severity, according to the meteorological conditions simulated, ranging from very smooth flights in fine weather to extremely rough flights in storm. Ground-Air-Ground loads and taxi loads are also taken into account. As a reference stress, which scales all the spectrum, the mean stress in level flight,  $S_{1g}$ , has been assumed. All the details necessary for the generation of this standardized load spectrum and a wider description can be found in /5/.

The Gaussian Random spectrum is a standard sequence of peaks and troughs, representing a stationary Gaussian process, obtained according to the procedure suggested in /6/. It is characterized by a given irregularity factor, i.e. number of mean level crossings/number of peaks (or troughs), and the total number of peaks, which are repeated periodically. The spectrum used in the fatigue tests was characterized by an irregularity factor equal to 0.7 and a total of 16.000 cycles. The severity of the spectrum is defined by the root mean square value of the stress, and a reference value of

2.5 Kg/mm<sup>2</sup> has been assumed in the tests; the spectrum was superposed to a mean stress of 7.0 Kg/mm<sup>2</sup>.

All the test data produced were collected in the form of the crack length versus the number of cycles or flights, whichever was appropriate. All the data were analyzed following the methodologies outlined in /7/.

At first, the a-n data from the sheet specimens tested under constant amplitude loading were processed, utilizing the SKESA computer program to obtain the constants that define the semiempirical laws of crack propagation.

The a-F data from the sheet specimens tested under variable amplitude spectrum loading were treated utilizing the results of the CADA V computer program. This produces a prediction of the test results, i.e. the values of crack length at progressive numbers of flights, according to the following methods: Non-interactive, Willenborg method and Wheeler method for different values of the plastic zone parameter, m. In the case of the FALSTAFF spectrum, the crack growth prediction was calculated also according to a method, deduced from /3/, which in the following will be called ONERA model. The predictions of the different methods are then evaluated to obtain the number of flights required for a crack growth of a given interval, so that, by means of a comparison with the test data on a statistical basis, the best method can be assessed, i.e. the one which better agrees on average with the experimental results.

The a-n data from built-up specimens tested under constant amplitude loading are analyzed to evaluate the overall junction flexibility, characterized by the rivet flexibility parameter,  $\xi^{(o)}$ , and the da/dn vs.  $\Delta K$  relationship. As far as the idealization of the load transfer pattern from sheet to

---

(<sup>o</sup>)  $\xi$  is the ratio of the actual flexibility and the flexibility as computed according to Swift's formula given in Ref./7/.

stiffener is concerned, the program utilized did not take friction into account. So friction effects are included in the optimum value of the rivet flexibility parameter, i.e. the one which minimizes the standard deviation between the test data and the relevant best fit, having  $\Delta K$  been evaluated with an attempt value for  $\xi$ , the rivet flexibility parameter. On this subject, a modified version of the SKESA computer program that improves the elasto-plastic idealization of the fasteners has been utilized; a description of which is given with more details in Appendix 2. Once the optimum value of  $\xi$  has been determined, the  $da/dn-\Delta K$  relationship relevant to stiffened panels is then obtained; it is found to be quite similar to that of the sheet specimens.

At last, the data collected in the most representative kind of test, i.e. built-up panels under variable amplitude loading, is analyzed. The computer program that processes this data has been improved on the basis of the observation that the shape of the plot of the a-F experimental data for long cracks is quite similar to the one of the unstiffened panels. This means that, under the action of the peak loads of a spectrum, the load transfer capability of the junction decreases. Improvements have been introduced in the CADAV program to take into account this progressive loss of efficiency (see Appendix 2 for a more detailed description). The following procedure has been accomplished:

- research, for the panel configuration under examination, of the load - crack length combinations for which yielding occurs in the most loaded rivets;
- computation of the stress intensity factor for a given panel configuration and efficiency, defined by the number of yielded rivets and the maximum load supported previously by the yielded rivets;
- computation of cycle by cycle growth due to the load spectrum sequence for different retardation methods, utilizing the  $da/dn-\Delta K$  relationship relevant to the stiffened panels;

- comparison of computed and experimental data, i.e. the number of flights necessary for the crack to grow a certain interval, and selection on a statistical basis of the most suitable retardation method.

#### 4 - ANALYSIS OF RESULTS

All the experimental results are collected in Tabs.2, expressed in terms of a-n or a-F, as appropriate according to the type of loading. All the data has been analyzed on the basis of the procedures described in the previous section and the main results are discussed in the following paragraphs.

##### 4.1 - SIMPLE SHEET-CONSTANT AMPLITUDE TESTS

The panel geometry and loading conditions in this group of tests are shown in Tab.1a. The experimental data has been analyzed by means of a least-squares regression technique to obtain the constants of the usual semiempirical crack growth laws.

Besides the well-known Forman's law:

$$\frac{da}{dn} = \frac{C \cdot \Delta K^n}{(1-R)K_C - \Delta K}$$

whose relationship is shown in Fig.1, the data has been treated also following another type of law, namely the one proposed by Schijve in /9/, obtained on the basis of previous works of Elber and Newman, and which, for the sake of brevity, will be called in the following "ELNES" law. It is based on the crack closure concept, that was proposed first by Elber in /10/. According to this theory, crack growth occurs only when the crack is fully open, i.e. in the part of the load cycle where the

applied stress is higher than the crack opening stress. In constant amplitude tests, the crack opening stress is supposed to be related to the maximum cyclic stress by means of a function of R, the stress ratio  $S_{min}/S_{max}$ , so that the effective stress intensity factor range can be expressed by:

$$\Delta K_{eff} = \Delta K \cdot U(R)$$

The expression for  $U(R)$  proposed by Newman /11/ on the basis of finite element calculations of the opening stress is:

$$U(R) = 0.55 + 0.35 R + 0.1 R^2$$

Schijve suggests to use a more flexible function, which depends also on the parameter  $\alpha$ :

$$U(R, \alpha) = 0.55 + (0.45 - \alpha) R + \alpha R^2$$

The value of the parameter  $\alpha$  must be selected on the basis of a best fit with experimental data, so that the scatter band of the regression in a plane  $da/dn - \Delta K_{eff}$  is minimum; the expression of the Elnes law is the following:

$$da/dn = C \cdot \Delta K_{eff}^n = C \cdot [\Delta K \cdot U(R, \alpha)]^n$$

The analysis of the experimental data from the point of view of the Elnes law is summarized in Figs.2.

Fig.2a shows that the Elnes law works fairly well, because the experimental points lie within a narrow scatter band centered around the best fit line. Nevertheless the points relevant to the stress ratio 0.7 do not agree very well with the others. Once this data has been disregarded, the analysis results are more grouped, as shown in Fig.2b. Some supplementary tests in the range of the high stress ratio values

have been carried out to check if the behaviour of the experimental data belonging to the test with  $R$  equal to 0.7 is accidental or systematic. Fig.2c shows the results relevant to the supplementary tests together with those of Fig.2b; it can be seen that the new results match quite well the old ones. The need for a deeper insight in the material behaviour at high stress ratio values is justified also by the content of some spectra, e.g. MINITWIST, which are densely populated with rather high stress ratio cycles.

The scatter of crack growth predictions has been analyzed by means of a plot of the cumulative probabilistic distribution of the random variable  $\text{Log}(N_{\text{ex}}/N_{\text{c}})$ , where  $N_{\text{c}}$  is the number of cycles necessary to reach a given crack length. The variable  $\text{Log}(N_{\text{ex}}/N_{\text{c}})$  conforms fairly well to a normal distribution with a small standard deviations, especially when  $N_{\text{c}}$  is calculated using the Elnes law (Fig.3) rather than Forman's law (Fig.4). The Elnes law seems to work more accurately, in relation to its sounder physical bases and to the fact that it optimizes three parameters ( $C$ ,  $n$  and  $\alpha$ ), whereas only two are optimized by Forman's law.

#### 4.2 - SIMPLE SHEET - VARIABLE AMPLITUDE TESTS

Three kinds of standard spectra have been used, viz. FALSTAFF, MINITWIST and GAUSSIAN random, whose main characteristics have been briefly outlined in section 3. The specimens geometrical dimensions and the parameters that define the loading spectrum are shown in Tabs.1b-1c-1d for the complete set of tests of this kind. It can be seen that for FALSTAFF and MINITWIST tests, the influence of two different load levels has been studied, thus giving

rise to a total number of five different groups of data. The experimental results are plotted in Figs. 5a-9a in the form of a-F curves. The predictions obtained by utilizing the Elnes law and the Willenborg model or the Wheeler model with various plastic zone parameters are compared with the experimental a-F (or a-n) plots in Figs. 5b-9b. For FALSTAFF spectra, the predictions have also been computed by means of the ONERA model, based on the evaluation of the stress intensity factor threshold in the spectrum. The results relevant to the non-interactive method are not shown, because for variable amplitude spectra they are usually too conservative.

For every group of tests, the accuracy of the predictions has been estimated also on the basis of a comparison of the number of flights required in the tests for a certain crack growth interval with the corresponding calculated number of flights. Two crack growth intervals have been selected for every type of tests and the cumulative probabilistic distribution of the random variable  $F_{ex}/F_C$  is plotted in Figs. 5c-9c. The analysis of these figures suggests the following observations:

- for tests under FALSTAFF spectrum with  $S_{max}=20.0 \text{ Kg/mm}^2$  a first group of six tests has been carried out. The optimum value of the plastic zone coefficient relevant to the Wheeler retardation method has been found to be in the range 1.3-1.4, for the data collected in this first group of tests (Fig. 5c). This value is slightly below the expected one (1.8 is a typical value) and therefore it has been considered worthwhile to produce further data, as an overall check and in order to consolidate the experimental results. The tests relevant to this supplement of investigation are indicated in Tab. 1b and in Fig. 5a with the symbol ( $^{\circ}$ ). The results of the supplementary tests confirm the validity of the first set of data, as a substantially good agreement has been

found (Fig.5d).

- The results of the tests under FALSTAFF spectrum with  $S_{max}=24.0 \text{ Kg/mm}^2$  look rather surprising, because the average crack growth rates are higher than expected, in comparison with other similar experimental results obtained previously in the same laboratory, during the research activity of the first year. The different behaviour can be ascribed both to differences in the material characteristics, as a different batch has been utilized, and to the testing methodology, described in Appendix 1, which is certainly much more accurate for the tests under examination. Nevertheless similar experimental results, available in literature /12/, show a substantial agreement with the present data. This has somehow proved the uselessness of further controls on the reliability of the data collected. The data has been analyzed also from the point of view of the ONERA method, and the predictions seem to be encouraging for the lower stress level, while slower crack growth rates are predicted for the other one. As already mentioned in section 3, this method has been deduced from /3/ and is based on the concept of threshold in crack growth. It requires a weighting parameter, which controls the overall variation of  $K_{th}$  in the spectrum. The same value suggested by the authors has been utilized in the computations, and slightly conservative predictions have been obtained for the lower stress level.
- The tests under MINITWIST spectrum are summarized in Figs. 7 and 8. It is noteworthy to point out that the predictions obtained by means of the Willenborg model may be conservative or slightly unconservative, according to the spectrum average stress. This fact shows that the modelling of the residual stresses, adopted by the Willenborg model to explain the retardation effects, is rather crude and in particular does not take in due consideration the influence

of the mean load in the spectrum. From the analysis of Figs. 7c and 8c, the optimum values of the Wheeler plastic zone coefficients are deduced, namely about 2.4 and 1.4 respectively. In this case too, as for the FALSTAFF spectrum, it can be pointed out that the higher stress level spectrum is associated with a lower value of the optimum Wheeler coefficient.

- The Gaussian random spectrum is characterized by an irregularity factor 0.7 and a stress root mean square value equal to 2.5 Kg/mm<sup>2</sup>, and has been superposed to an average stress of 7.0 Kg/mm<sup>2</sup>. The experimental data, (Fig.9b), matches fairly well the prediction obtained with the Wheeler method, with a value of  $m$ , the plasticity zone parameter, equal to 1.9. The Willenborg model gives slightly conservative predictions.

#### 4.3 - STIFFENED PANEL - CONSTANT AMPLITUDE TESTS

Ten tests have been carried out, as shown in Tab. 1e, on strip stiffened panels under a constant amplitude loading, characterized by a stress ratio equal to 0.2. The experimental data, summarized in Tab.2e, has been treated to obtain the necessary information on rivet flexibility, following the procedure discussed in /7/, improved, as outlined in section 3, by means of a more accurate approach in the  $\Delta K$  evaluation, which takes into account the elastic unloading subsequent to plastic deformation in a yielded rivet.

Friction forces have not been taken into account and a regression analysis has been performed to define the optimum value of the flexibility parameter,  $\xi$ , i.e. the one which is related to the lowest scatter. Figs. 10a, 10b and 10c show  $da/dn - \Delta K$  plots, where  $\Delta K$  has been computed by as-

suming different values of  $\xi$ , i.e. 0.1, 0.3 and 0.7. It can be seen that in the second figure the points relevant to experimental results are grouped in a narrow scatter band around the best fit line.

Fig.11 shows a plot of the Fischer variable, assumed as the statistical quantity whose maximum must be searched, as a function of  $\xi$ . The best assessment of  $\xi$  derived from the analysis of all the data is 0.3 and the optimum values of  $\xi$  relevant to single tests fall within a narrow interval near that value.

The regression analysis to obtain the constants of Forman's law for the optimum value of  $\xi$  is shown in Fig.10b, and it must be pointed out that the slope of the best fit line is very similar to the one pertinent to the simple sheet tests. This means that the stress intensity factor calculation approach that has been adopted, which is explained in detail in Appendix 2, works quite satisfactorily. Once the best value of  $\xi$  has been assessed by following the usual procedure, /7/, a reliability analysis has been performed by comparing  $N_{ex}$  with  $N_c$  for two different crack growth intervals, chosen in a suitable way, i.e. one ending before and the other beyond the first stiffener. Fig. 12 shows the cumulative probabilistic distribution of the variable  $N_{ex}/N_c$  for the same three values of  $\xi$  in Figs.10.

#### 4.4 - STIFFENED PANEL - VARIABLE AMPLITUDE TESTS

Three groups of tests have been carried out with a variable amplitude standard spectrum, namely FALSTAFF, MINITWIST and Gaussian random, on built-up specimens of the same geometry as those tested under a constant amplitude loading. Tab. 1f and Tab.2f report the main characteristics and the re-

sults of all the tests. A plot of  $\Delta K$  versus the number of flights is shown in Figs. 13a÷15a.

A comparison with the predicted crack growth, evaluated by means of the CADAV program, described in detail in Appendix 2 as far as the  $\Delta K$  evaluation procedure is concerned, is shown in Figs. 13b÷15b. The retardation methods utilized are Wheeler's model, with different values of the plastic zone parameter, and the Willenborg model. The usual plots of the random variable  $\log F_{ex}/F_c$  are shown in Figs. 13c÷15c.

The analysis of the figures suggests the following considerations:

- for tests under FALSTAFF spectrum with  $S_{max}=20.0 \text{ Kg/mm}^2$ , the ONERA method works again quite well, resulting in slightly conservative predictions, while the Willenborg prediction curve falls just in the middle of the scatter band of the experimental curves. The most suitable value of Wheeler's parameter is about 2.0. It is different from the optimum value for flat panels, because, besides some uncertainties concerning the  $K$  evaluation in stiffened panels, the same asymptotic stress history does not produce the same  $K$  history at the crack tips.
- The panels tested under MINITWIST spectrum had quite a long initial damage, because the crack growth rates were low and it was decided to study with more accuracy the stiffener crossing. The Willenborg model gives too conservative results, whereas a high optimum value of the Wheeler plastic zone parameter is obtained, 3.5.
- The asymptotic stress history applied in the tests under Gaussian random loading was the same as that of the flat panels tests. This group of tests is characterized by a very low scatter in the experimental results. The comparison with the predictions shows that the Willenborg model

appears to be slightly conservative, while the optimum value of Wheeler's parameter is about 2.2.

## 5 - CRACK GROWTH PREDICTION RELIABILITY

All the data collected during the present research (1st, 2nd and 3rd year of activity) covers a large variety of loading spectra, geometrical configurations and materials.

In the previous sections the tests carried out in the third year's research activity have been analyzed, group by group, in order to highlight the main features of each group of tests. In the present paragraph almost the whole data obtained in the entire research has been treated, with the aim of evaluating the capacity of the existing methods to predict reliably the crack growth. To this end the statistical variable  $\text{Log } F_{\text{ex}}/F_c$  has been analyzed, irrespective of the kind of test in which the data has been collected, to evaluate its distribution and scatter.

$F_c$  has been evaluated according to the following retardation models:

- Wheeler's method with the optimum value of  $m$ , the plastic zone parameter, different of course from test to test, Fig.16a;
- Wheeler's method with a fixed average value of  $m$ , 1.8, Fig.16b;
- Willenborg model, Fig.16c;
- ONERA model, Fig.16d (in this case, only data obtained under FALSTAFF spectrum in 2024-T3 specimens has been considered).

The results shown in Figs.16 include data from almost every type of tests. The crack growth interval for which  $F_{\text{ex}}/F_c$  has been evaluated is not strictly the same for all tests.

The results show that:

- in the case of Fig.16a, in which  $F_c$  has been evaluated according to the Wheeler's method with the optimum value of the plastic zone parameter, the alignment of the points is satisfactory and the standard deviation of the normal distribution is assessed to be about 0.10, quite a low value;
- to assume a fixed value of the plastic zone coefficient,  $m$ , brings to a significant increase in the standard deviation (about 0.24) and the alignment of the points is not so good as in the first case, due to the bias introduced by the average value of  $m$ ;
- the Willenborg model curve shows a good alignment of the points, but the standard deviation is even higher than in the previous case (about 0.34). This means that the predictions obtained using this method can be affected by a large inaccuracy;
- the ONERA method results refer only to tests obtained in 2024-T3 specimens under FALSTAFF spectrum, because of the lack of information about the threshold variations in the 7075-T6 material. The standard deviation is assessed to be about 0.16, higher than in the case of Fig.16a, but still acceptable.

It can be seen that the best results are those obtained with Wheeler's method, using each time the most suitable value of  $m$ , but its evaluation is not a simple problem, as it is strongly affected by the kind of spectrum, the specimen geometrical configuration and the stress level. This difficulty strongly limits the validity of Wheeler's method, because an inaccurate evaluation of  $m$  can give rise to misleading results, as shown in Fig.17.

On the other hand, Wheeler's method with a fixed para-

meter does not provide accurate results. The Willenborg model is defined once for all and does not require any parameter to be optimized, but its predictions are not very good, because they are affected by a very large scatter.

The ONERA method seems to work satisfactorily and to provide generally conservative predictions, but the data analyzed is limited only to one load spectrum and, anyway, for every load spectrum, a proper weighting parameter is required, variable according to the spectrum "severity".

The survey of the prediction methods here analyzed shows that further research is required, and a particular effort must be focused in the development of new retardation models, e.g. those based on the crack closure phenomenon, which seem to be more flexible in use and more accurate than those based on the modelling of residual stresses.

## 6 - CONCLUSIONS

The research carried out during the third year of the programme was centered on tests of sheets and stiffened panels loaded both at constant and variable amplitudes. The specimens were made of 2024-T3 aluminium alloy, cut from the same batch of sheets. Three types of standard loading spectra have been utilized: FALSTAFF representative of fighter aircraft wing loading, MINITWIST typical for transport aircraft wings and Gaussian random, representative of the loading on a transport aircraft fin. The results of these tests, processed with the methods developed during the whole period of research activity, have been presented in previous sections.

A set of conclusions concerning the two types of tests, namely constant amplitude and variable amplitude, is worth remarking:

- as far as the constant amplitude tests are concerned, two

different types of specimen have been tested, namely simple sheets and stiffened panels. The data obtained with the sheet specimens has been treated prevalently with the aim of evaluating the existing formulas for crack growth. A significant conclusion concerns the relationship:

$$\frac{da}{dn} = C \cdot \Delta K_{eff}^n = C \cdot [\Delta K \cdot U(R, \alpha)]^n$$

which fits quite well with the test results when the function  $U(R, \alpha)$  is chosen conforming to the Schijve proposal:

$$U(R, \alpha) = 0.55 + (0.45 - \alpha) R + \alpha R^2$$

This law works quite well in the intermediate  $\Delta K$  range and this is in accordance with the results of other investigators. So this law is more recommended than the well-known Forman's relationship.

- Tests from stiffened panels allow us to obtain further information on rivet flexibility. The improvements in the modeling of the rivet elasto-plastic behaviour for the stress intensity factor computation increase the reliability of the flexibility evaluation. The method developed in the course of the present investigation seems to work fairly accurately in the final version utilized in the third year's research activity even if a slightly stiffer fastener behaviour is likely to be predicted.
- As far as simple sheets-variable amplitude tests are concerned, a rather wide set of results has been obtained, utilizing three different spectra and different load levels. The data has been utilized to evaluate the Willenborg and Wheeler methods, while only data from tests under FALSTAFF spectrum has been utilized to evaluate the ONERA model. The Willenborg method is unable to provide a reliable fit to the

test data. On the contrary, the Wheeler method with a suitable selection of the plastic zone parameter,  $m$ , predicts correctly, on the average, the number of flights necessary for a crack growth of given length. Nevertheless  $m$  is very sensitive to the type of spectrum and, for a given spectrum, to the load level. As far as the ONERA method is concerned, the predictions comply with the data from FALSTAFF spectrum tests with an acceptable scatter.

- The stiffened panels tests have been performed with three different types of spectra. The tests results have been compared, as usual, with the predictions obtained by means of the methods devised by Willenborg, by Wheeler and by ONERA. The computations have been made utilizing the optimum value of the rivet flexibility obtained from constant amplitude tests on the basis of an improved version of the CADAV program to take into account the progressive rivet yielding. With such changements, the trends in predictions and test data are quite similar, with a significative improvement with respect to the previous year's results.
- As far as the relative merits of the prediction methods are concerned, similar conclusions to the case of simple sheets also can be drawn. It is worth noting that the best values of the Wheeler plastic zone parameters are different from the case of simple sheets with the same stress level, denoting a dependence of this parameter on the geometry.
- All the data from variable amplitude tests has been eventually treated to obtain a general assessment of the reliability of the prediction methods. The results of this analysis are shown in Figs.16, which include also data obtained from 7075-T6 specimens tested in the previous year's research activity. The set of data reported in Figs.16 is relevant to three different spectra, different load levels, materials and geometry. Therefore it can be considered a sig-

nificant sample to evaluate the prediction methods reliability.

The results confirm the inadequacy of the Willenborg model and, on the contrary, show that Wheeler's method, with the selection of the best values of  $m$  for each group of tests, provides quite accurate predictions, characterized by low values of scatter. Nevertheless this positive assessment is weakened by the strong dependence of the optimum value of  $m$  on spectrum, geometry and load level; this dependence nowadays is difficult to be predicted either "a priori" or on the basis of simple test programs. Fig.16b, obtained utilizing the predictions of the Wheeler method with a fixed value of the plastic zone parameter ( $m=1.8$ ), does not show satisfactory results, similarly to those relevant to the Willenborg model.

Therefore, the present state of affairs about predictions is not fully satisfactory and further developments are necessary, particularly in the area of interaction effects modelling, to make it possible to have a reliable prediction for a given geometry, spectrum and load level.

#### REFERENCES

- /1/ Willenborg J.D., Engle R.M., Wood H.A.: "A Crack Growth Retardation Model Using an Effective Stress Concept", AFFDL-TM-FBR-71-1, Air Force Flight Dyn.Lab., 1971.
- /2/ Wheeler O.E.: "Spectrum Loading and Crack Growth", J. of Basic Eng., Trans. ASME, Series D, 1962, pp.181-186.
- /3/ Baudin G., Robert M.: "Crack Growth Model for Flight-Type Loading".

- /4/ Anon.: "Description of a Fighter Aircraft Loading STAn-  
dard For Fatigue evaluation", Combined Report of the  
NLR,LBF,IABG and F+W, March 1976.
- /5/ Lowak H., De Jonge J.B., Franz J.,Schütz W.: "MINITWIST,  
a Shortened Version of TWIST", NLR MP 79018 U, 1979,ICAF  
Doc.1147.
- /6/ Hück M., Schütz W., Fischer R., Köbler G.: "A Standard  
Random Load Sequence of Gaussian Type Recommended for  
General Application in Fatigue Testing; its Mathemati-  
cal Background and Digital Generation", Presented at the  
42nd AGARD Meeting of the Structures and Materials Pan-  
el , Ottawa, April 1976.
- /7/ Salvetti A., Cavallini G.,Lazzeri L.: "The Fatigue Crack  
Growth Under Variable Amplitude Loading in Built-Up Struc-  
tures",DA ERO-78-G-107, 1st Annual Technical Report, Nov.  
1979, ICAF Doc.1139.
- /8/ Salvetti A., Cavallini G., Lazzeri L.: "The Fatigue Crack  
Growth Under Variable Amplitude Loading in Built-Up Struc-  
tures",DA ERO-78-G-107, 2nd Annual Technical Report, Jan.  
1981, ICAF Doc.1200.
- /9/ Schijve J.: "Some Formulas for the Crack Opening Stress  
Level", Delft University of Technology, Department of  
Aerospace Engineering, Memorandum M-368, April 1980, ICAF  
Doc.1161.
- /10/ Elber W.: "The Significance of Crack Closure", ASTM STP  
486, 1971, pp. 230-242.
- /11/ Newman J.C.Jr.: "A Finite-Element Analysis of Fatigue  
Crack Closure", Mechanics of Crack Growth, ASTM STP 590,  
1976, pp.281-301.

- /12/ Wanhill R.J.H.: "Manoeuvre Spectrum Fatigue Crack Propagation in Aluminium Alloy Sheet Materials", NLR MP 78025 U.
- /13/ Lanciotti A.: "A Method to Improve the Performance of Fatigue Machines in Variable Amplitude Loading Tests", to be published.
- /14/ Poe C.C.Jr.: "Stress Intensity Factor for a Cracked Sheet with Riveted and Uniformly Spaced Stringers", NASA TR R-358, 1971.

## APPENDIX 1 - TESTING METHODOLOGY FOR VARIABLE AMPLITUDE LOADING SPECTRA.

Fatigue testing under variable amplitude loading is often a hard job, because a very difficult problem arises, viz. how to guarantee within acceptable limits that the applied load sequence follows quite faithfully the desired one. In the following the testing methodology adopted at the Institute of Aeronautics is briefly summarized, but a wider description can be found in /13/.

The testing equipment available in the Institute of Aeronautics fatigue laboratory consists of a Servotest hydraulic power pack, that can supply pressure to two actuators, controlled in closed loop by means of servovalves and capable of a force range in dynamic of  $\pm 500$  KN the first and  $\pm 250$  KN the second, and a process computer, Digital PDP 11/34, with analog-to-digital (A/D) and digital-to-analog (D/A) converters.

The computer, by means of the A/D converter, can measure the electrical signal from the load cell, proportional to the load actually applied by the actuator, with an accuracy of about 2.5 mV, i.e. 1/2000 of the full scale range. If a computer program feeds the machine with an electrical signal, varying with time, identical to the spectrum required, the response of the machine will introduce appreciable differences, which cannot be accepted from the point of view of the load spectrum accuracy. On this basis, a group of programs have been developed with the aim of handling the complete spectrum data in such a manner that, by making successive corrections, the machine response is improved until it becomes fully satisfactory. The loads actually applied by the fatigue machine are monitored by means of the A/D converter.

For every kind of variable amplitude loading tests, a statistical analysis of the machine response has been carried out, to assess the accuracy of the applied loading. For each load level (e.g. levels 1-32 for FALSTAFF and Gaussian random loading), a comparison was performed between the applied load, measured by the computer by means of the A/D converter, and the expected load. Two cases are distinguished, in which only the peaks or the valleys, respectively, are processed. The average percentage error, referred to the maximum load in the spectrum, is well below 1%, thus assuring a good accuracy in load control. For each load level, the actual response of the machine is highlighted by means of a histogram of the error occurrences. A plot is shown in Fig.18, where both load levels and errors are expressed in computer internal units, used by the A/D and D/A converters.

With the available facilities, most tests have been performed with an average working frequency of about 18 Hz., a compromise between accuracy in load control and time required to carry out the test.

## APPENDIX 2 - STRESS INTENSITY FACTOR IN BUILT-UP STRUCTURES.

The problem of  $K$  evaluation in stiffened panels is of great importance in the analysis of the experimental data collected in tests on such specimens. Both programs, SKESA and CADAV, developed at the Institute of Aeronautics of the University of Pisa, utilize for the  $K$  evaluation a scheme which derives from that proposed by C.C.Poe /14/. In this approach a cracked stiffened panel is considered as a redundant system, whose unknowns are the rivet forces, which can be determined by means of displacement compatibility equations.

The original version proposed by Poe has been improved by taking into account also the rivet flexibility, i.e. by adding in the displacement compatibility equations the terms due to the rivet deflection. A further development has been made by introducing plastic deformation effects, i.e. whenever the load carried by a rivet exceeds the yielding load, a different load-deflection relationship is assumed for that rivet, still of linear type, Fig.19. According to this scheme, a more accurate evaluation of  $\Delta K$  can be made, assuming that in the unloading part of a cycle the rivet behaves elastically, i.e. with the same slope of the fully elastic phase.

In the analysis of test data from stiffened specimens under constant amplitude loading, the  $\Delta K$  pertinent to each crack length has been evaluated by first calculating  $K_{max}$ , and then checking if any rivet carried a load higher than the yielding load. In case this occurred, the evaluation of  $K_{min}$  in the cycle was performed by taking into account the elastic unloading just described when writing the term relevant to that rivet in the deflection compatibility equations.

The  $\Delta K$  values evaluated in this manner have then been

associated with the computed crack growth rate values,  $da/dn$ , to get the constants of the semiempirical crack propagation laws. Figs.10 show the results of the analyses carried out assuming three different values of the flexibility parameter in the computation of  $\Delta K$ .

In variable amplitude loading tests on stiffened panels, under the combined action of increasing crack length and peak loads, a progressive yielding of the most loaded rivets occurs, so that the load transfer capability of the junction decreases. The computer program for the crack growth evaluation has been modified in the  $\Delta K$  computation block for stiffened panels, according to the following scheme:

- a) at first, for the panel geometry under examination, a research has been made to identify the possible combinations of crack lengths and peak loads for which yielding occurs in the most loaded rivets, according to the double-linear elasto-plastic behaviour outlined in Fig.19;
- b) according to the scheme above described,  $K$  is computed for a sufficiently high number of crack lengths and loads, and for different situations of the rivets, i.e.
  - all the rivets behave elastically;
  - only the first rivet has carried a higher load than the yielding load while all the others are still in the fully elastic range;
  - the first and the second most loaded rivets have been yielded, and so on.
- c) in the computer program, the progressive efficiency decrease of the junction is monitored by means of a comparison with the limiting situations outlined in a) and, according to the estimated model for the rivets behaviour,  $K$  is evaluated by interpolating through the values calculated in b). This solution has been chosen because it is accurate enough,

while a direct K computation would be too long and bring to an unacceptable computing time.

The results obtained are encouraging, (see Figs.13b-15b), because the predicted a-F curves show a shape similar to the one of the experimental data, with an accurate location of the flex point in the region of the stiffener crossing.

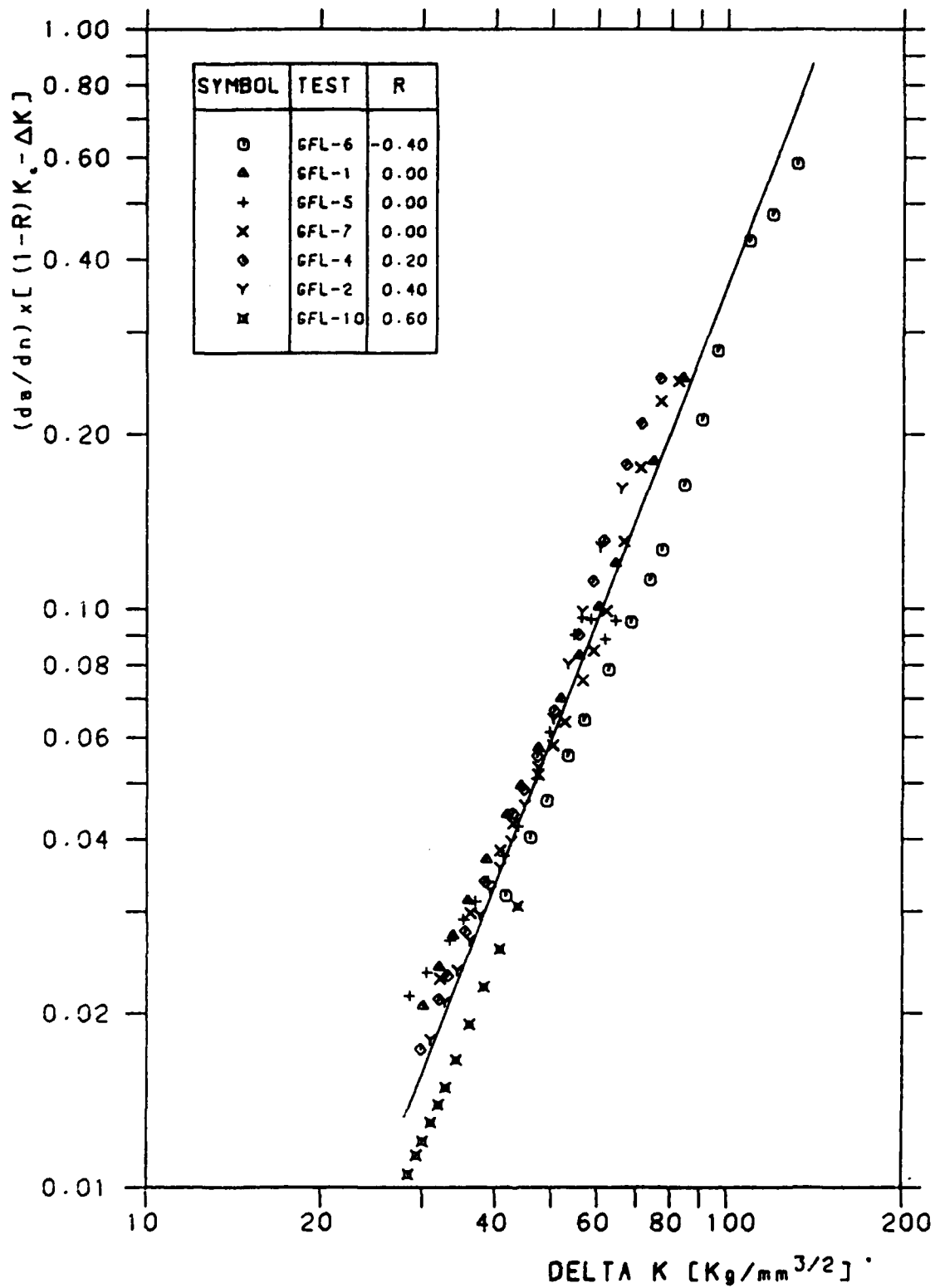


Fig.1 - Regression analysis on experimental data for evaluating Forman's law. The best-fit values are:  $C=0.22686 \times 10^{-5}$ ,  $n=2.6027$ .

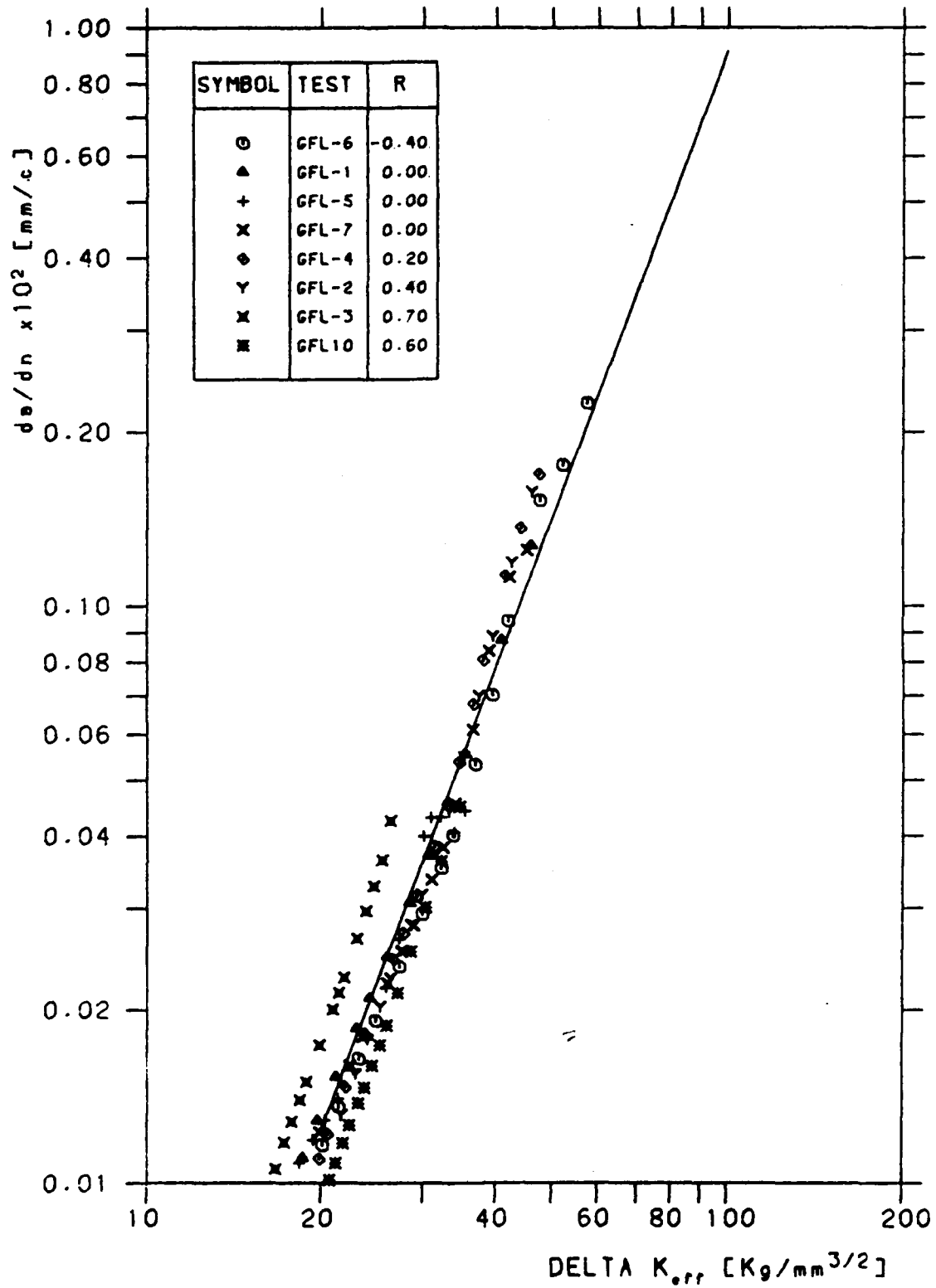


Fig.2a - Regression analysis on experimental data for evaluating Elnes law.

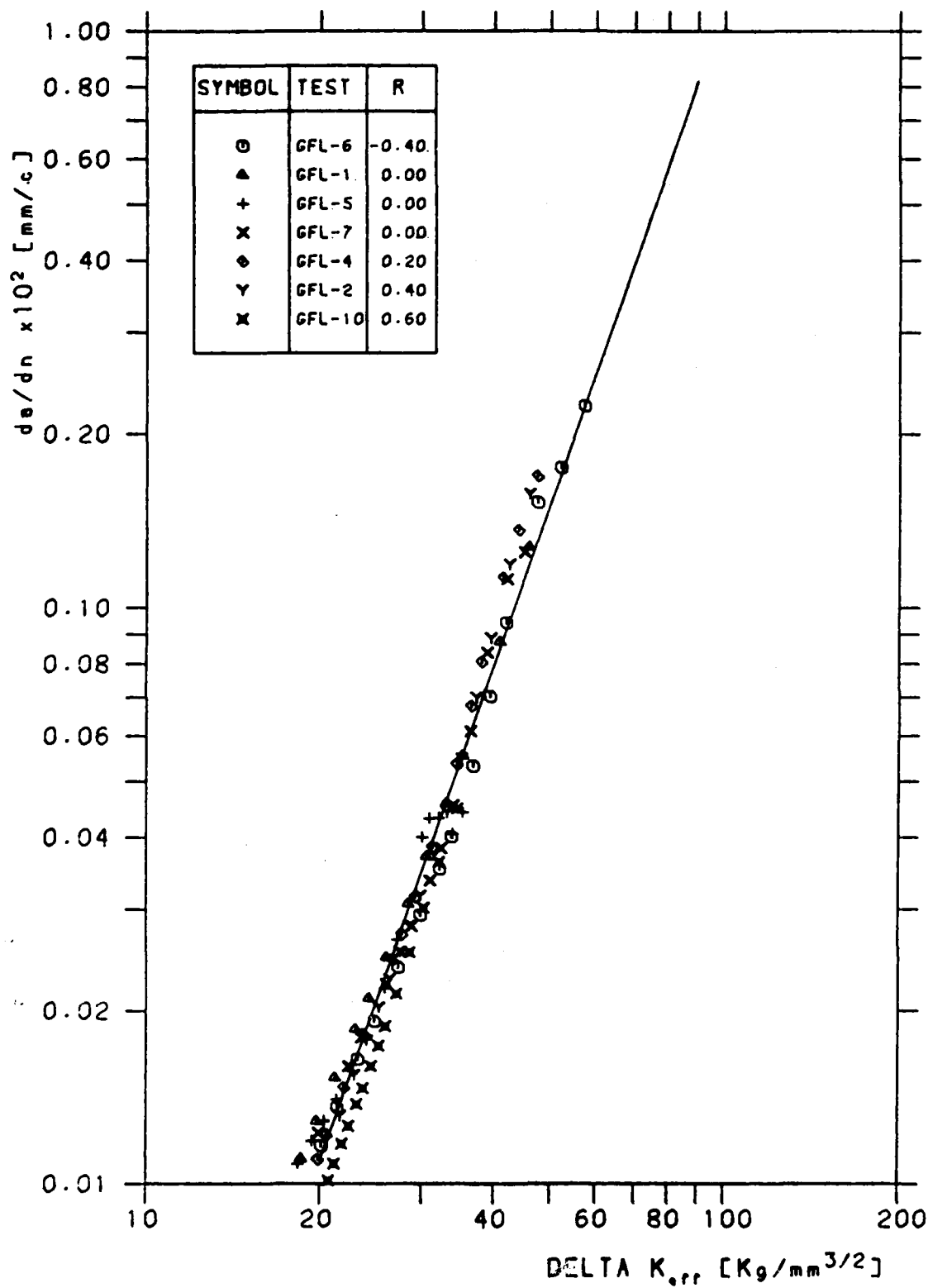


Fig.2b - Regression analysis on a reduced set of experimental data for evaluating the Elnes law. The best-fit values are:  $\alpha=0.12$ ,  $C=0.2019 \times 10^{-7}$ ,  $n=2.87$ .

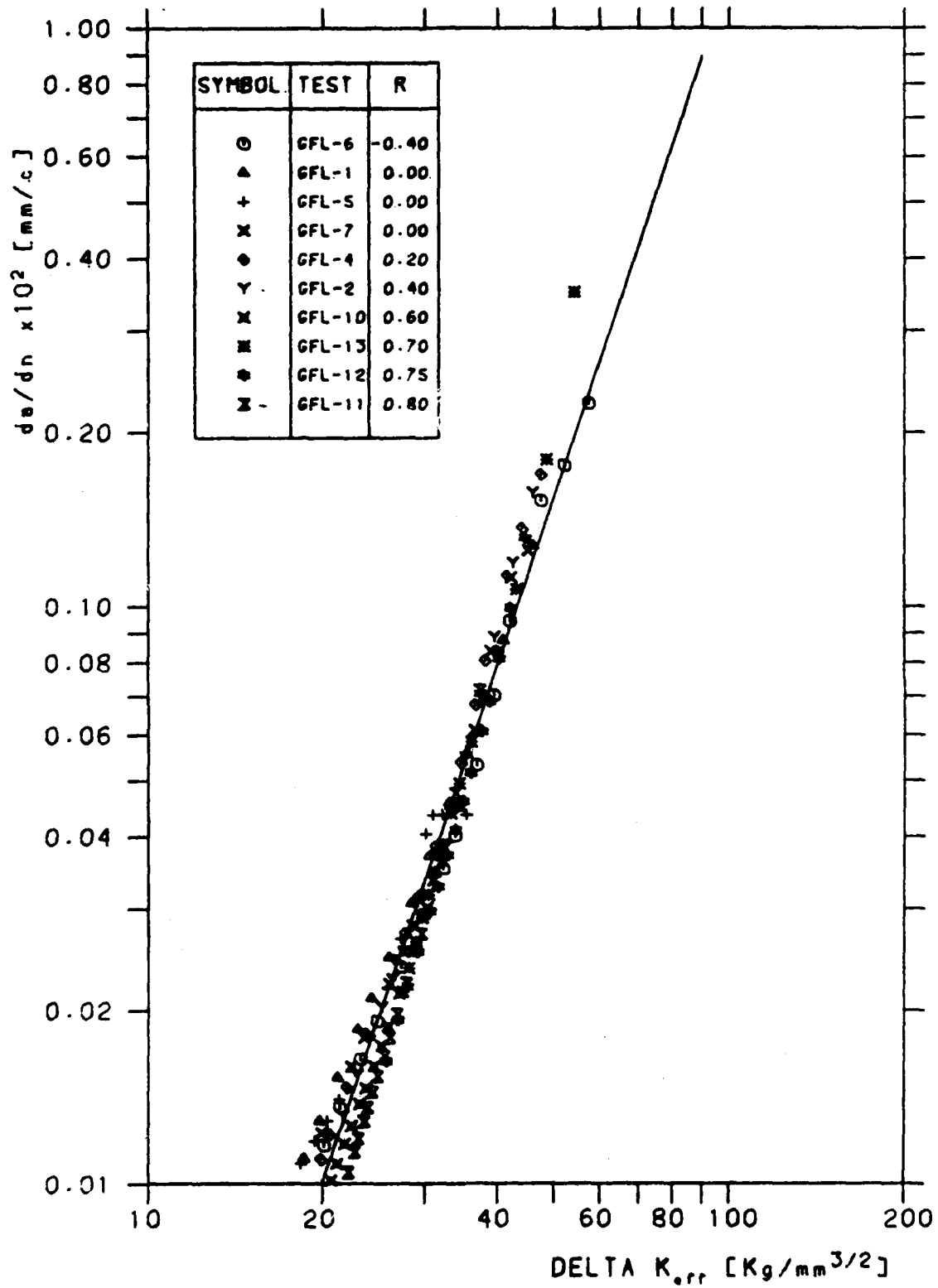


Fig.2c - Regression analysis on a wider set of experimental data for evaluating the Elnes law.

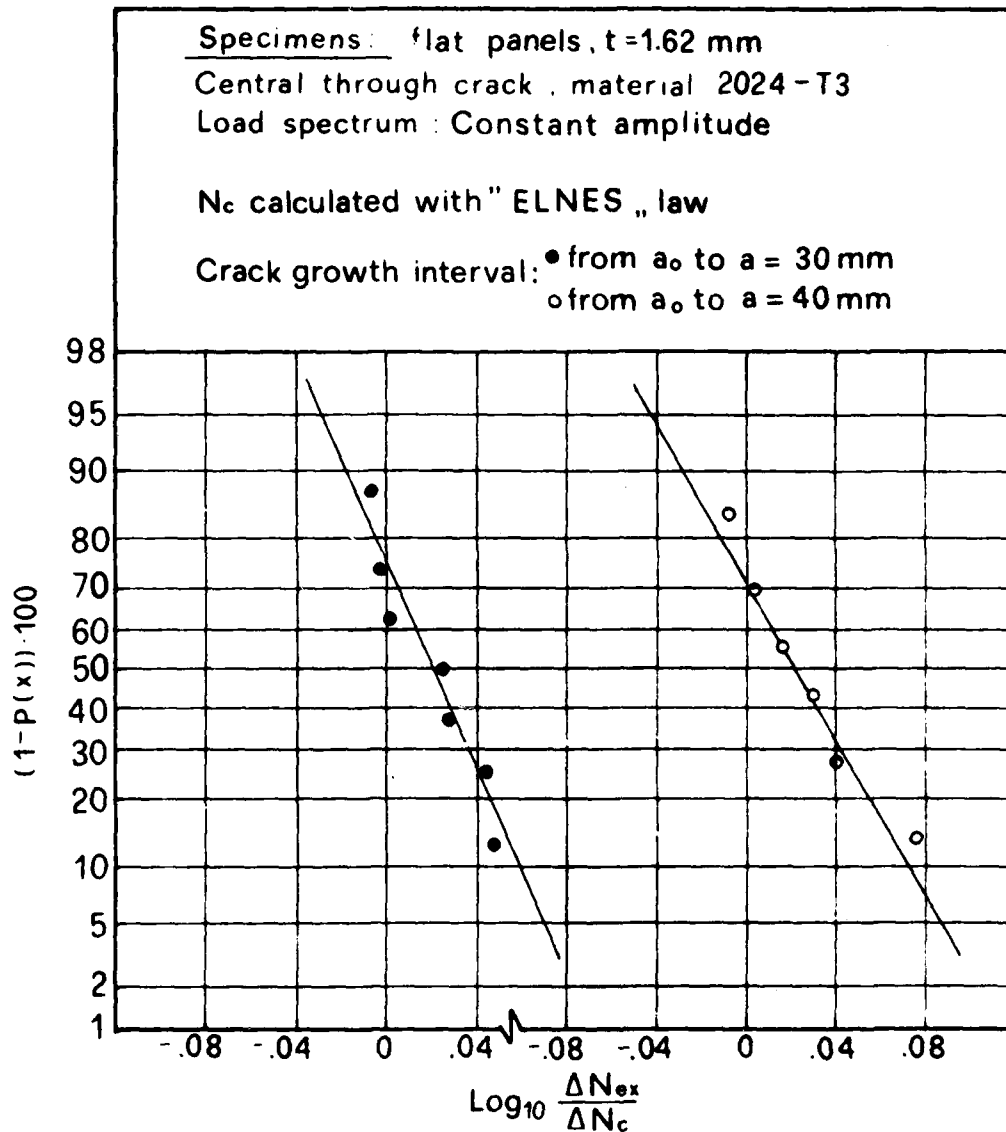


Fig.3 - Lognormal cumulative distributions of the variable  $\Delta N_{ex}/\Delta N_c$  for two ranges of damage growth.

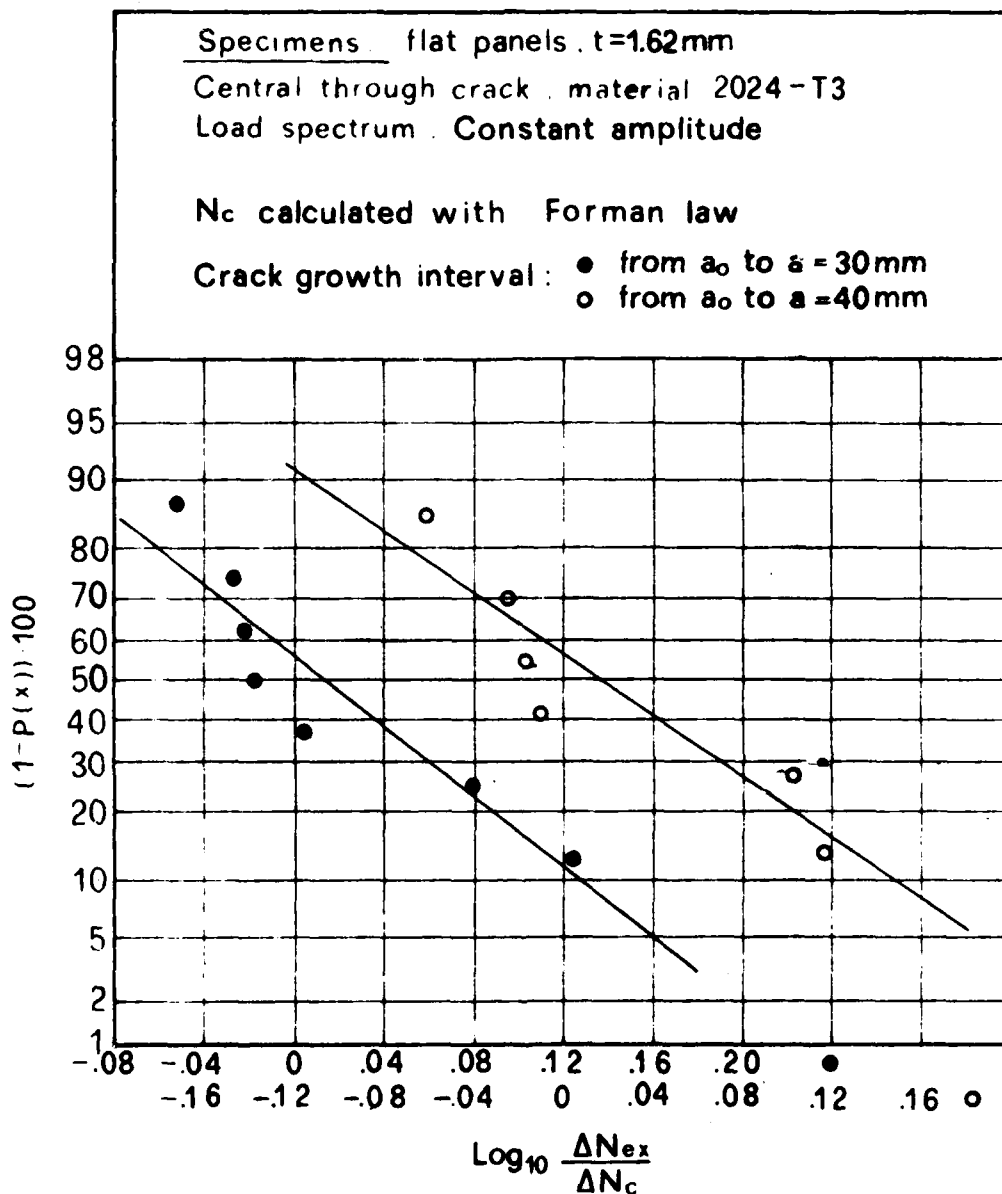


Fig.4 - Lognormal cumulative distributions of the variable  $\Delta N_{ex}/\Delta N_c$  for two ranges of damage growth.

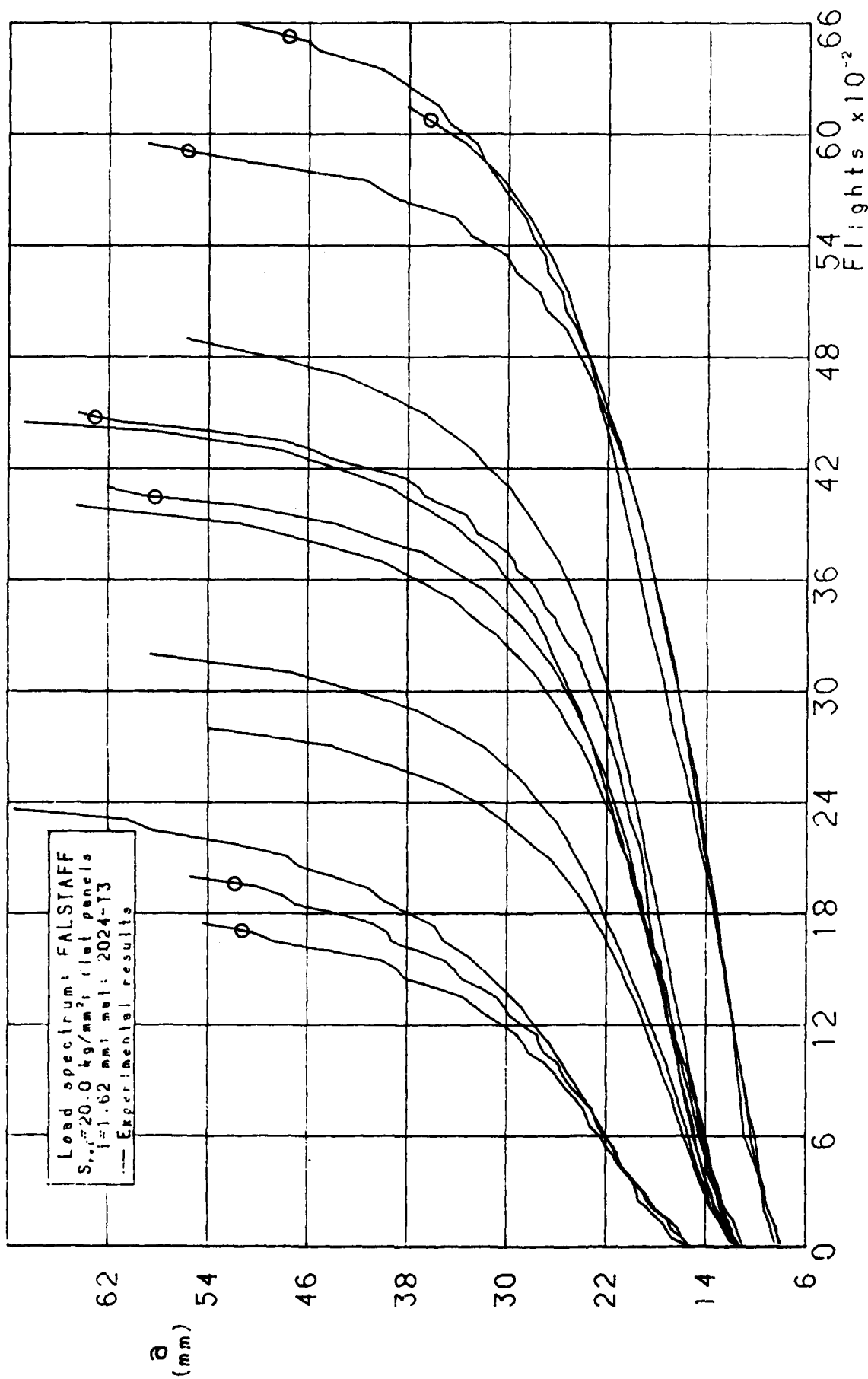


Fig. 5a - Experimental results of flat panels tests under FALSTAFF spectrum loading with  $S_{max} = 20.0 \text{ Kg/mm}^2$ .

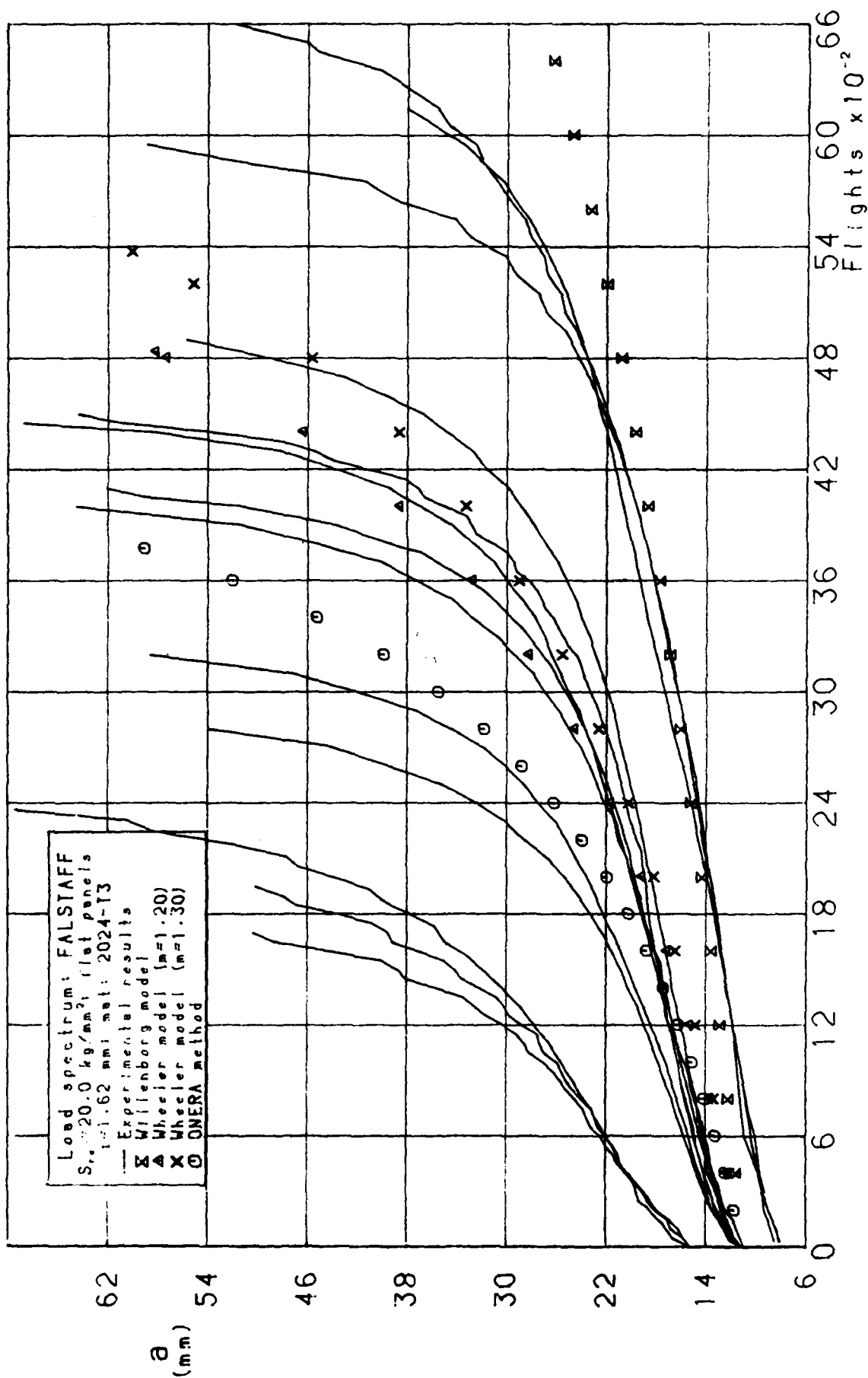
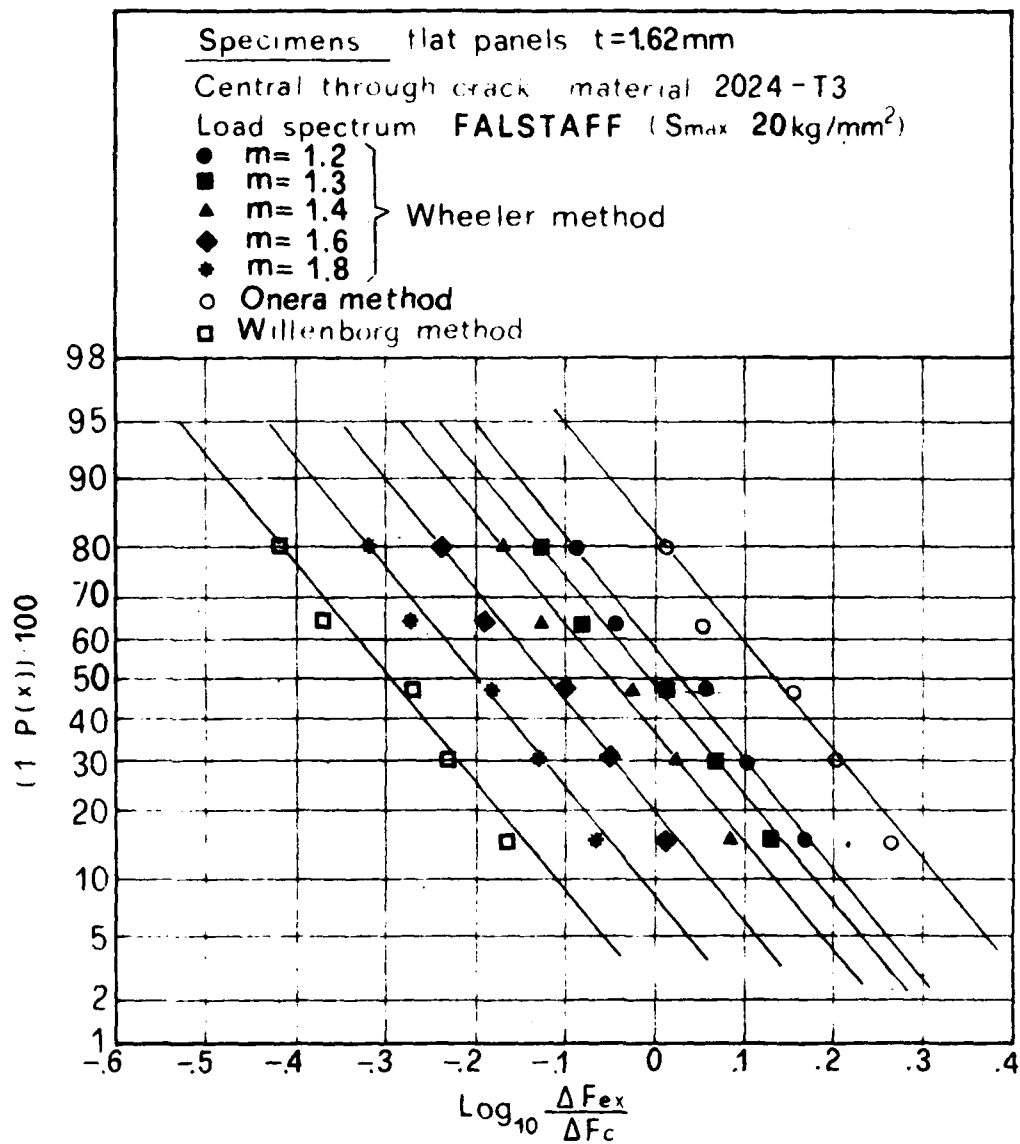
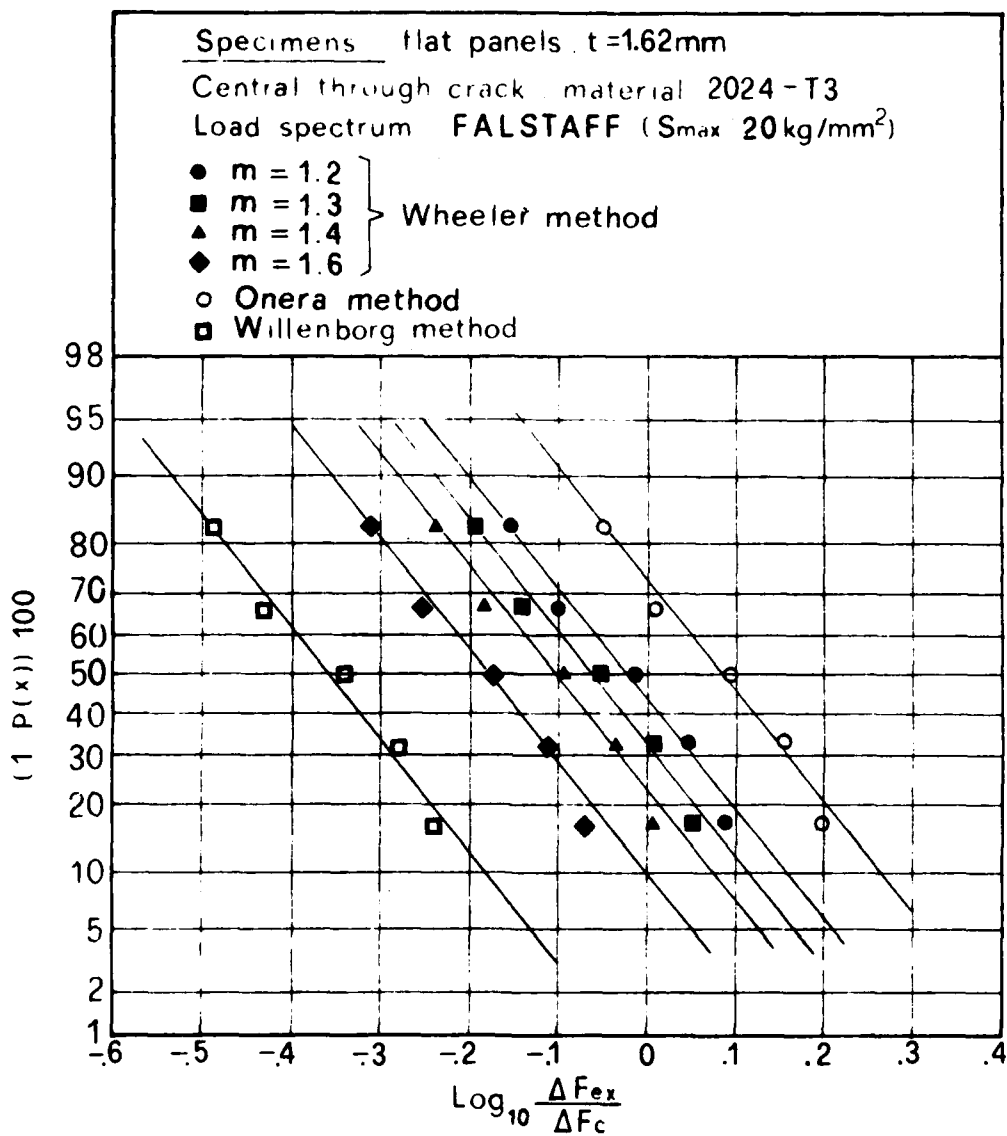


Fig.5b - Comparison of experimental results with predictions obtained with Elnes law for flat panels tests under FALSTAFF spectrum loading with  $S_{max}=20.0 \text{ Kg/mm}^2$ .



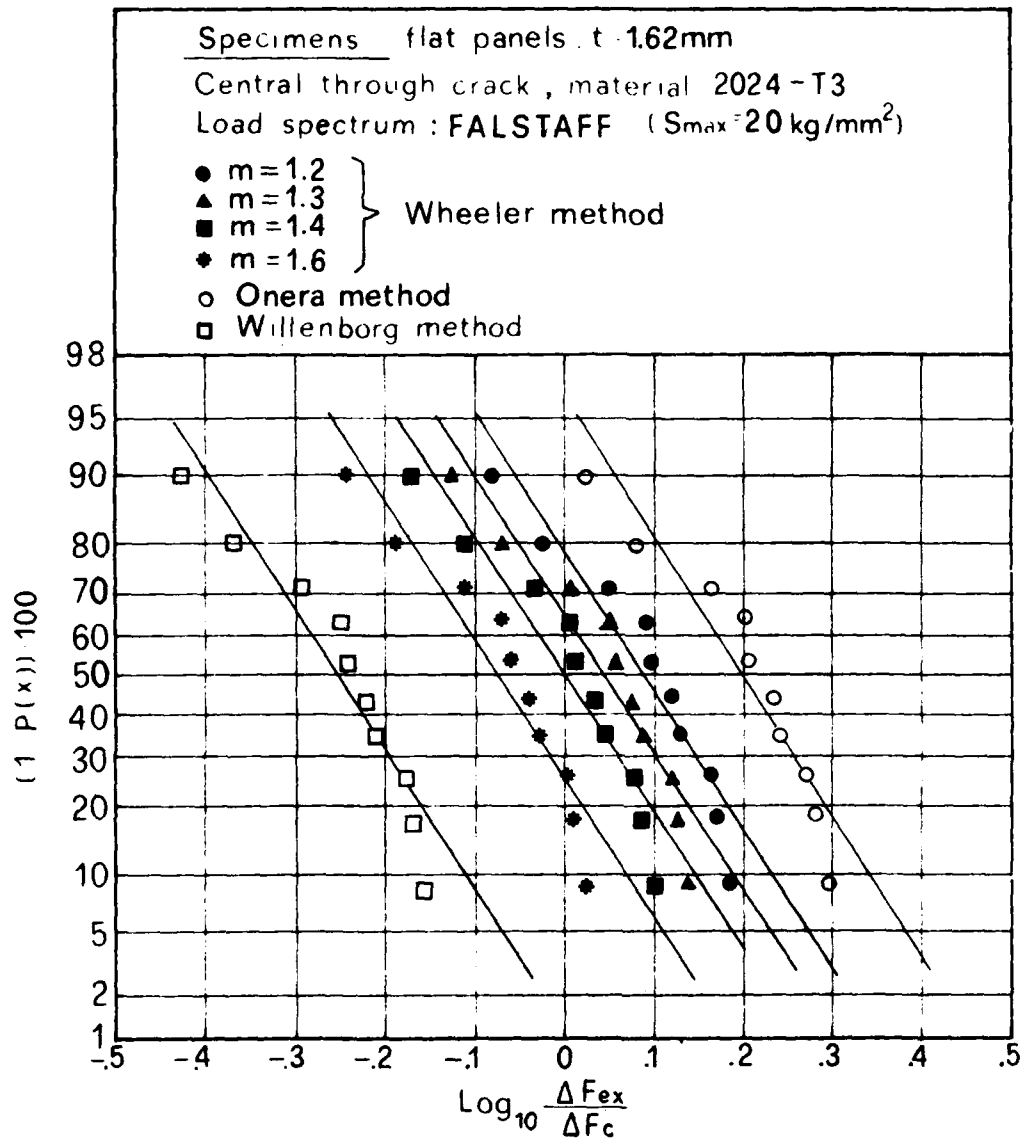
Crack growth interval : from  $a = 13\text{mm}$  to  $a = 25\text{mm}$

Fig.5c - Lognormal cumulative distributions of the variable  $\Delta F_{ex}/\Delta F_c$  for the first series of flat panels tests under FALSTAFF spectrum loading with  $S_{\max}=20.0\text{ Kg/mm}^2$ .  $F_c$  has been calculated using the Elnes law.



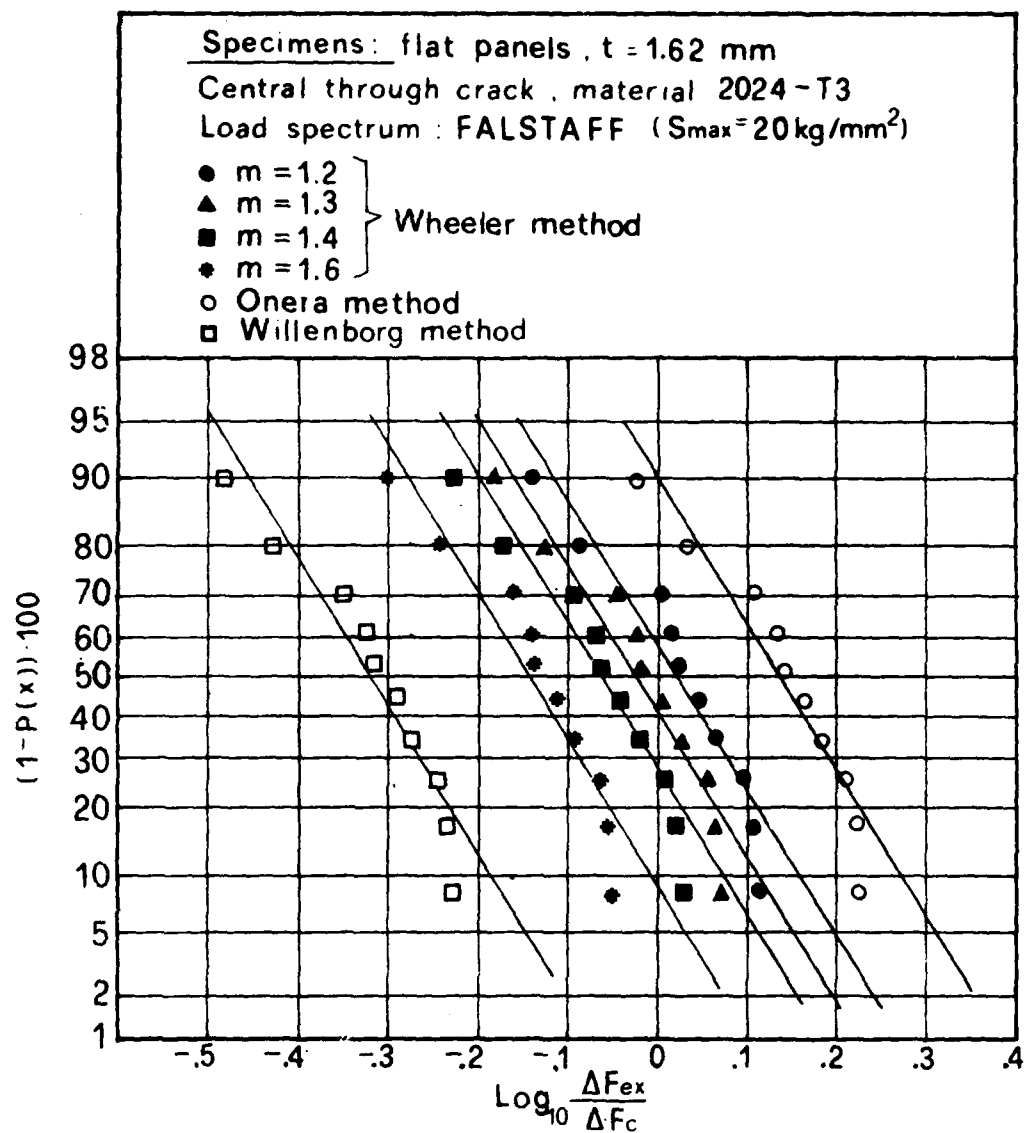
Crack growth interval : from  $a=13\text{mm}$  to  $a=42\text{mm}$

Fig.5c - Concluded.



Crack growth interval : from  $a=15 \text{ mm}$  to  $a=30 \text{ mm}$

Fig.5d - Lognormal cumulative distribution of the variable  $\Delta F_{ex}/\Delta F_c$  for the complete series of flat panels tests under FALSTAFF spectrum loading with  $S_{max}=20.0 \text{ Kg/mm}^2$ .  $F_c$  has been calculated using the Elnes law.



Crack growth interval: from  $a = 15$  mm to  $a = 42$  mm

Fig.5d - Concluded.

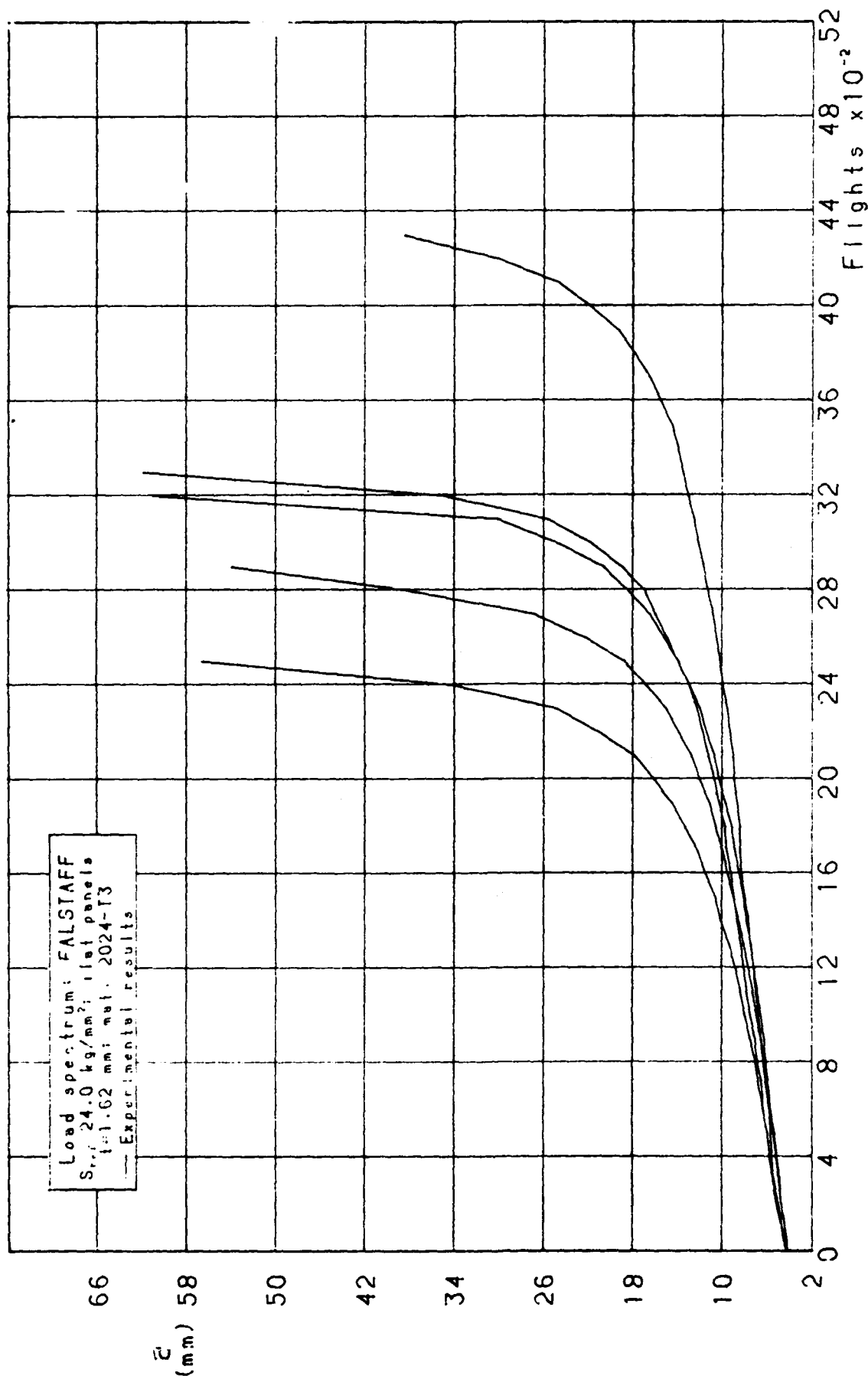


Fig. 6a - Experimental results of flat panels tests under FALSTAFF spectrum loading with  $S_{max}=24.0$  Kg/mm<sup>2</sup>.

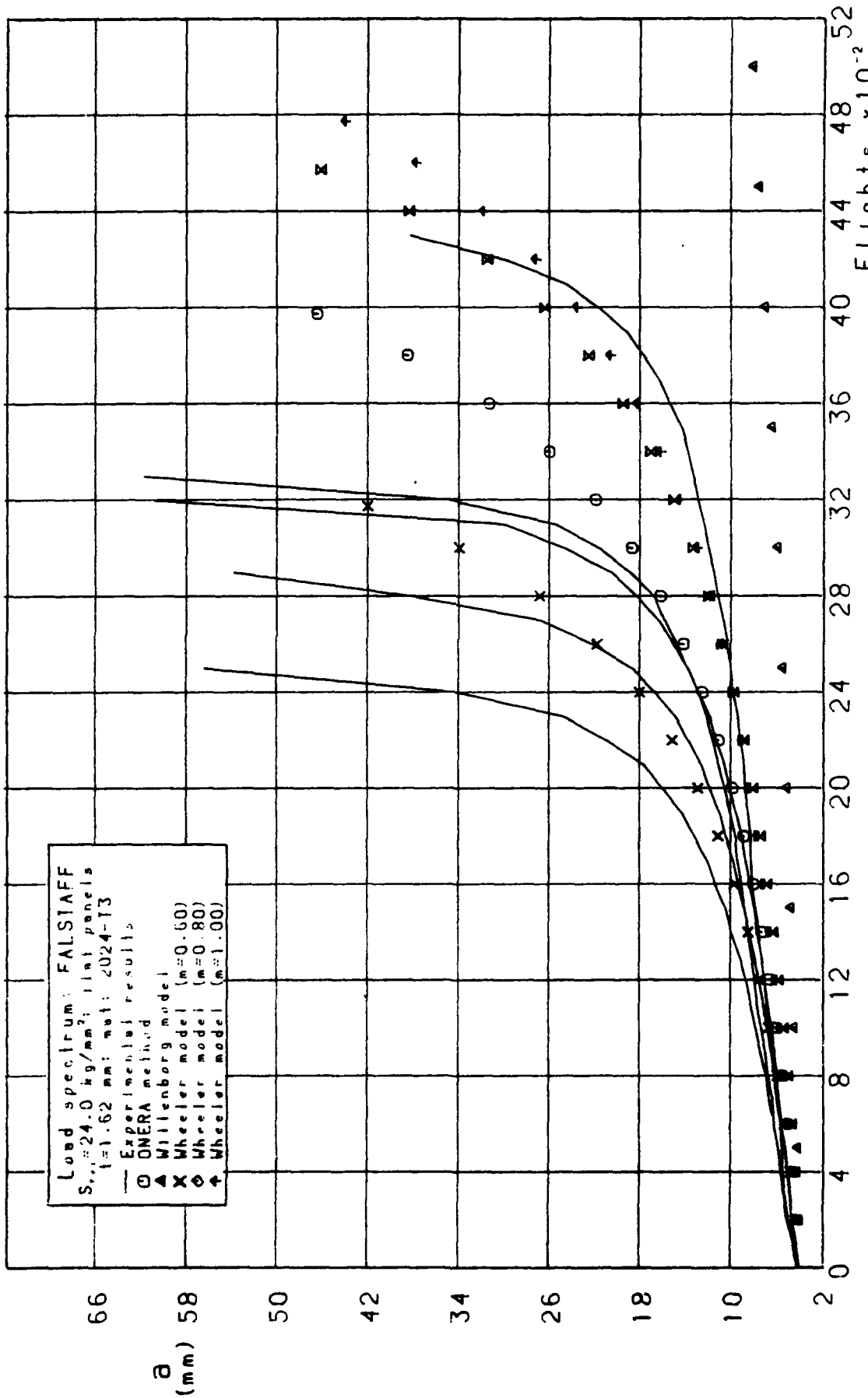
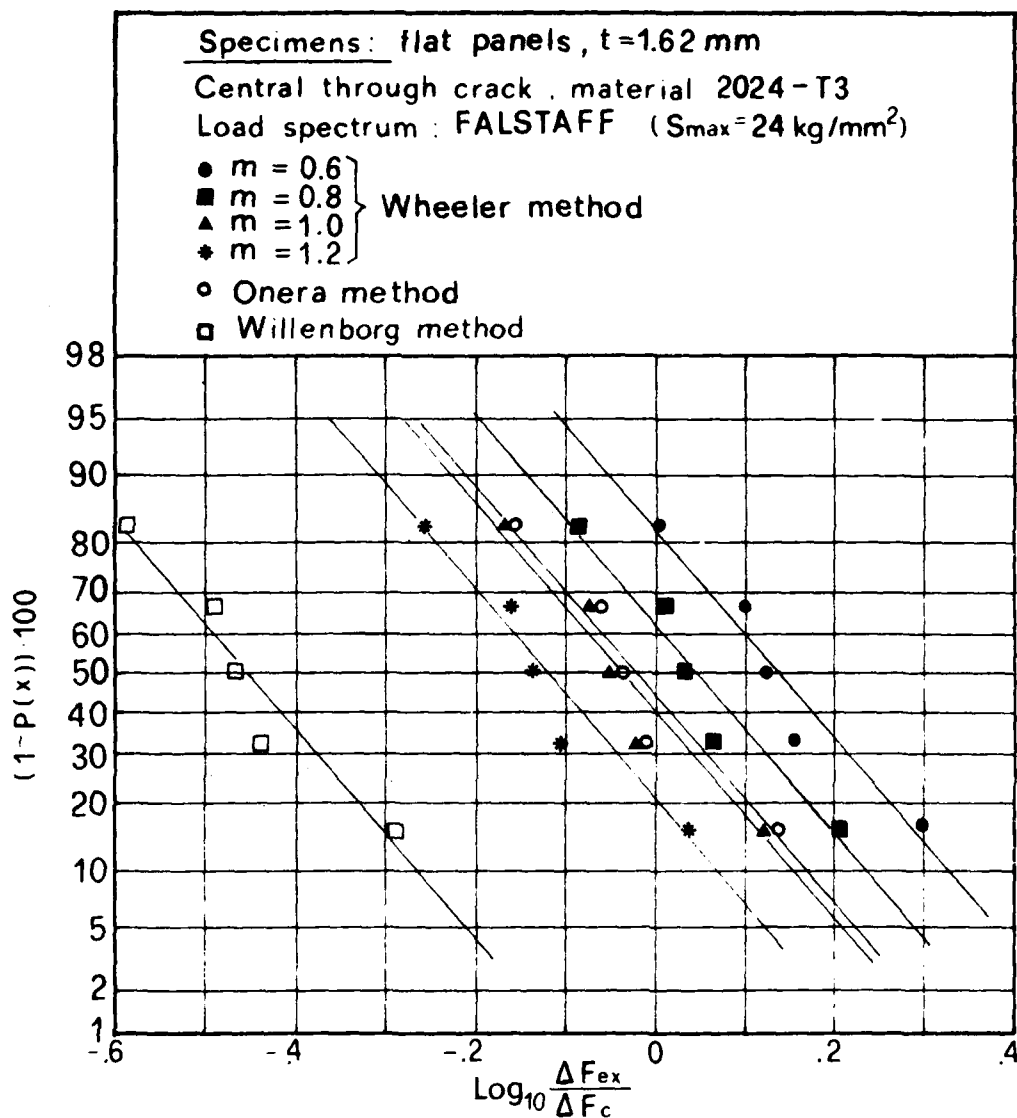
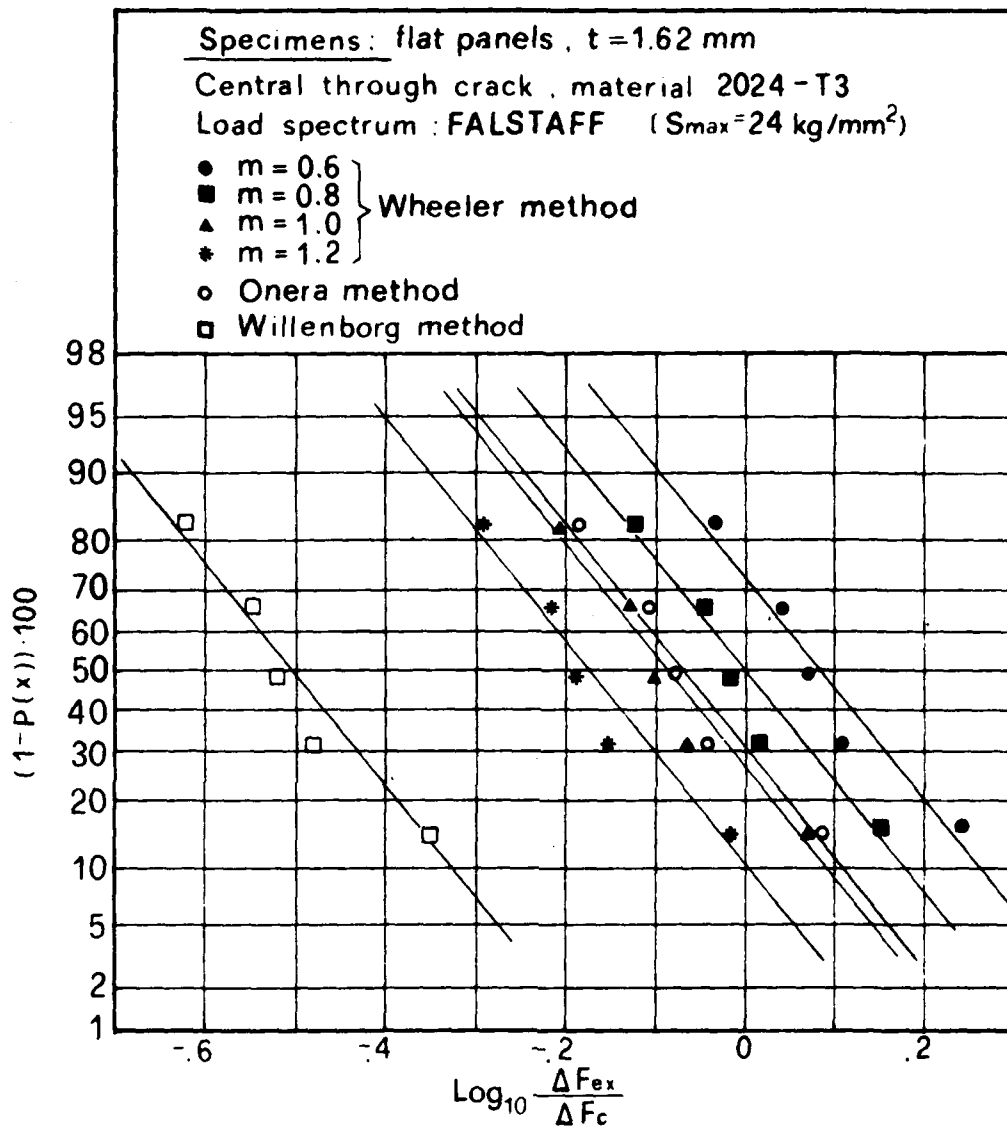


Fig.6b - Comparison of experimental results with predictions obtained with Elmes law for flat panels tests under FALSTAFF spectrum loading with  $S_{max}=24.0 \text{ Kg/mm}^2$ .



Crack growth interval : from  $a = 5$  mm to  $a = 14$  mm.

Fig.6c - Lognormal cumulative distribution of the variable  $\Delta F_{ex}/\Delta F_c$  for flat panels tests under FALSTAFF spectrum loading with  $S_{max}=24.0$  Kg/mm<sup>2</sup>.  $F_c$  has been calculated using Elnes law.



Crack growth interval: from  $a = 5 \text{ mm}$  to  $a = 24 \text{ mm}$

Fig.6c - Concluded.

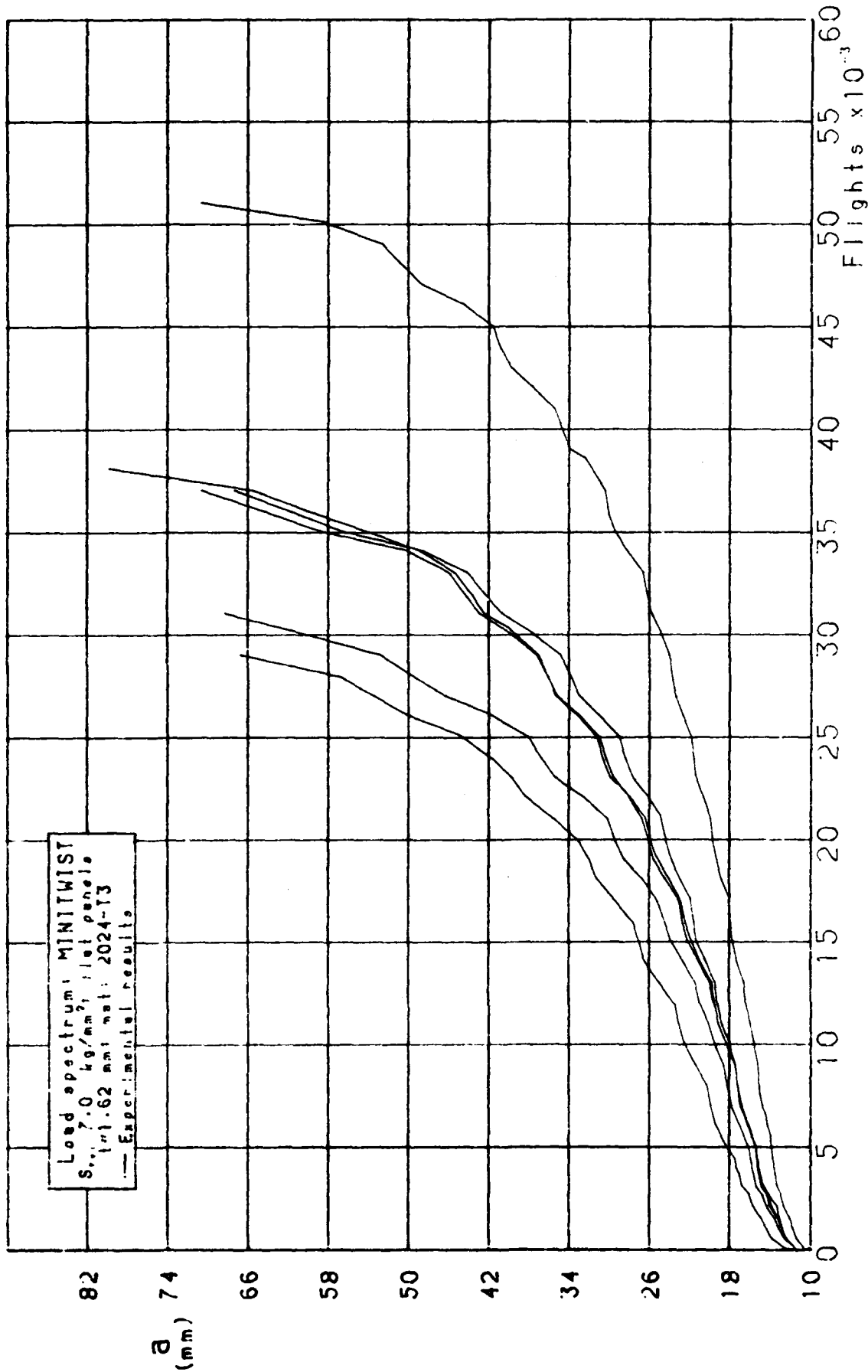


Fig.7a - Experimental results of flat panels tests under MINITWIST spectrum loading with  $S_{ig} = 7.0 \text{ kg/mm}^2$ .

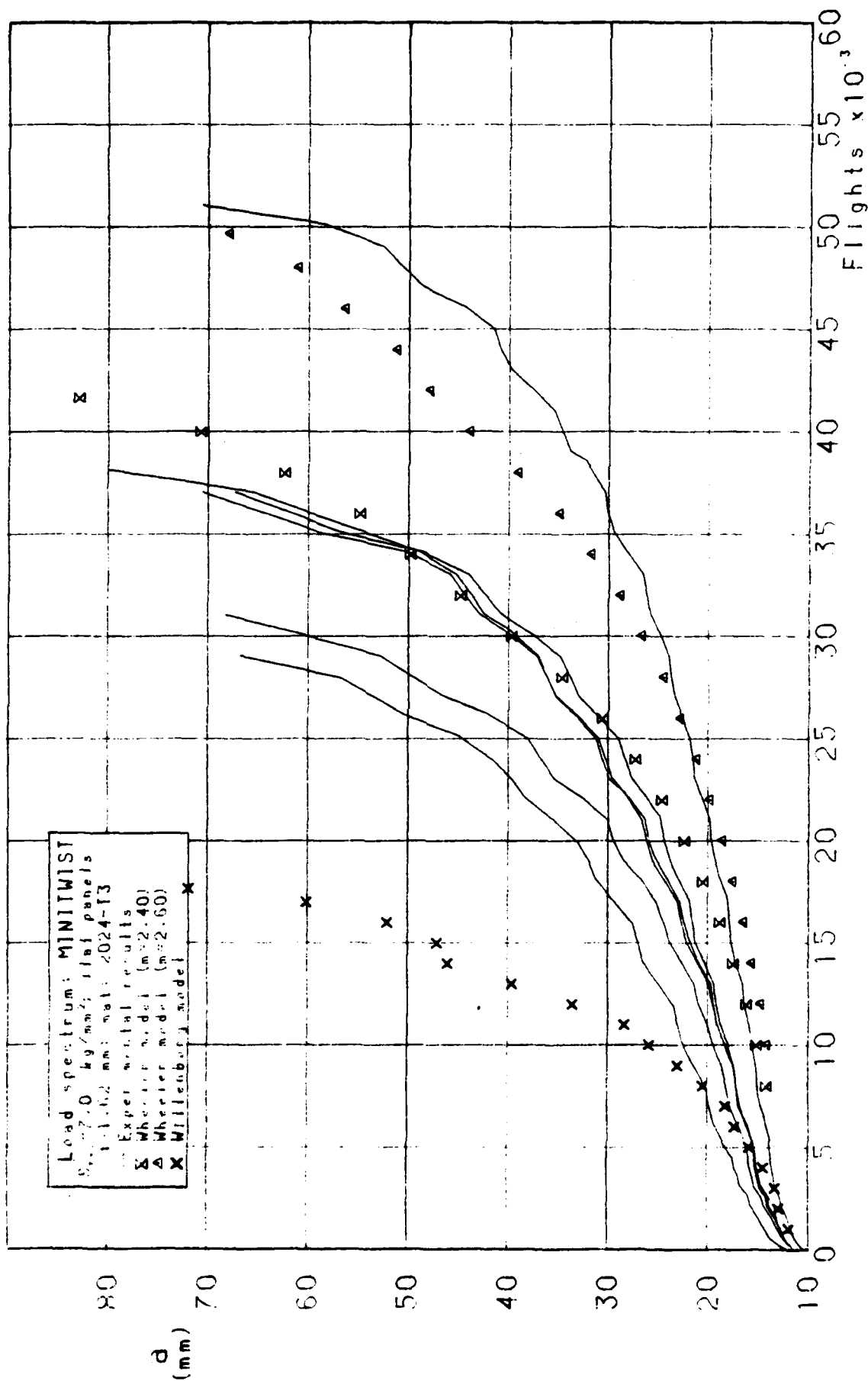
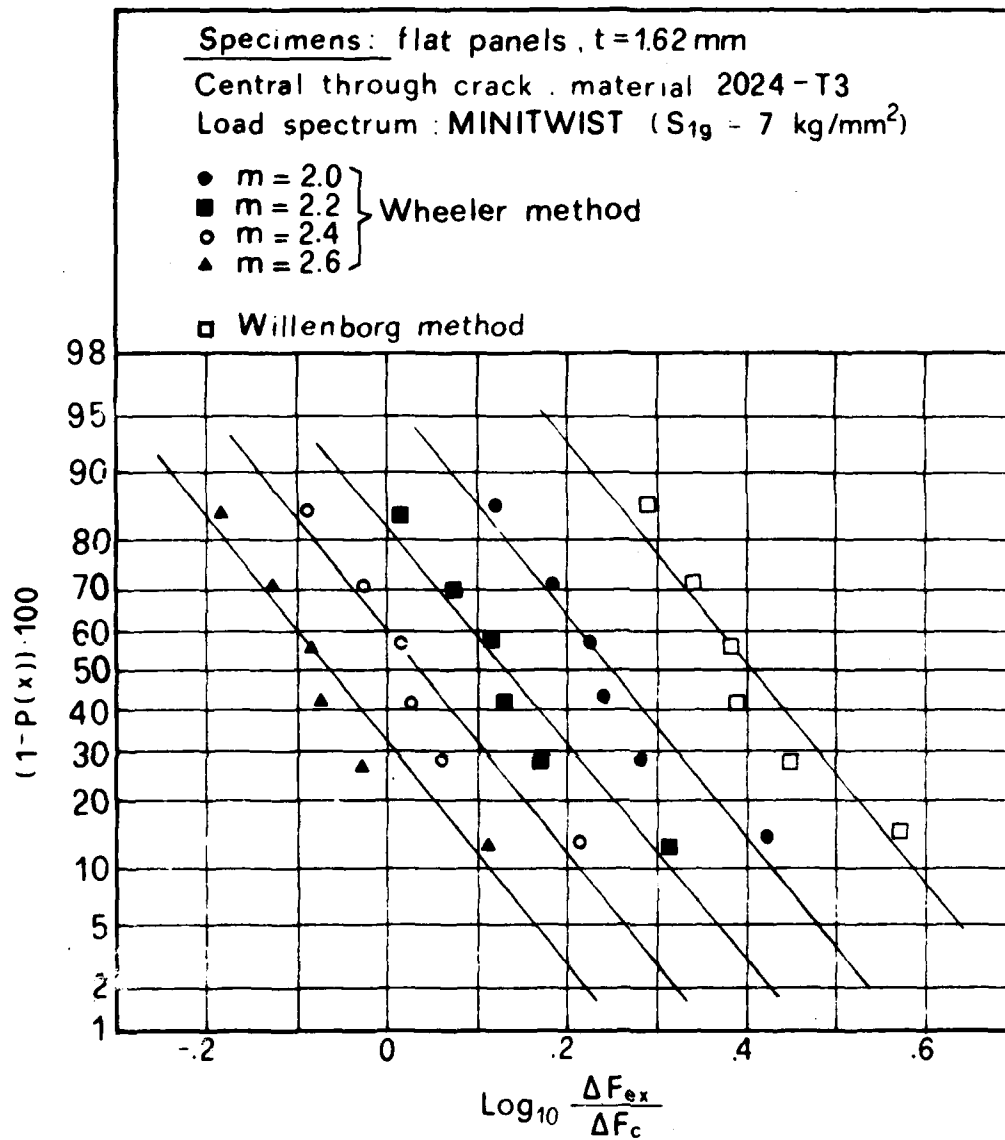
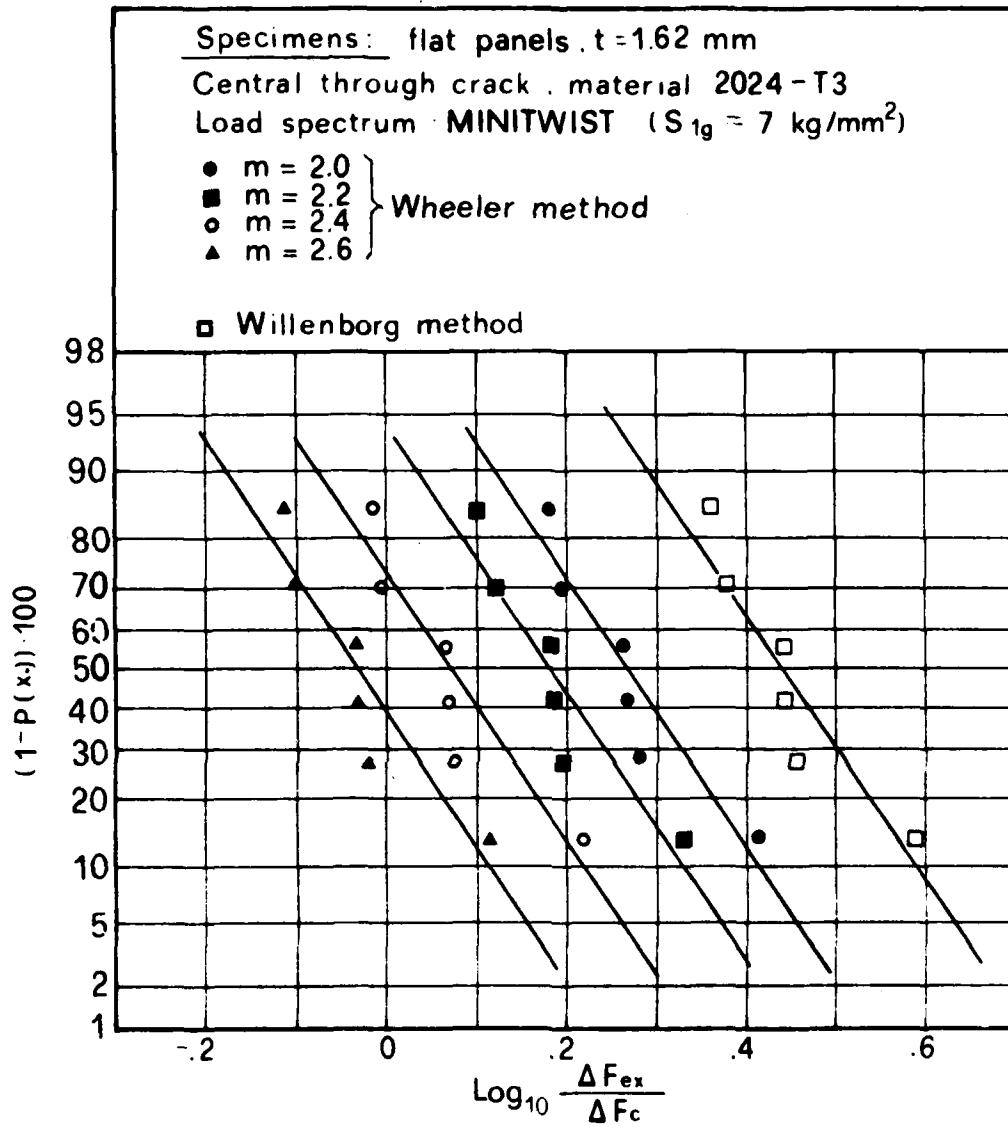


Fig.7b - Comparison of experimental data with predictions obtained with Elmes law for flat panels tests under MINITWIST spectrum loading with  $S_{11}=7.0 \text{ Kg/mm}^2$ .



Crack growth interval : from  $a = 13$  mm to  $a = 26$  mm

Fig.7c - Lognormal cumulative distribution of the variable  $\Delta F_{ex}/\Delta F_c$  for flat panels tests under MINITWIST spectrum loading with  $S_{1g}=7.0$  Kg/mm<sup>2</sup>.  $F_c$  has been calculated using the Elnes law.



Crack growth interval : from  $a = 13$  mm to  $a = 40$  mm

Fig.7c - Concluded.

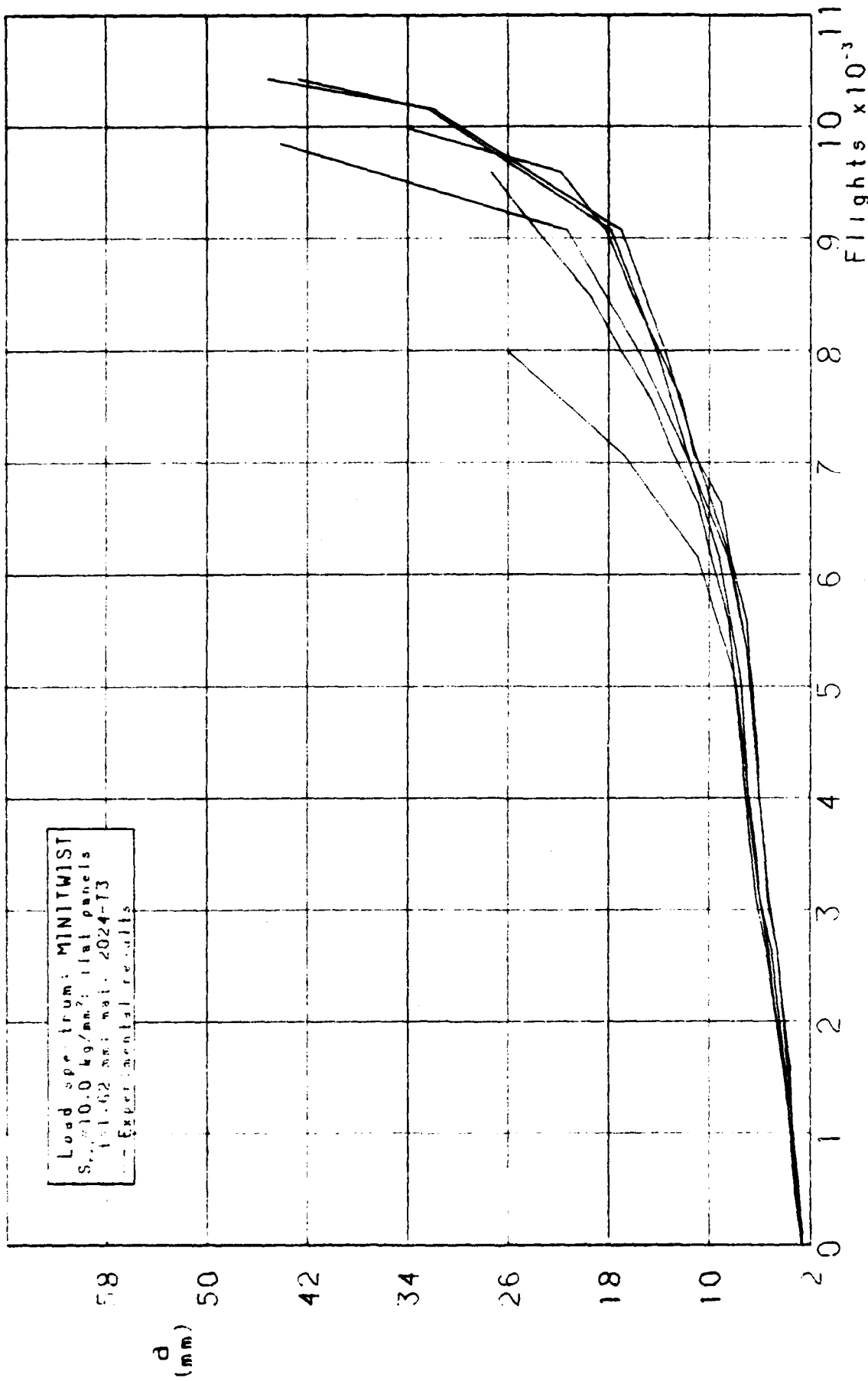


Fig.8a - Experimental results of flat panels tests under MINITWIST spectrum loading with  $S_{ig}=10.0 \text{ Kg/mm}^2$ .

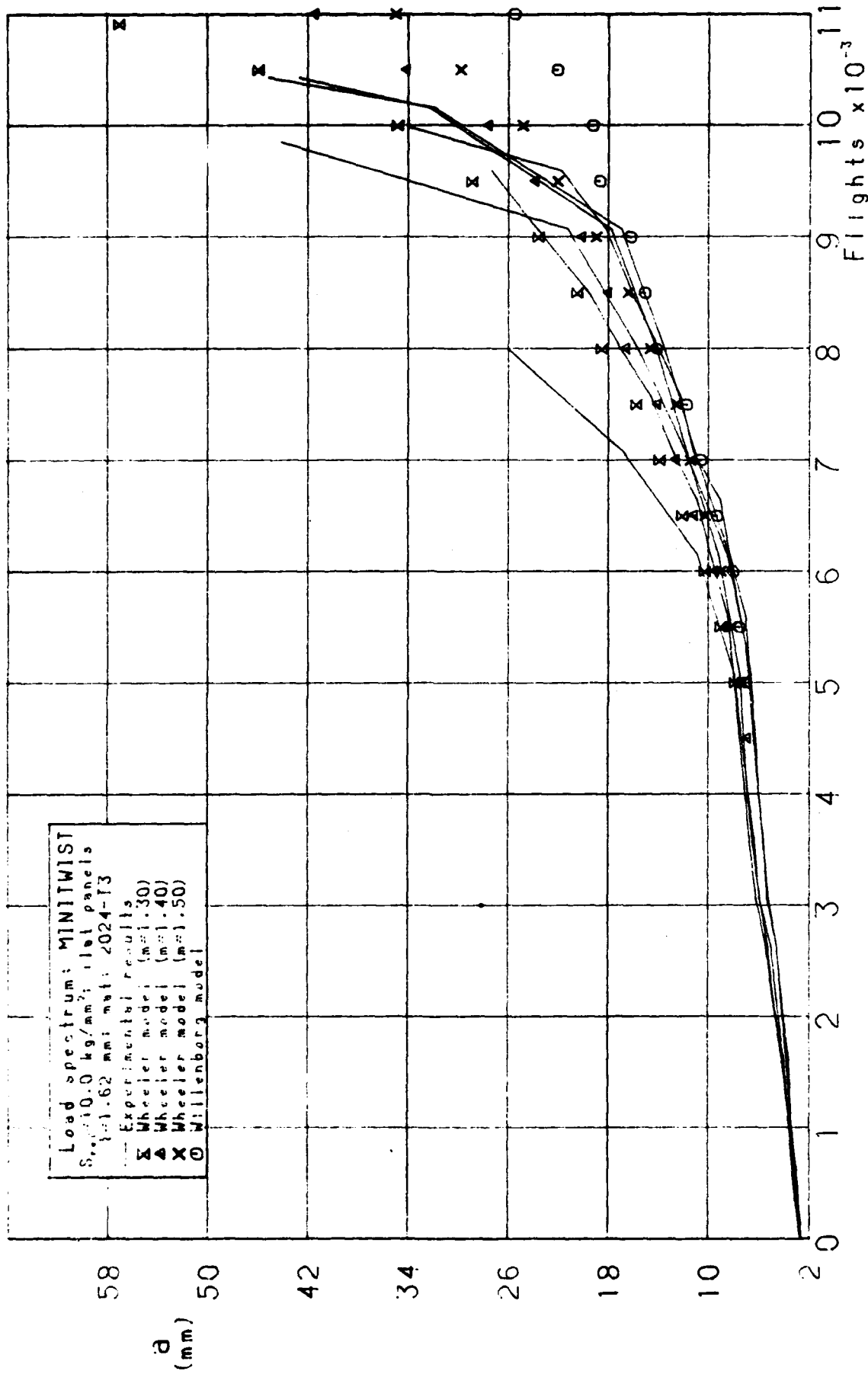
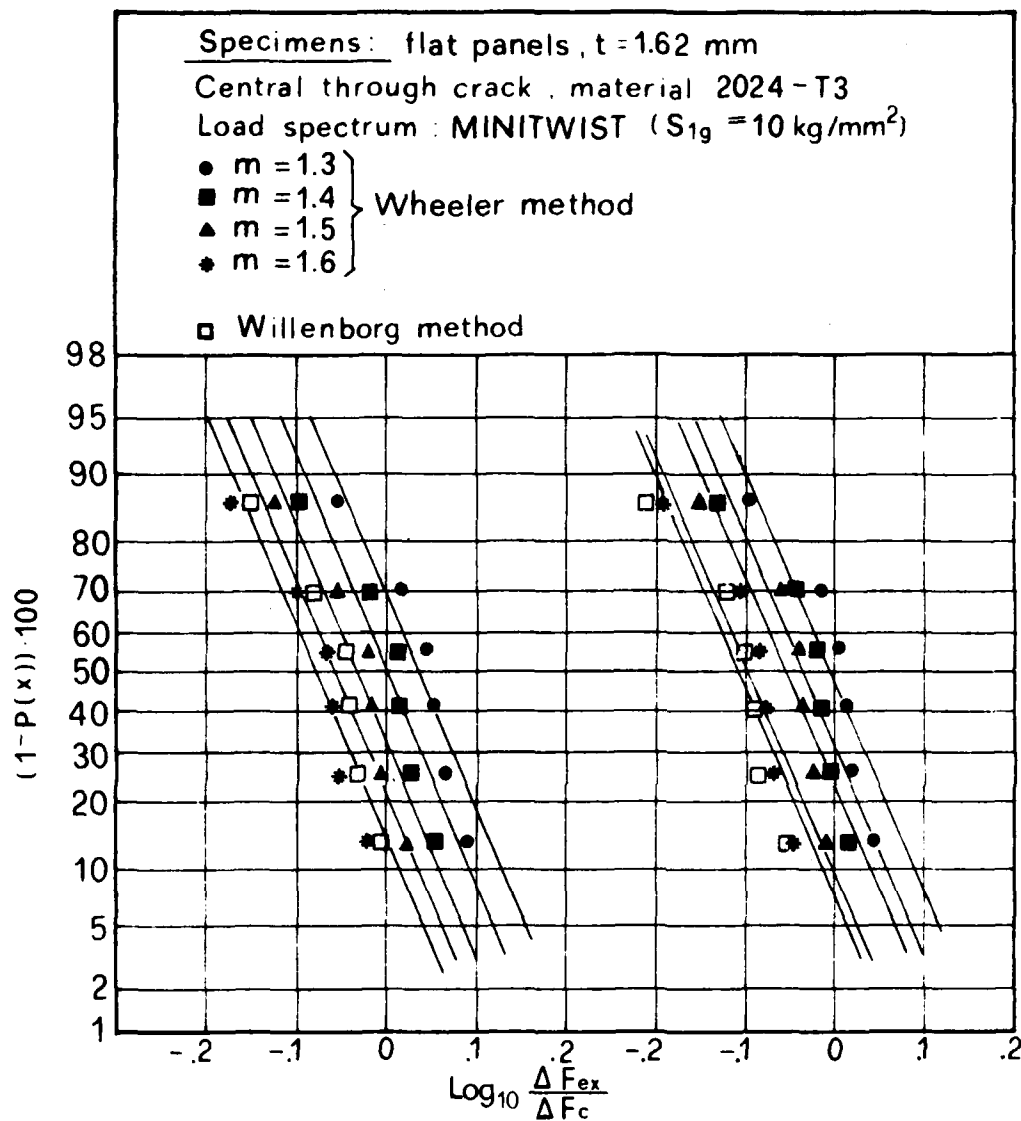


Fig.8b - Comparison of experimental data with predictions obtained with Elmes law for flat panels tests under MINITWIST spectrum loading with  $S_{1g} = 10.0 \text{ Kg/mm}^2$ .



Crack growth interval:

from  $a = 5$  mm to  $a = 15$  mm

from  $a = 5$  mm to  $a = 24$  mm

Fig.8c - Lognormal cumulative distributions of the variable  $\Delta F_{ex}/\Delta F_c$  for flat panels tests under MINITWIST spectrum loading with  $S_{1g} = 10.0 \text{ Kg/mm}^2$ .  $F_c$  has been calculated using Elnes law.

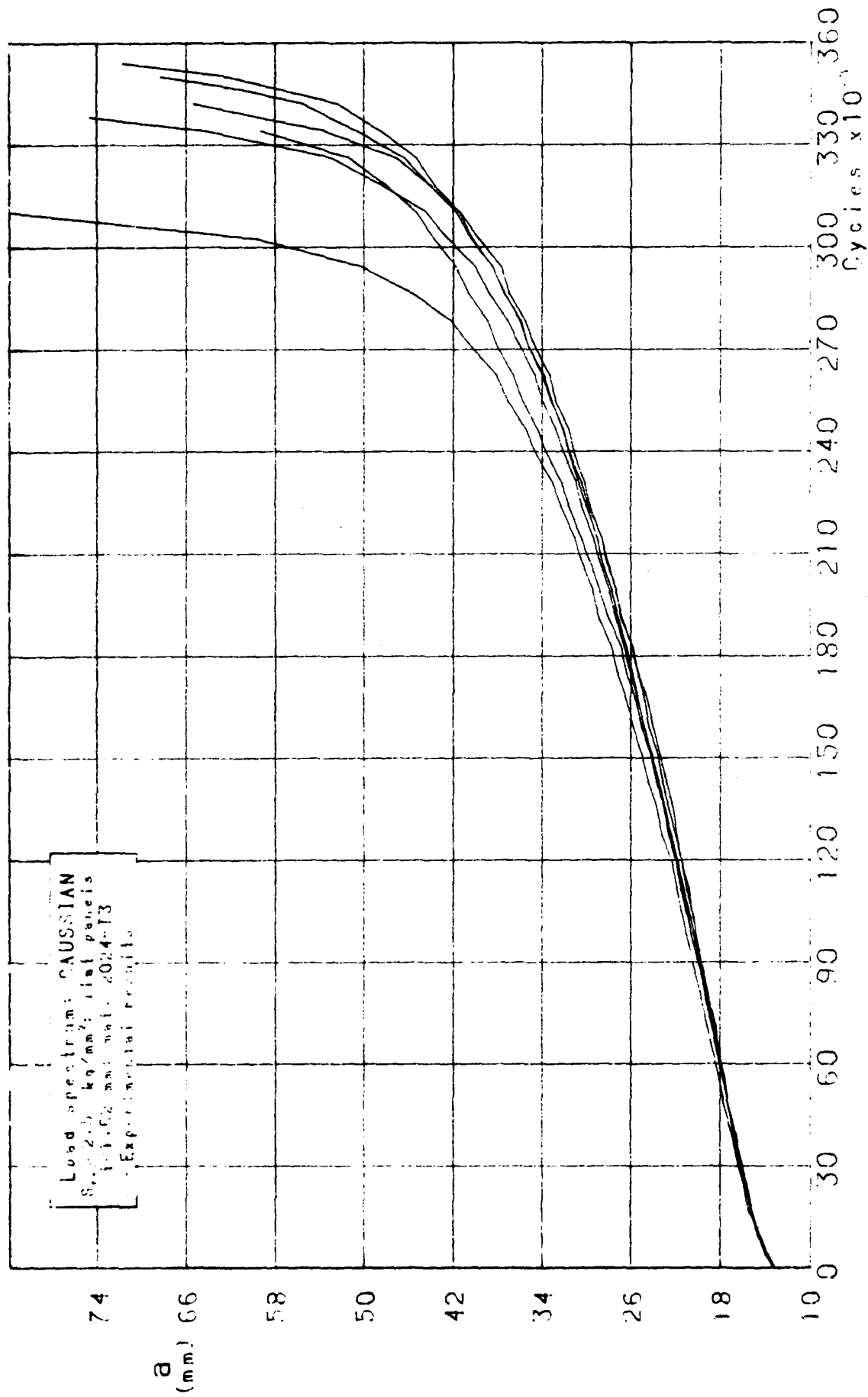


Fig.9a - Experimental results of flat panels tests under Gaussian random spectrum loading with  $S_{rms} = 2.5 \text{ kg/mm}^2$ .

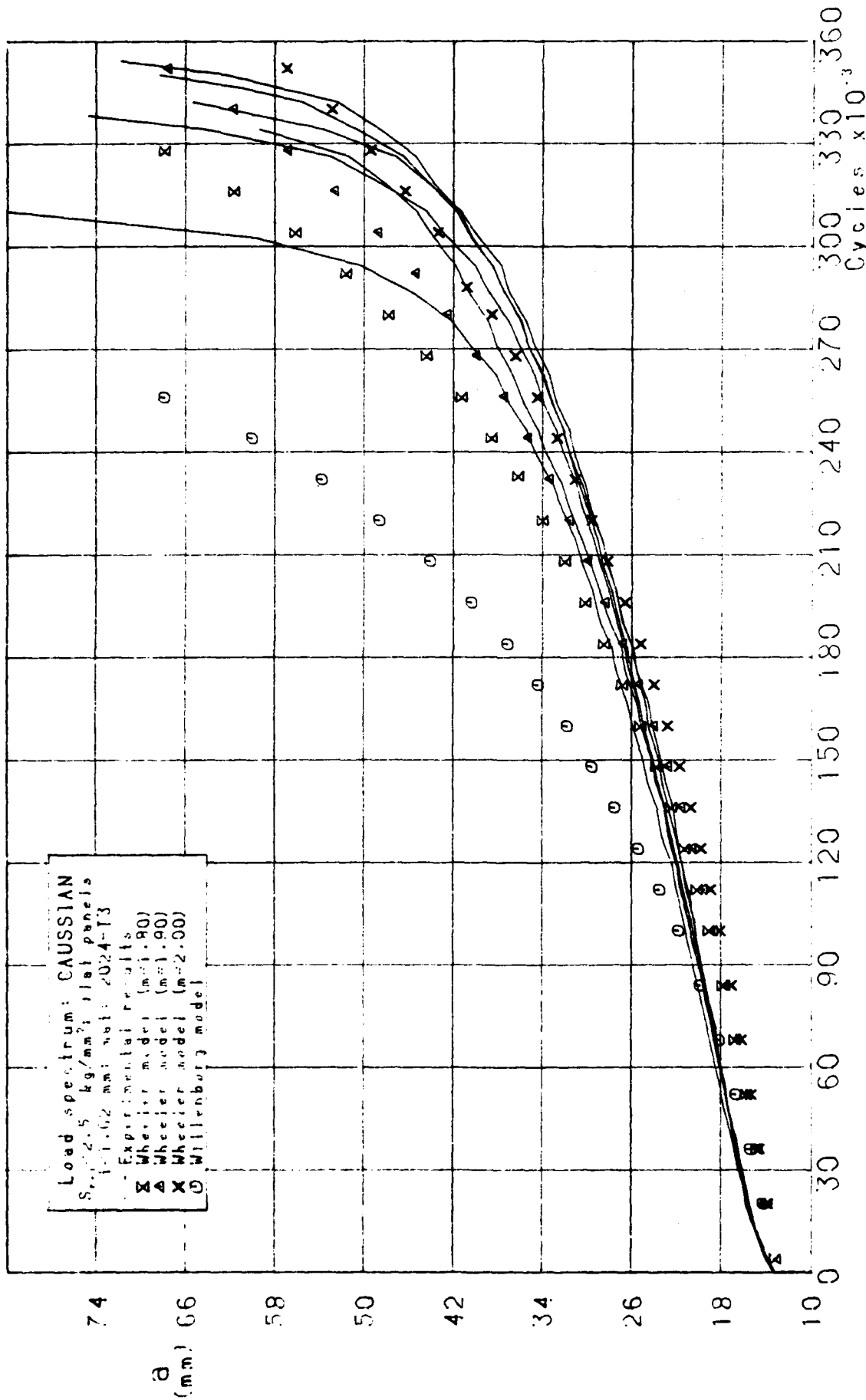
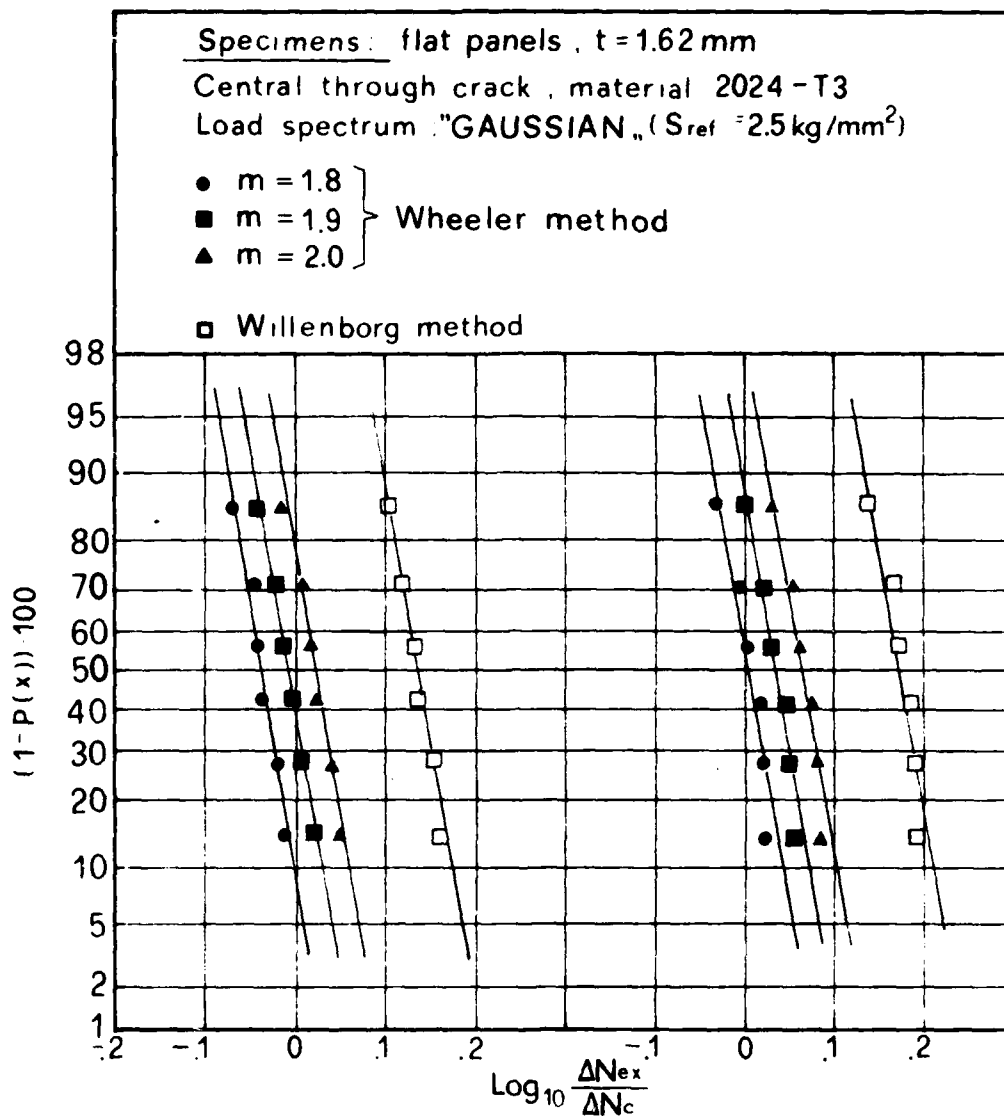


Fig.9b - Comparison of experimental data with predictions obtained with Elmes law for flat panels tests under Gaussian random spectrum loading with  $S_{rms} = 2.5 \text{ Kg/mm}^2$ .



Crack growth interval:

from  $a = 13 \text{ mm}$  to  $a = 26 \text{ mm}$       from  $a = 13 \text{ mm}$  to  $a = 42 \text{ mm}$

Fig.9c - Lognormal cumulative distributions of the variable  $\Delta N_{ex}/\Delta N_c$  for flat panels tests under Gaussian random spectrum loading with  $S_{rms} = 2.5 \text{ Kg/mm}^2$ .  $N_c$  has been calculated using Elmes law.

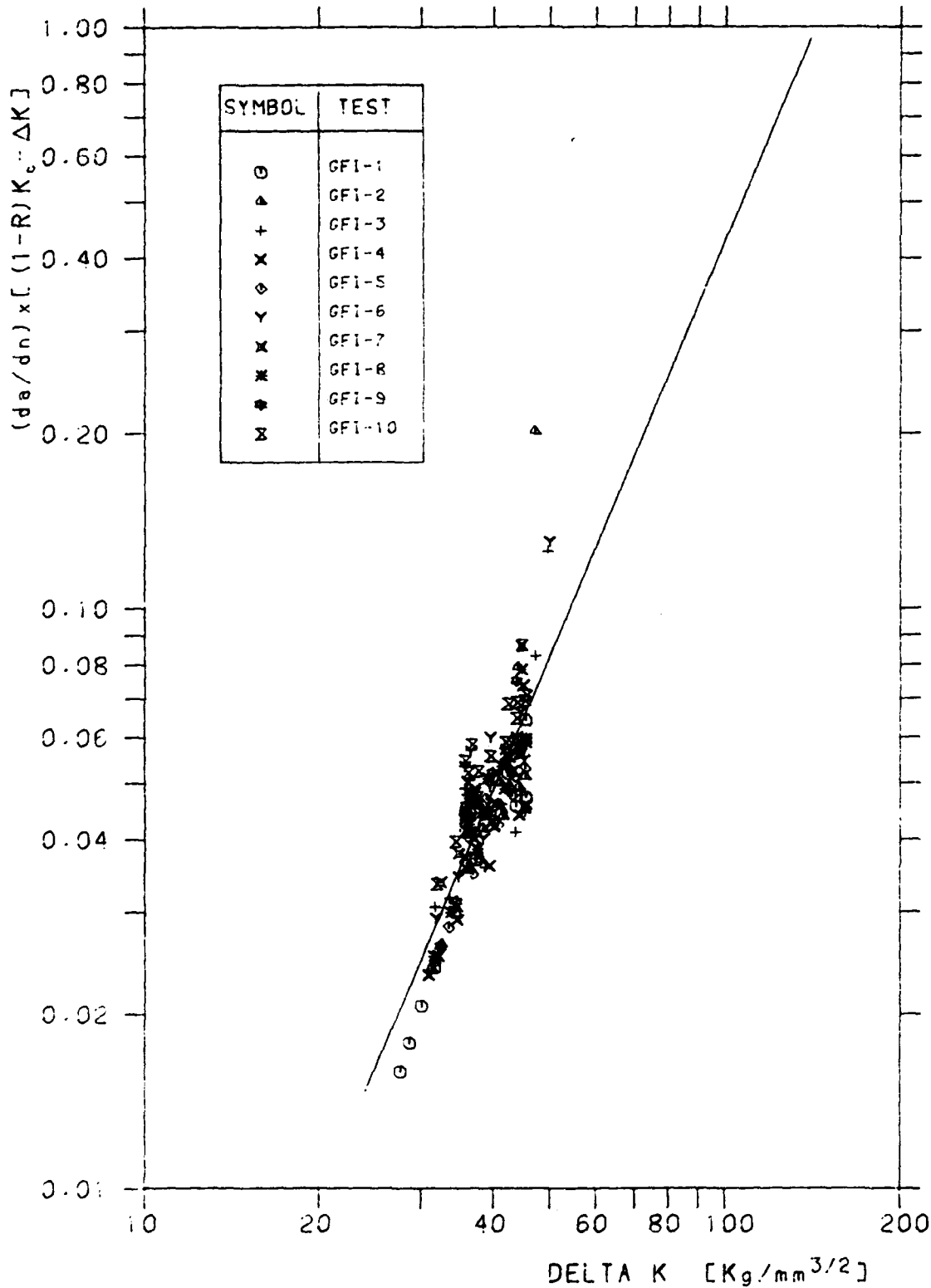


Fig.10a - Regression analysis of experimental data from constant amplitude tests on stiffened panels.  $\Delta K$  has been evaluated disregarding friction forces and assuming for the rivet flexibility parameter the value  $\xi=0.10$ .

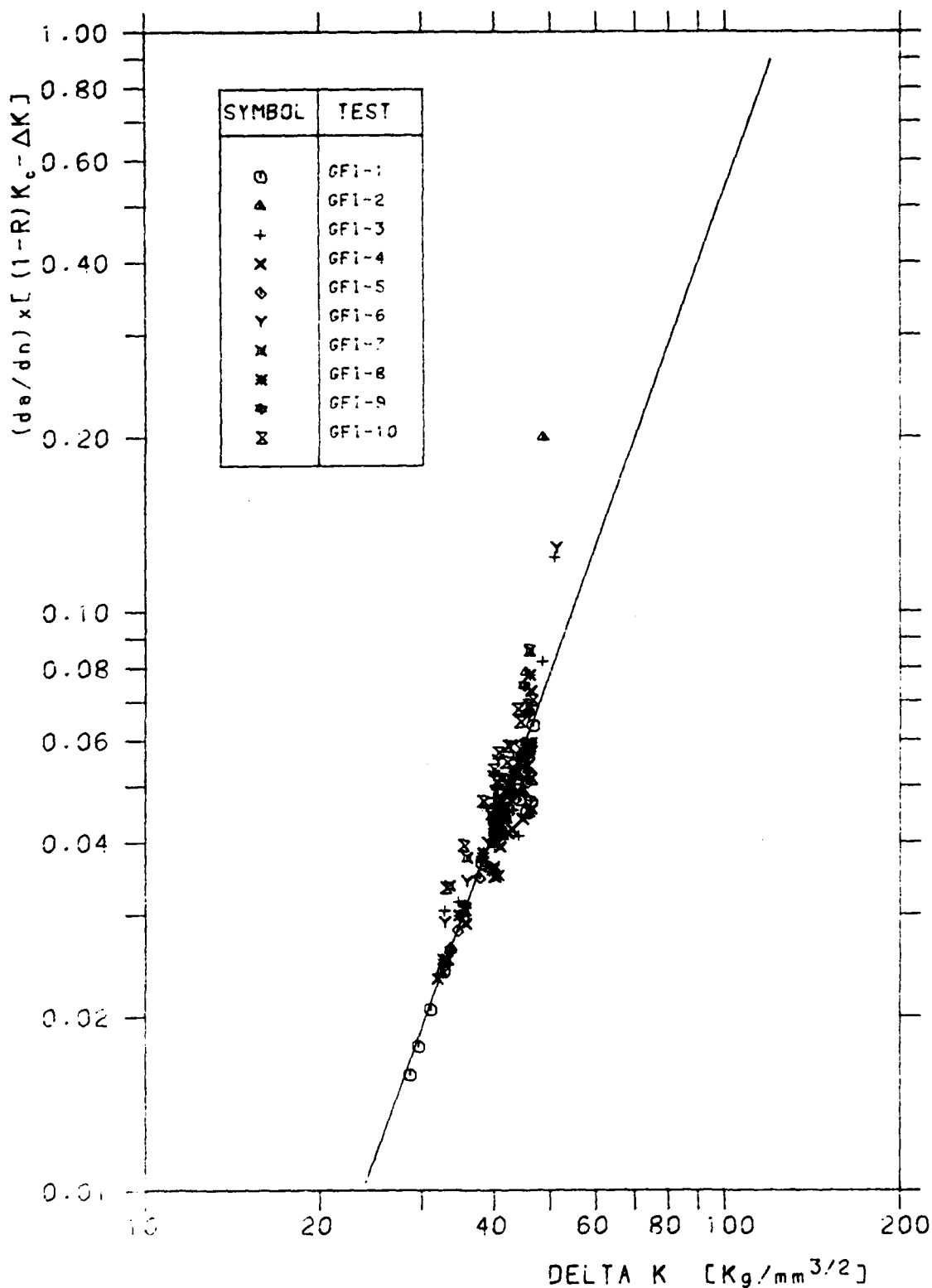


Fig.10b - Regression analysis of experimental data from constant amplitude tests on stiffened panels.  $\Delta K$  has been evaluated disregarding friction forces and assuming the optimum value  $\xi=0.30$ . The best-fit Forman's law is defined by  $C=0.1532 \times 10^{-5}$ ,  $n=2.774$ .

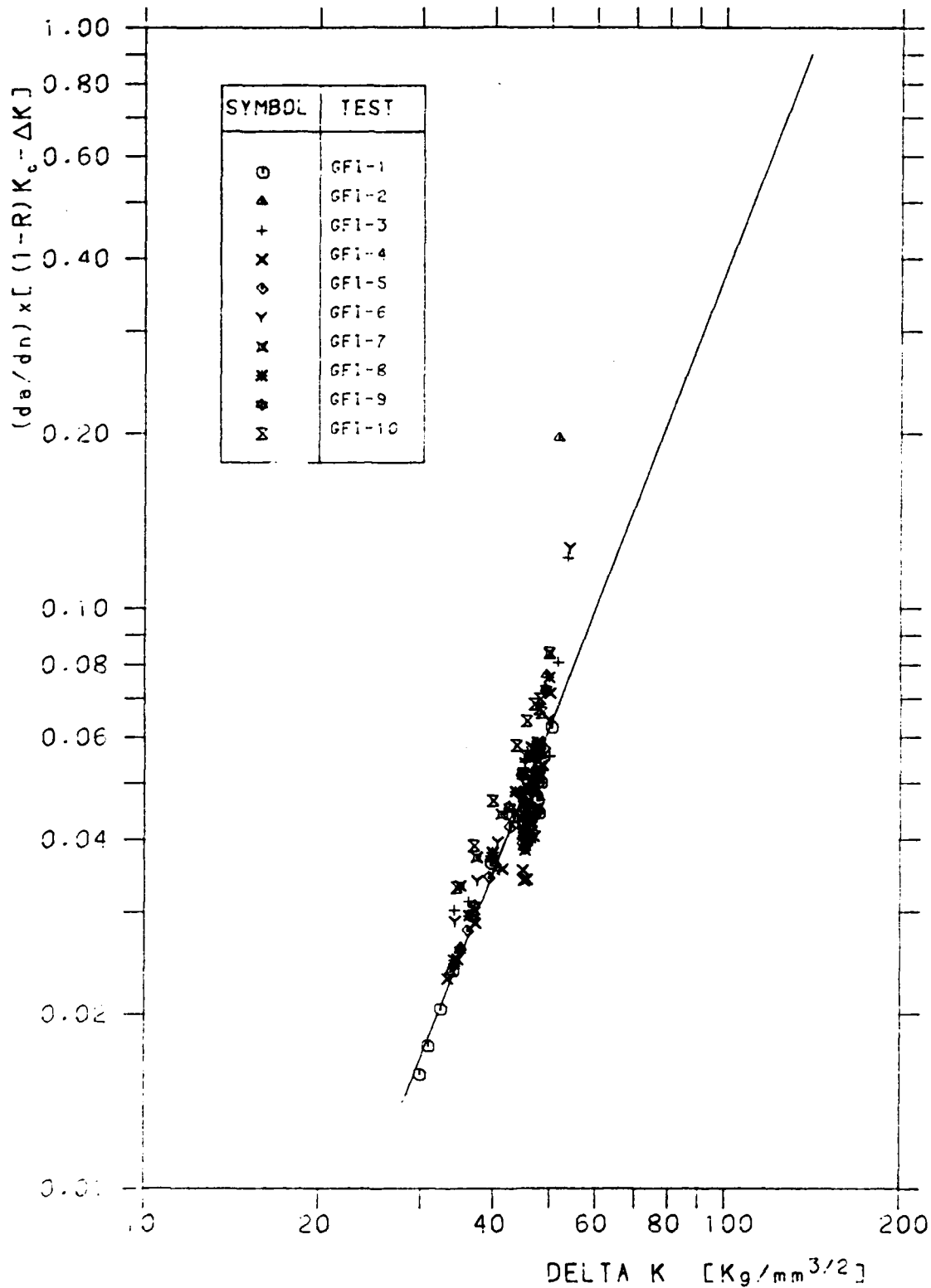


Fig.10c - Regression analysis of experimental data from constant amplitude tests on stiffened panels.  $\Delta K$  has been evaluating disregarding friction forces and assuming  $\xi=0.70$ .

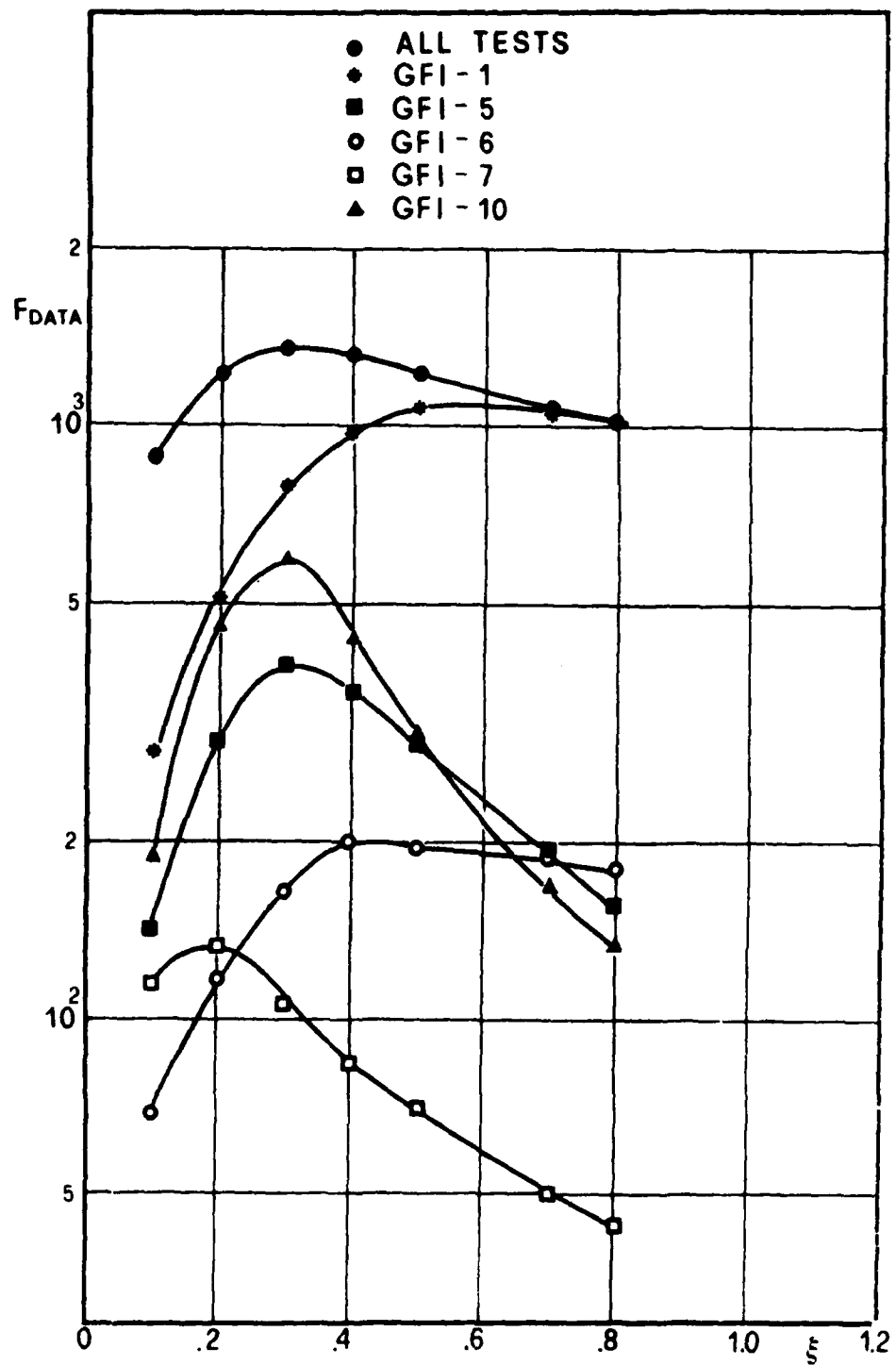
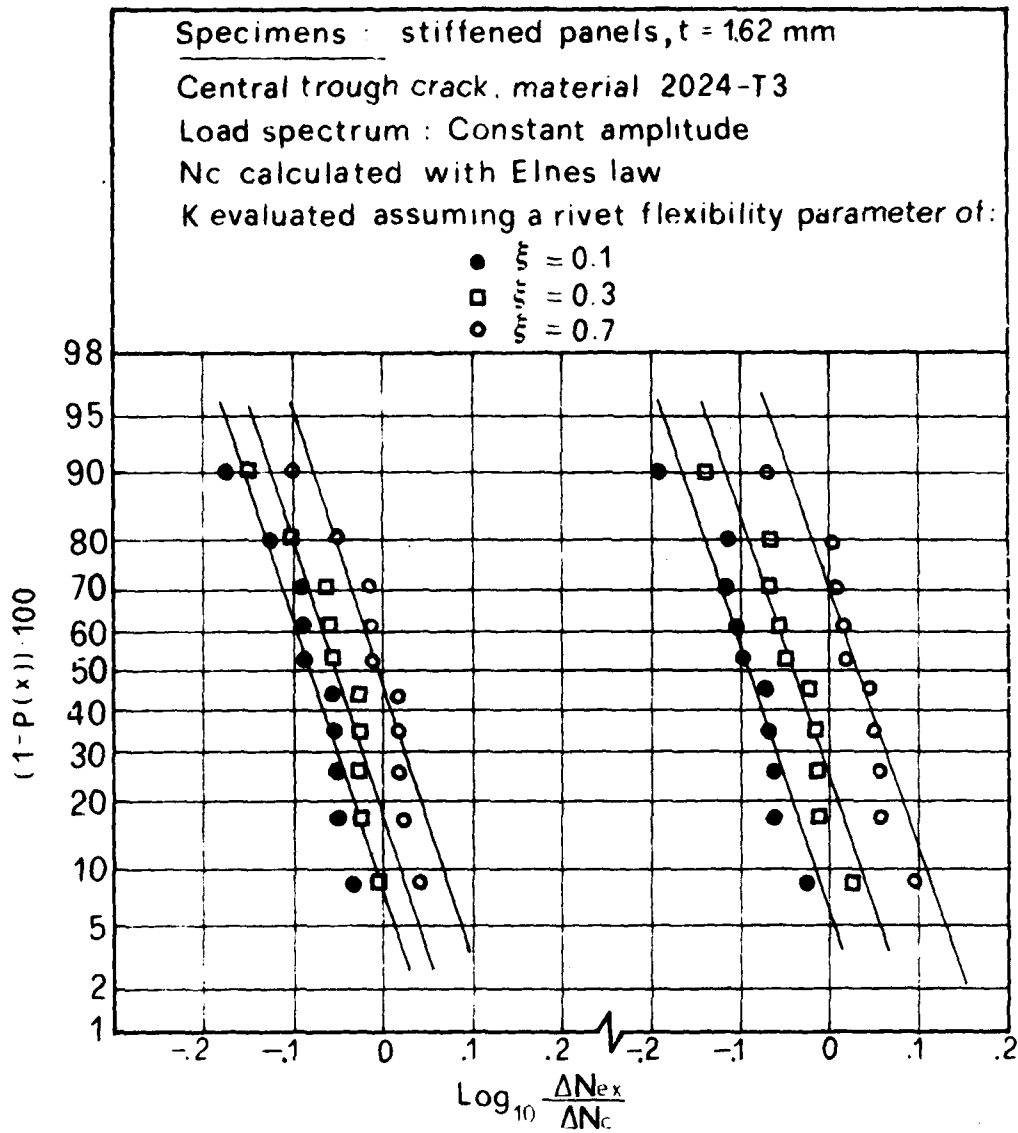


Fig.11 -  $F_{DATA}$  versus flexibility parameter  $\xi$  for some constant amplitude-stiffened panels tests.



Crack growth interval

from  $a = 25$  mm to  $a = 45$  mm      from  $a = 25$  mm to  $a = 75$  mm

Fig.12 - Lognormal cumulative distributions of the variable  $\Delta N_{ex}/\Delta N_c$  for stiffened panels tests under constant amplitude loading.  $N_c$  has been calculated using Forman's law and assuming different values of the rivet flexibility.

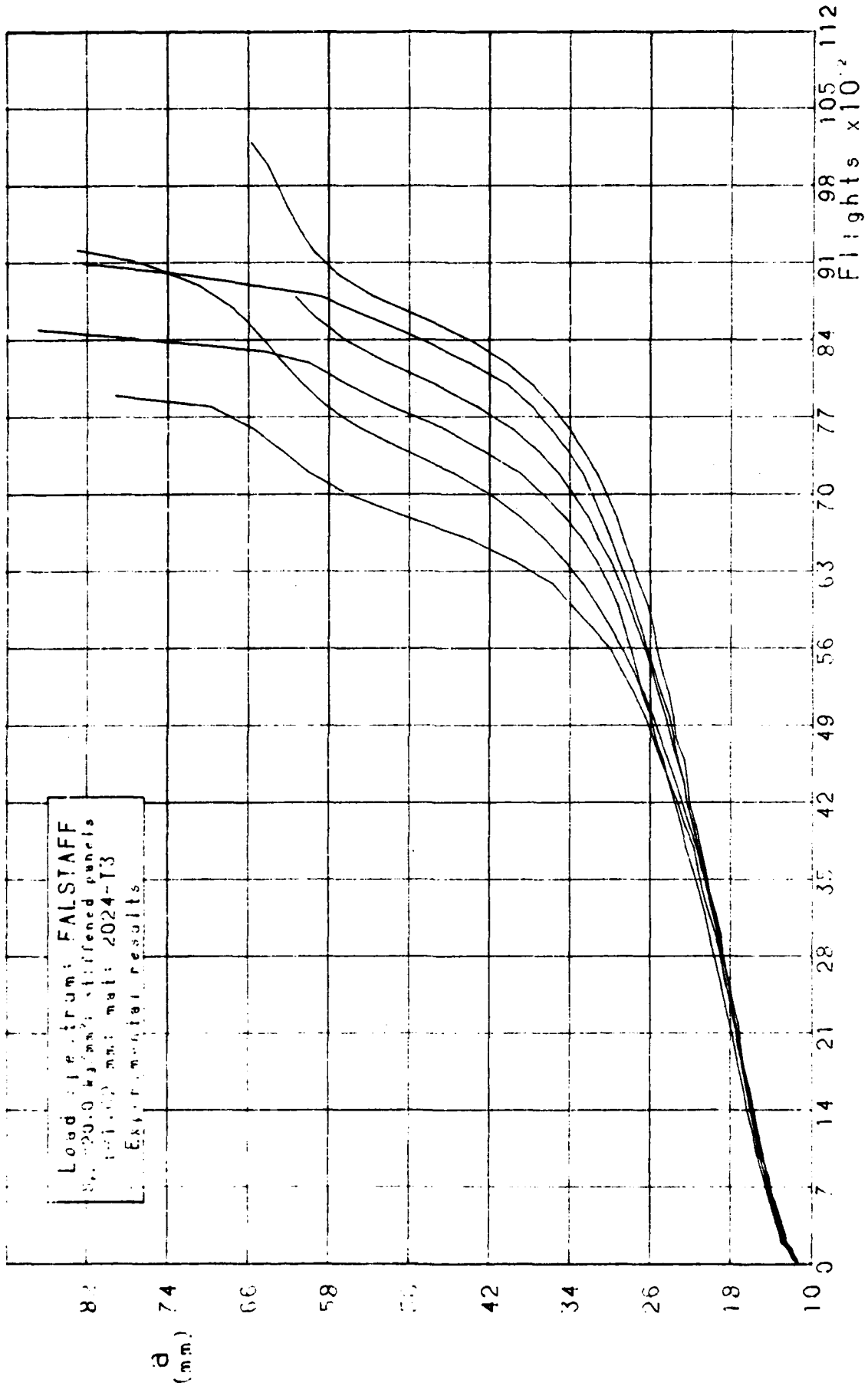


Fig.13a - Experimental results of built-up panels tests under FALSTAFF spectrum loading with  $S_{max} = 20.0 \text{ kg/mm}^2$ .

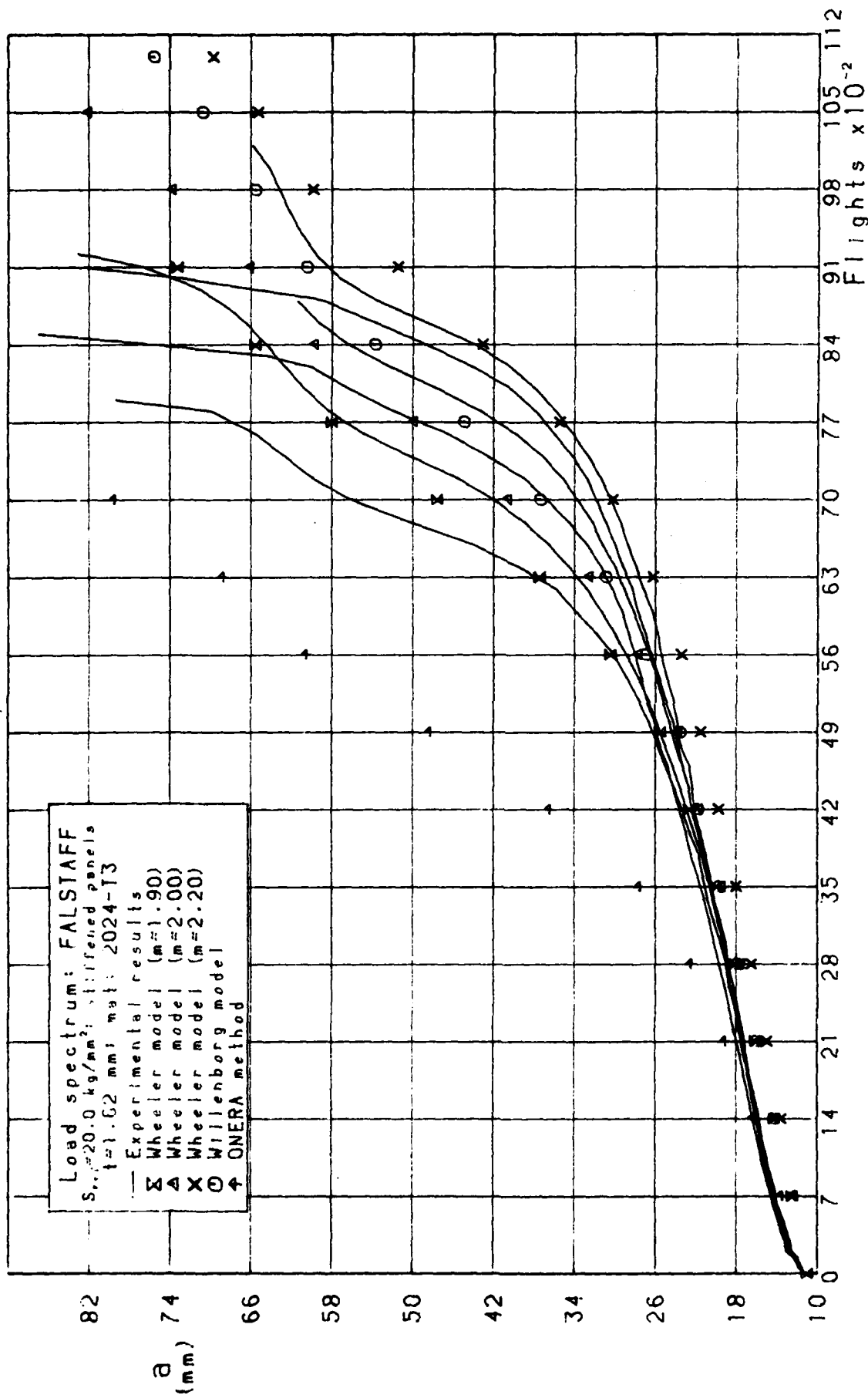
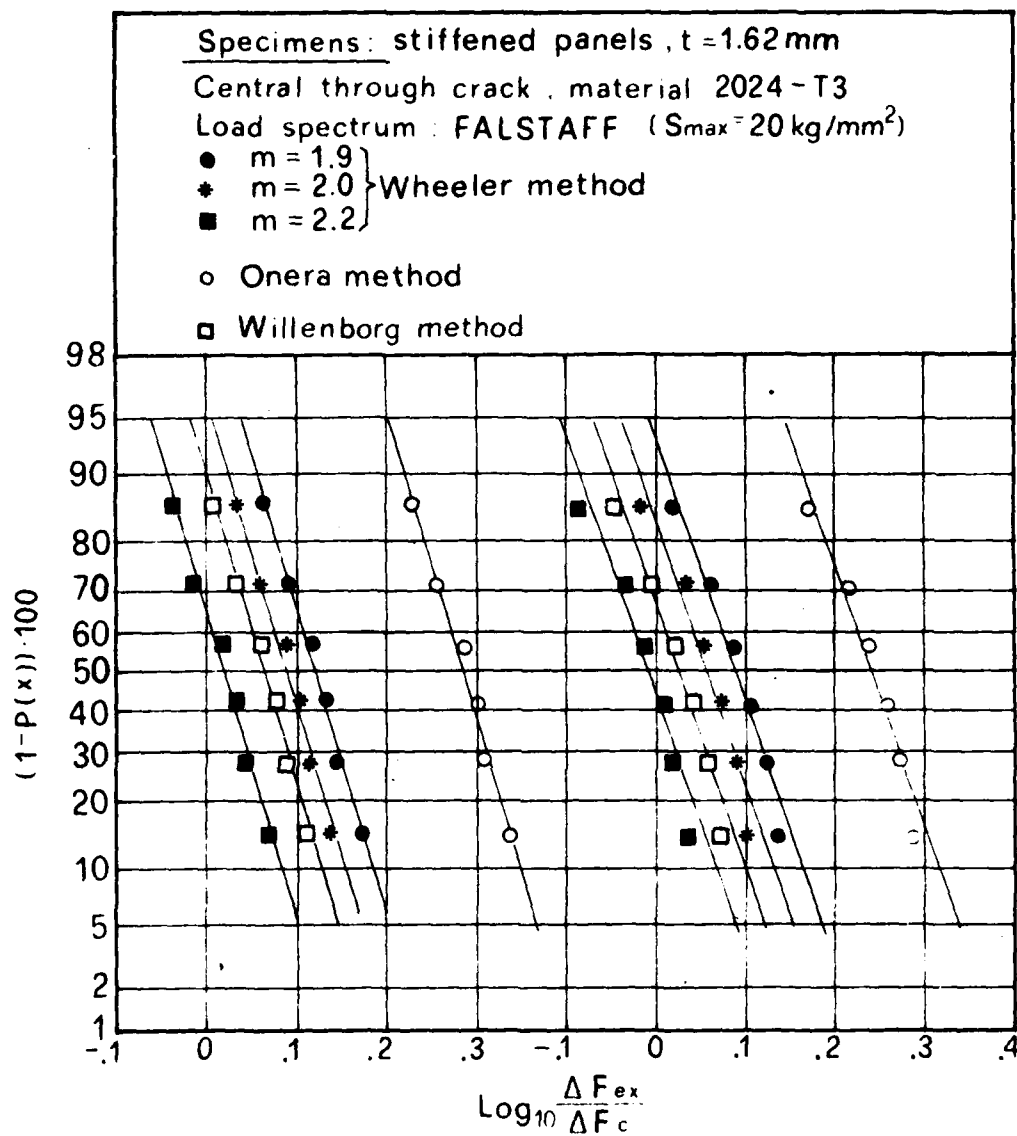


Fig.13b - Comparison of experimental results with predictions obtained with Forman's law for built-up panels tests under FALSTAFF spectrum loading with  $S_{max}=20.0 \text{ Kg/mm}^2$ .



Crack growth interval :

from  $a = 14 \text{ mm}$  to  $a = 30 \text{ mm}$       from  $a = 14 \text{ mm}$  to  $a = 50 \text{ mm}$

Fig.13c - Lognormal cumulative distributions of the variable  $\Delta F_{ex}/\Delta F_c$  for built-up panels tests under FALSTAFF spectrum loading with  $S_{\max} = 20.0 \text{ Kg/mm}^2$ .  $F_c$  has been calculated using the Forman's law of built-up panels.

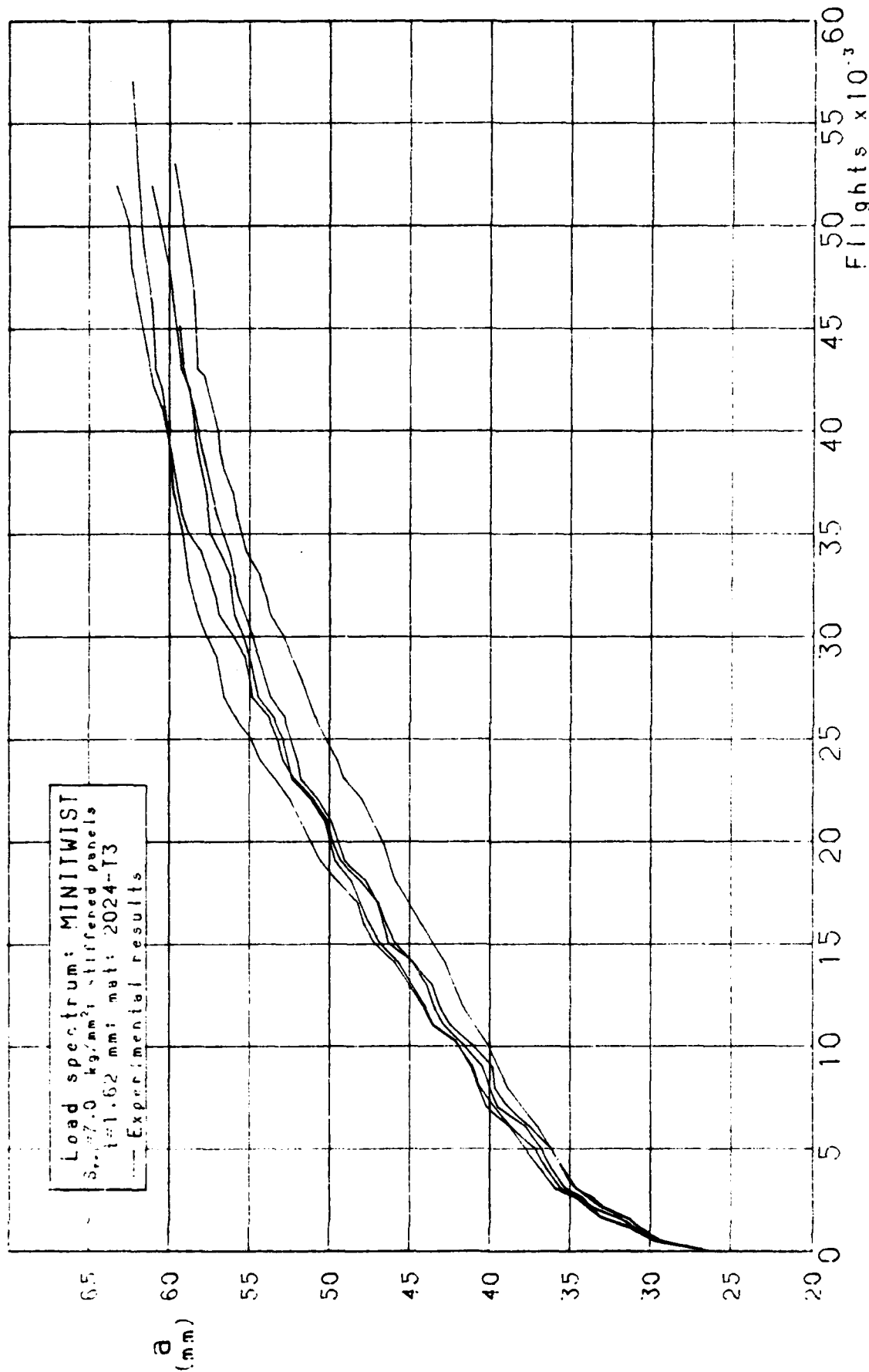


Fig.14a - Experimental results of built-up panels tests under MINITWIST spectrum loading with  $S_{ig}=7.0 \text{ Kg/mm}^2$ .

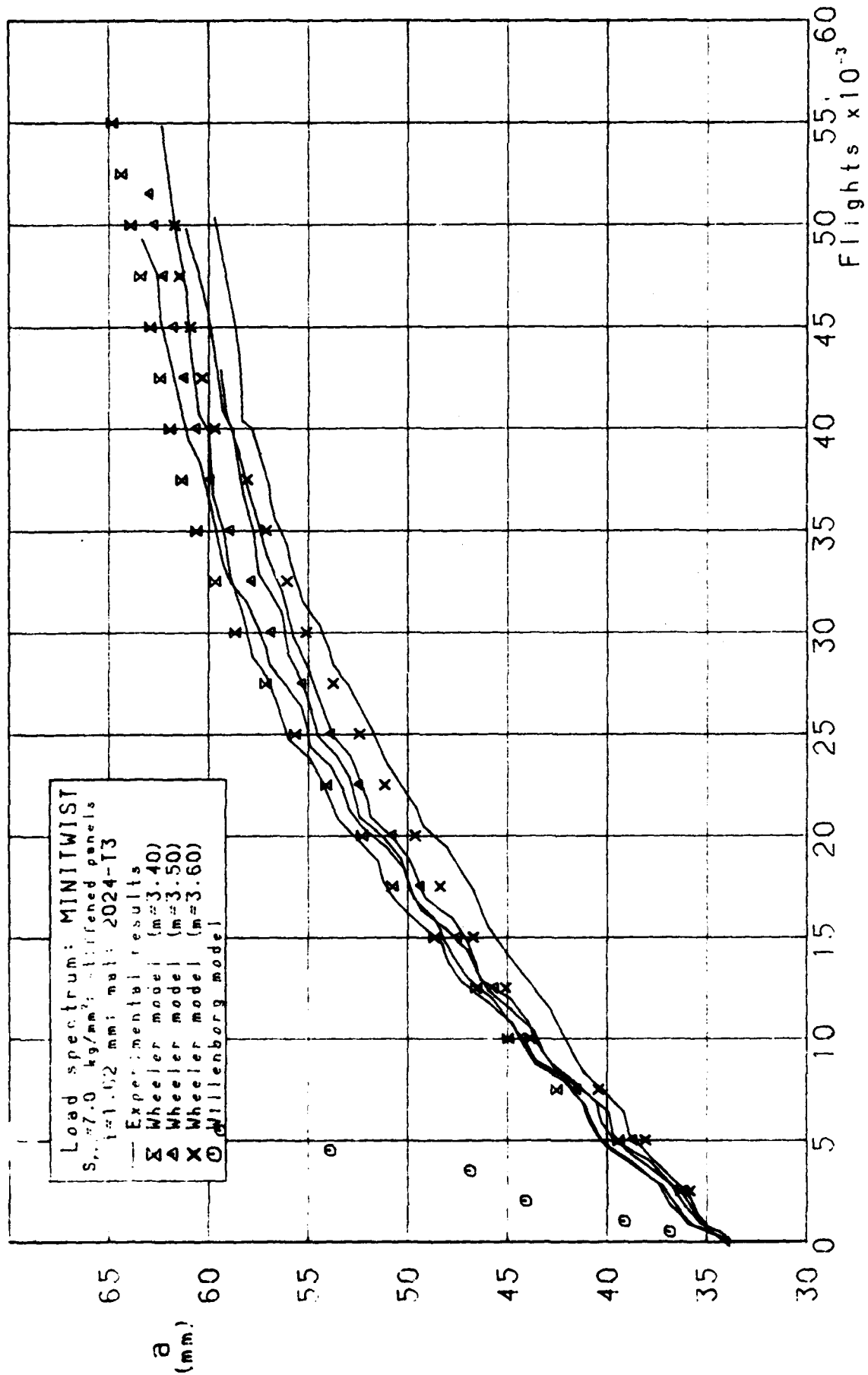
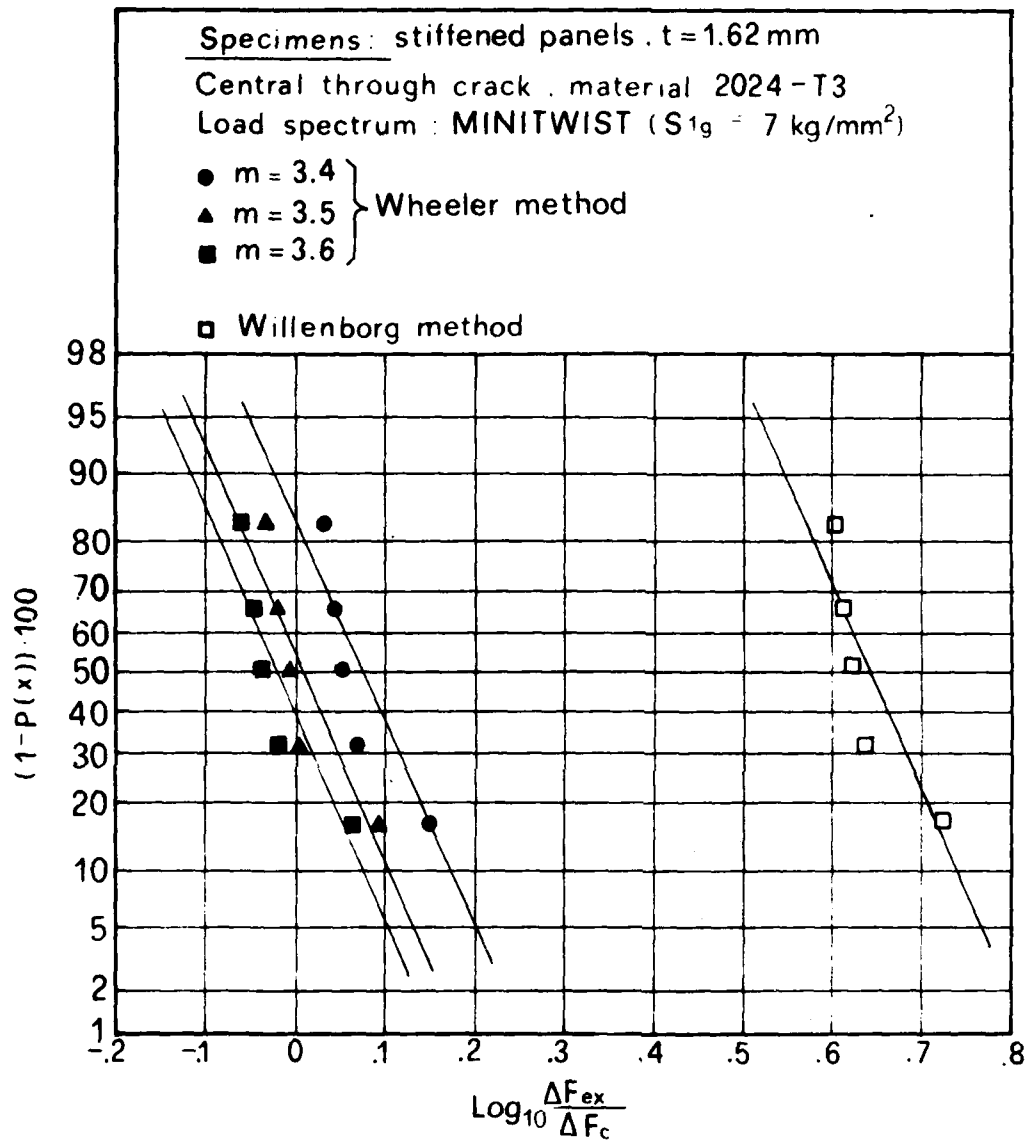
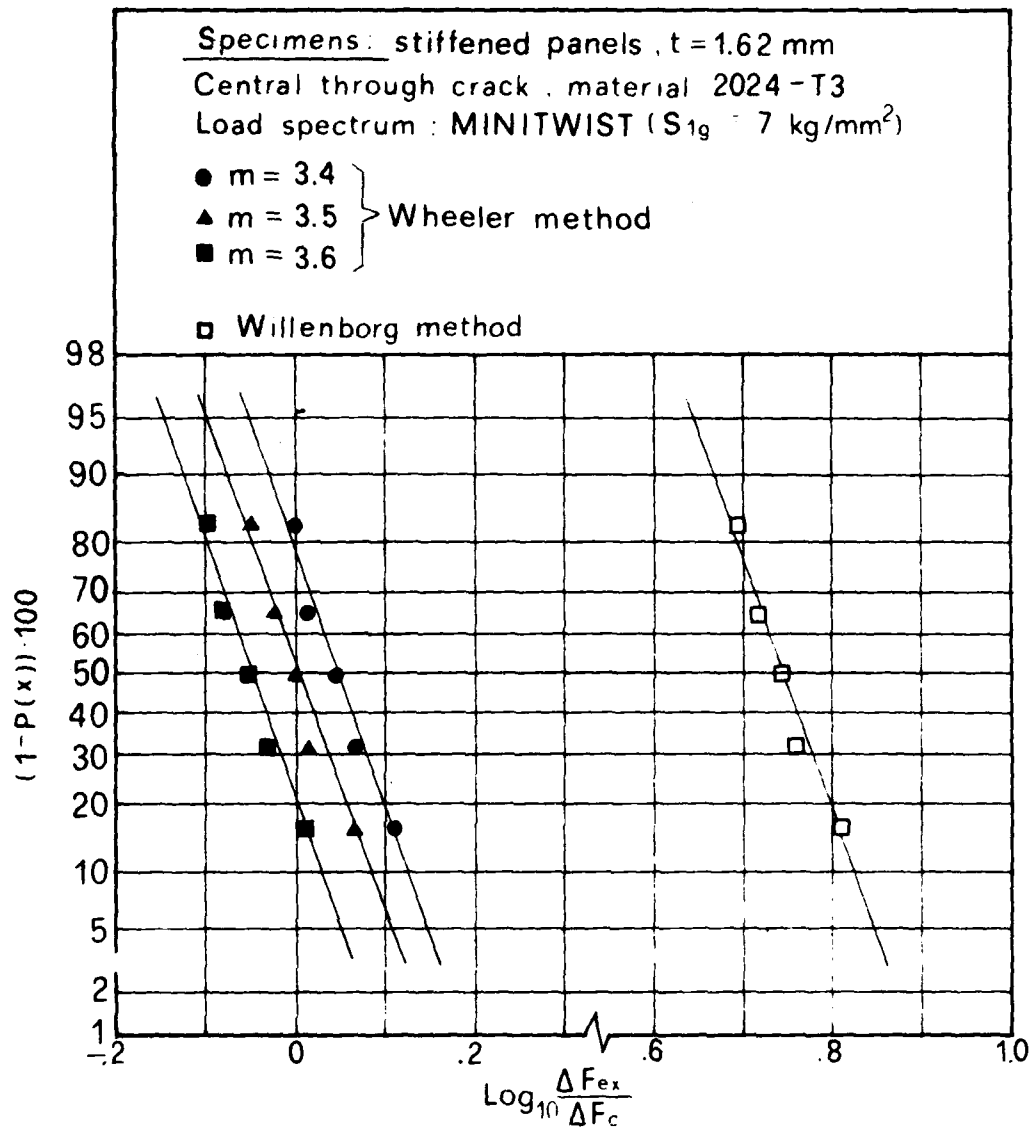


Fig. 14b - Comparison of experimental results with predictions obtained with Forman's law for stiffened panels tests under MINITWIST spectrum loading with  $S_0 = 7.0 \text{ Kg/mm}^2$ .



Crack growth interval : from  $a = 34 \text{ mm}$  to  $a = 45 \text{ mm}$

Fig.14c - Lognormal cumulative distributions of the variable  $\Delta F_{ex}/\Delta F_c$  for stiffened panels tests under MINITWIST spectrum loading with  $S_{1g} = 7.0 \text{ Kg/mm}^2$ .  $F_c$  has been calculated using the Forman's law of stiffened panels.



Crack growth interval: from  $a = 34$  mm to  $a = 55$  mm

Fig.14c - Concluded.

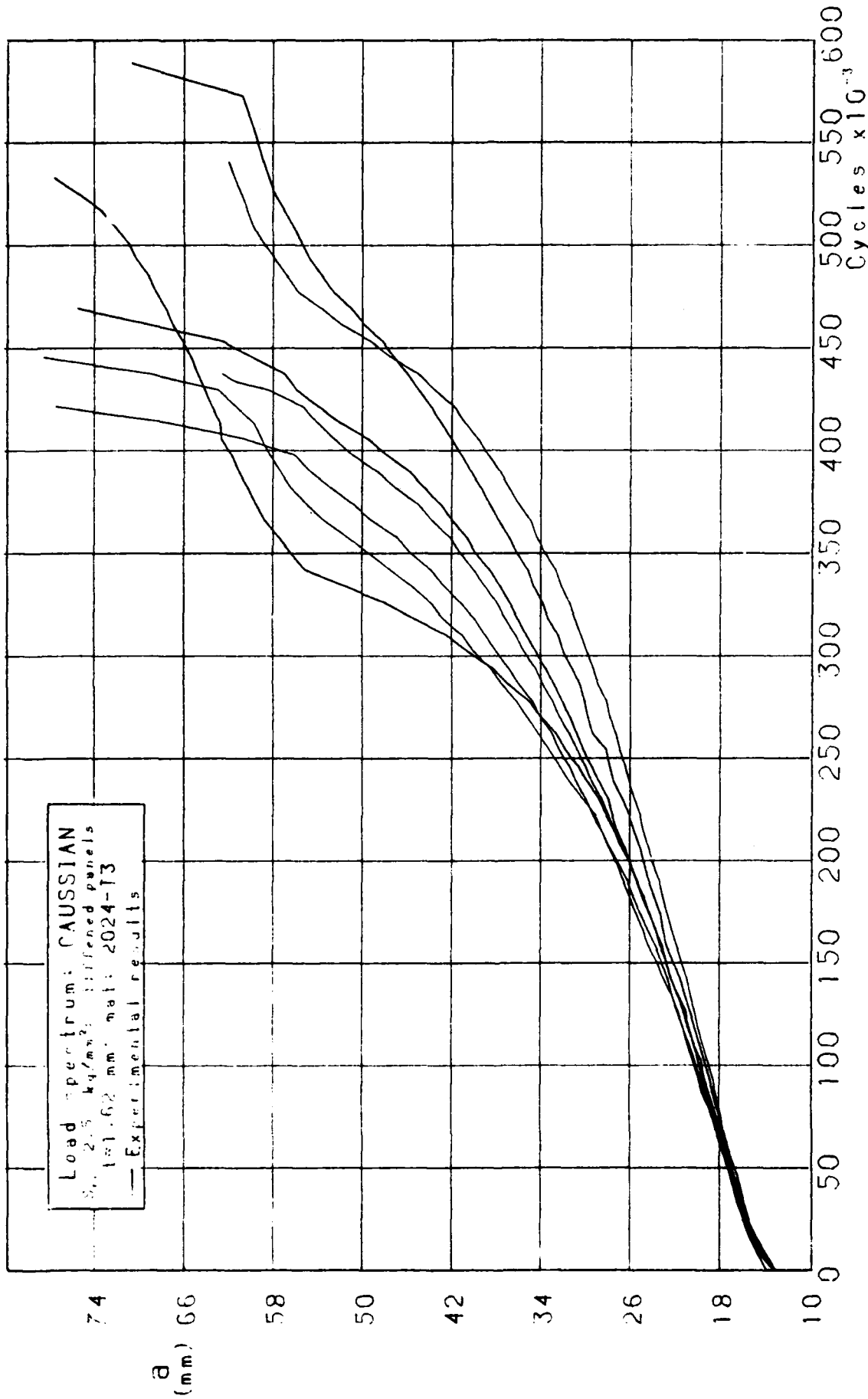


Fig.15a - Experimental results of built-up panels tests under Gaussian random spectrum loading with  $S_{rms} = 2.5 \text{ kg/mm}^2$ .

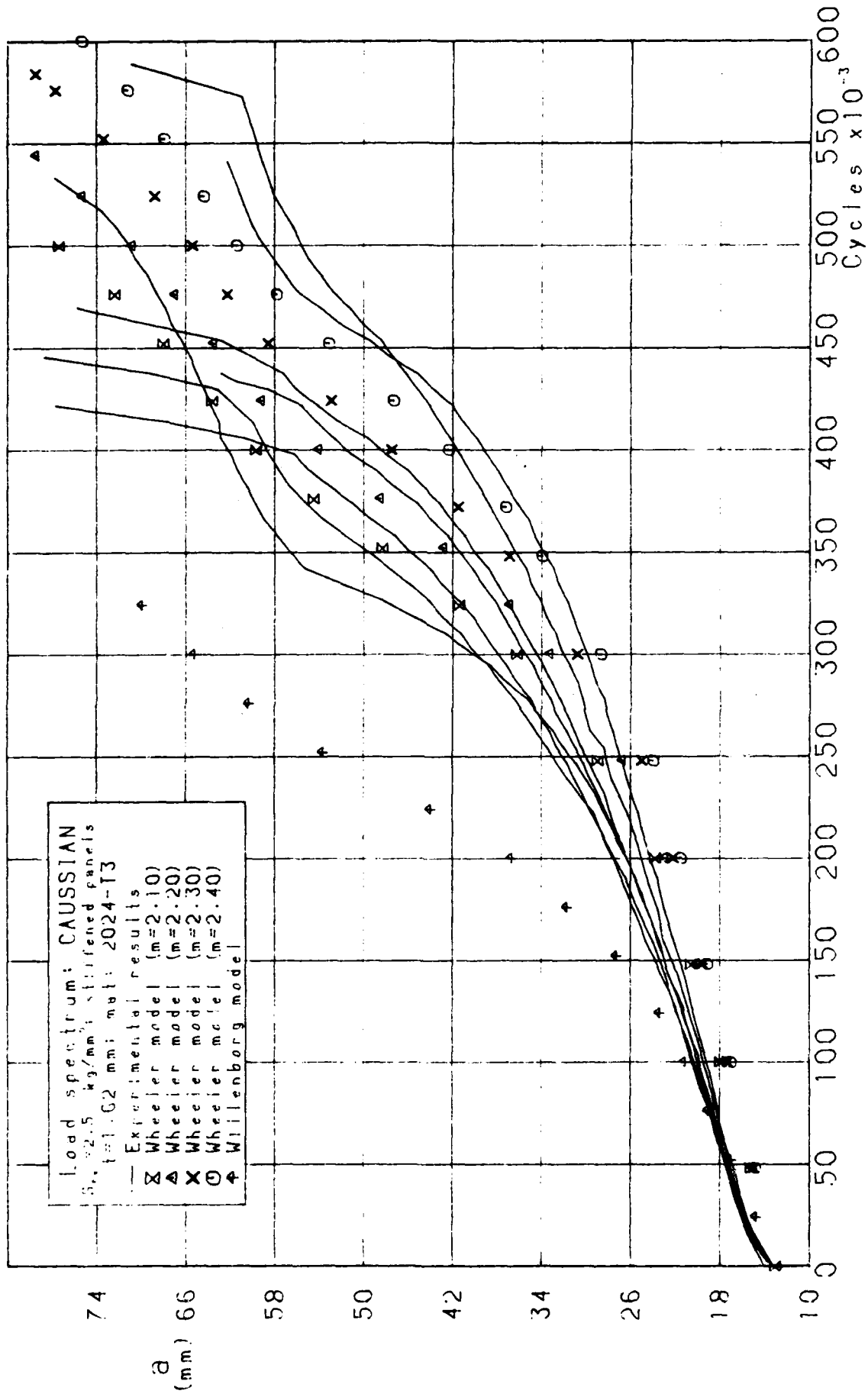
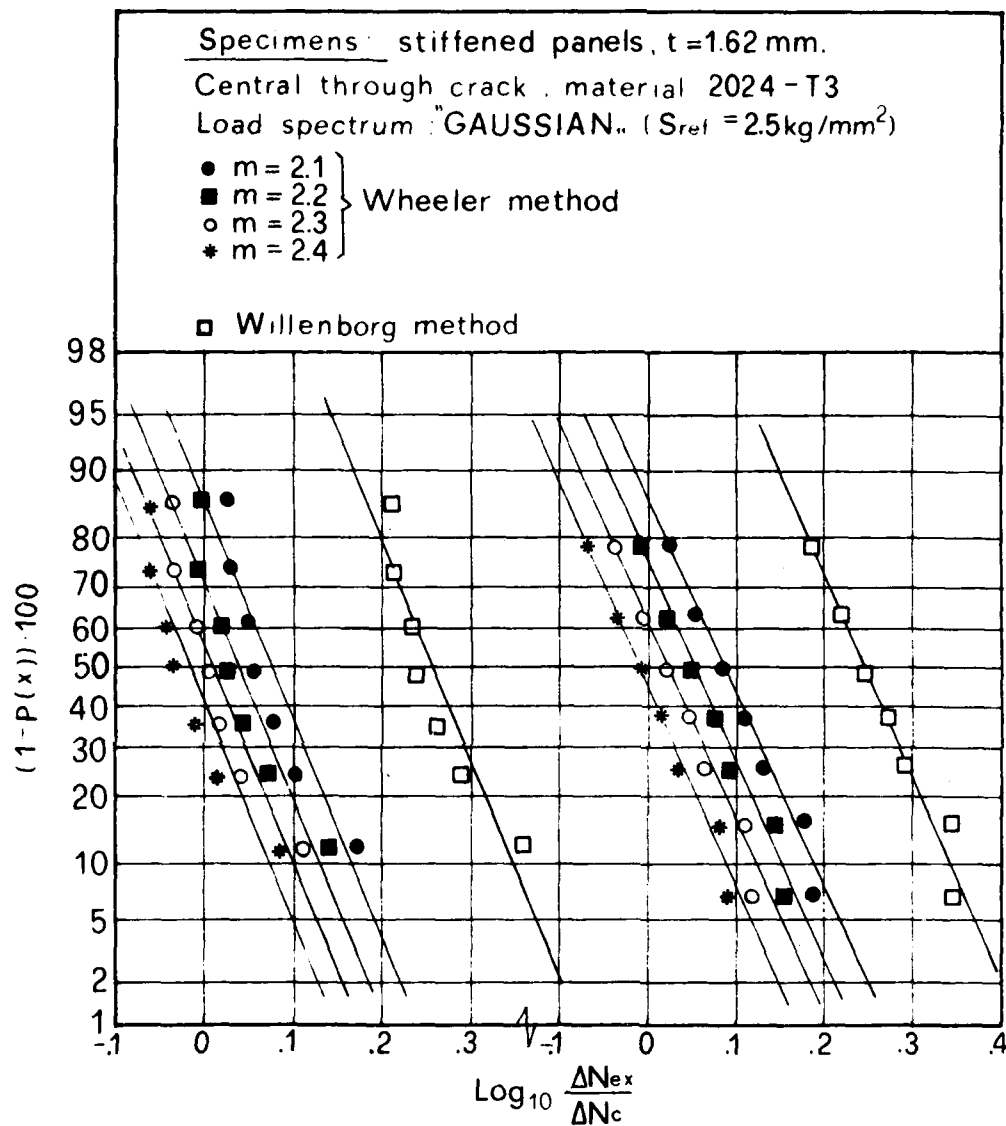


Fig.15b - Comparison of experimental results with predictions obtained with Forman's law for stiffened panels tests under Gaussian random spectrum loading with  $S_{rms}=2.5 \text{ Kg/mm}^2$ .

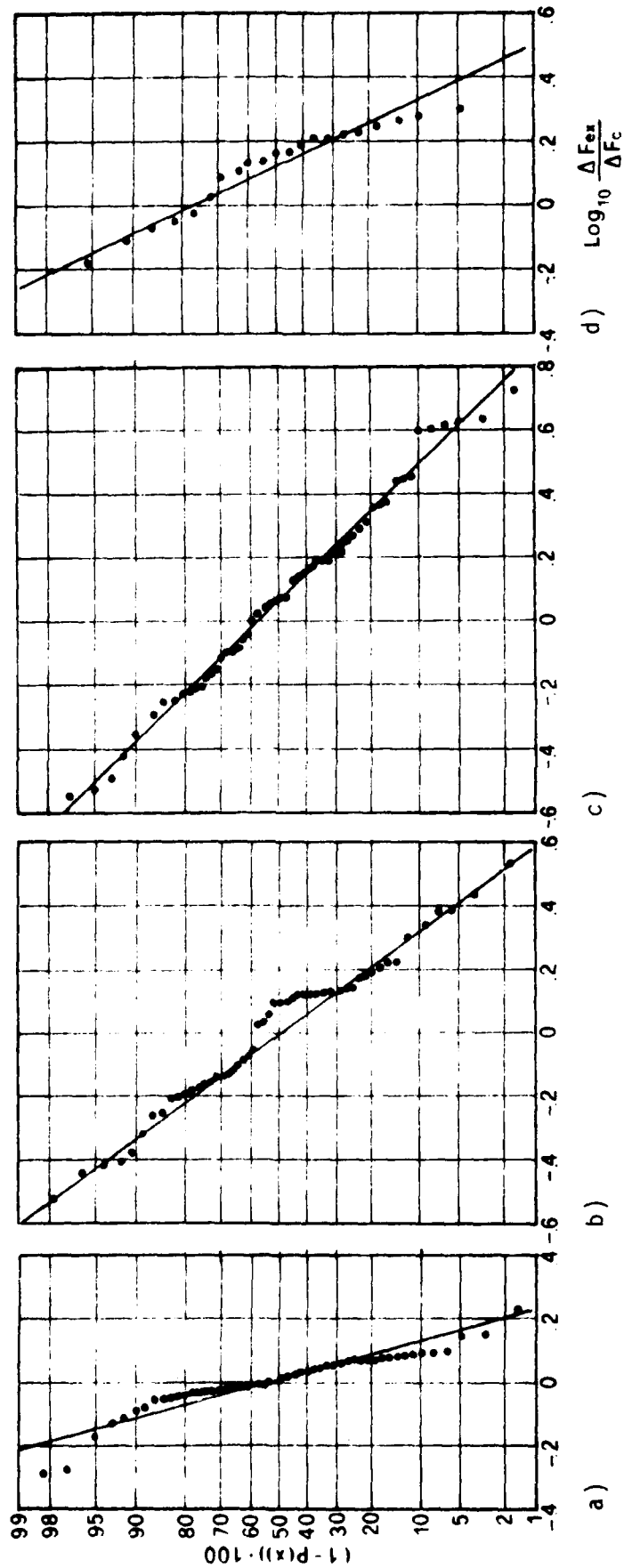


Crack growth interval :

from  $a = 16$  mm to  $a = 30$  mm

from  $a = 16$  mm to  $a = 50$  mm

Fig.15c - Lognormal cumulative distributions of the variable  $\Delta N_{ex}/\Delta N_c$  for stiffened panels tests under Gaussian random spectrum loading with  $S_{rms} = 2.5 \text{ Kg/mm}^2$ .  $N_c$  has been calculated using the Forman's law of stiffened panels.



Figs.16 - Comparison of variable amplitude tests results with predictions obtained according to various retardation methods. Lognormal distributions of the variable  $\Delta F_{ex}/\Delta F_c$ .

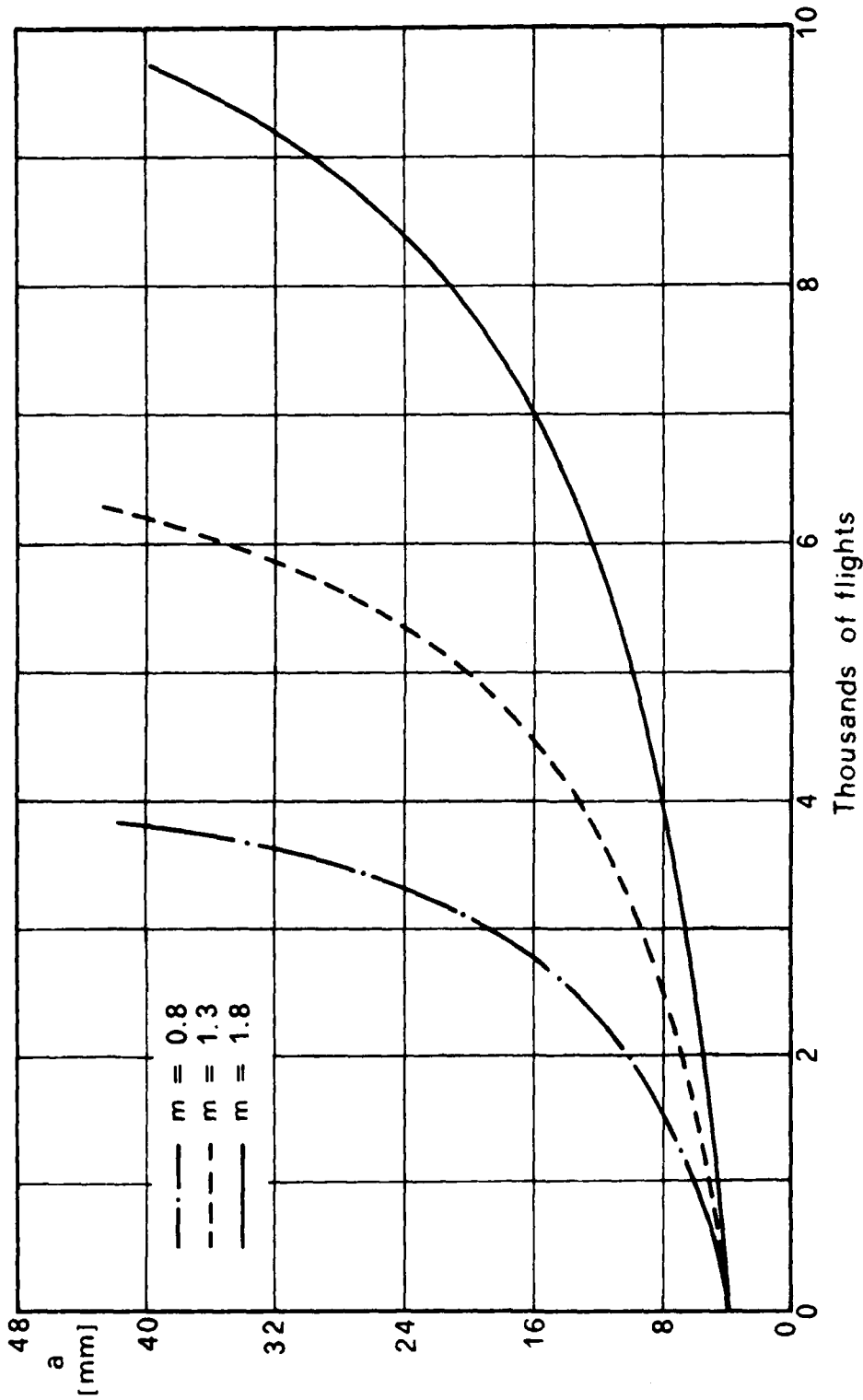


Fig.17 - Predictions sensibility to the Wheeler's plastic zone parameter. The curves are relevant to flat panels subjected to FALSTAFF spectrum loading with  $S_{max} = 24.0 \text{ Kg/mm}^2$ .

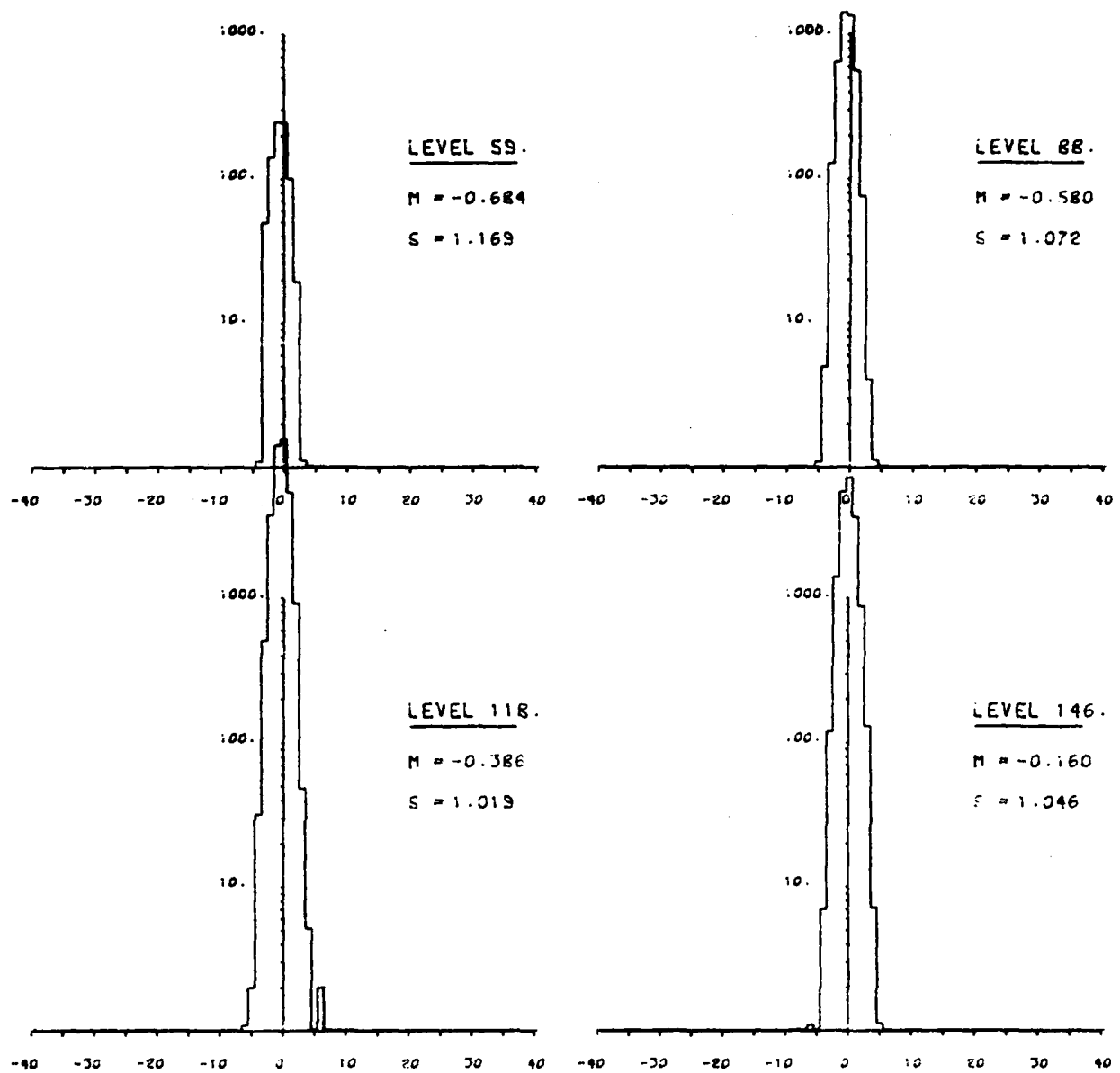


Fig.18 - A sample histogram of error occurrences in the fatigue machine setting up phase for variable amplitude loading tests.

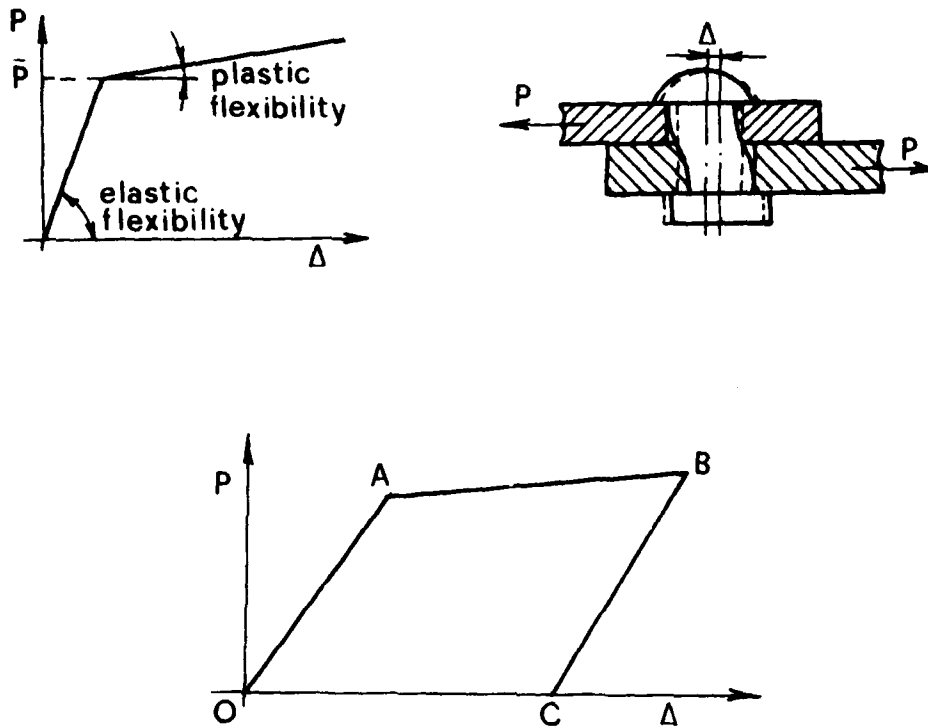
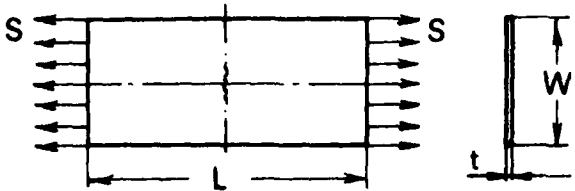
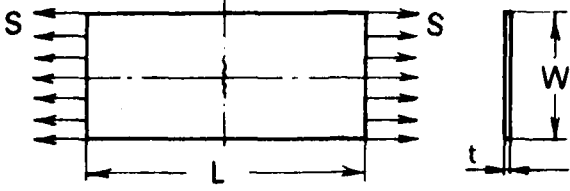


Fig.19 - The model adopted for the description of the rivet elasto-plastic behaviour.

FLAT PANELS					
					
TYPE	W mm	L mm	t mm	n. panels	
				2024-T3	7075-T6
F <sub>2</sub>	400	500	1.62	10	0

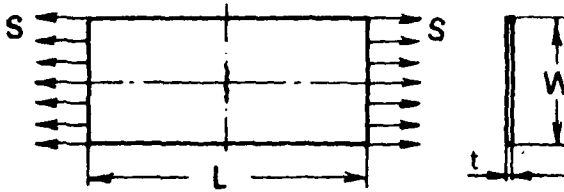
TEST	panel type	a <sub>0</sub> mm	S max kg/mm <sup>2</sup>	R	material
GFL6	F <sub>2</sub>	5.0	7.0	-0.40	2024-T3
GFL1	"	"	"	0.00	"
GFL5	"	6.0	6.0	0.00	"
GFL7	"	5.0	7.0	0.00	"
GFL4	"	8.0	"	0.20	"
GFL2	"	16.0	6.94	0.40	"
GFL10	"	24.0	7.0	0.60	"
GFL13	"	35.0	10.0	0.70	"
GFL12	"	40.0	"	0.75	"
GFL11	"	44.0	"	0.80	"

Tab.1a - Main characteristics of the constant amplitude-flat panels tests.

FLAT PANELS					
					
TYPE	W mm	L mm	t mm	n. panels	
				2024-T3	7075-T6
F <sub>2</sub>	400	500	1.62	18	0

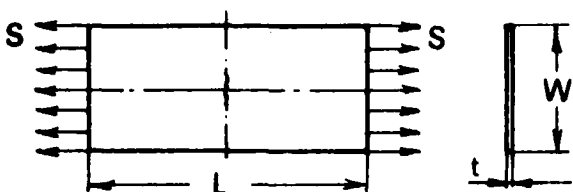
TEST	panel type	a <sub>0</sub> mm	spectrum	S <sub>ref</sub> kg/mm <sup>2</sup>	material
GFF1	F <sub>2</sub>	15.0	FALSTAFF	20.0	2024-T3
GFF7-D °	"	"	"	"	"
GFF7-E °	"	"	"	"	"
GFF7-F °	"	11.0	"	"	"
GFF5	"	"	"	"	"
GFF3	"	"	"	"	"
GFF6	"	"	"	"	"
GFF2	"	"	"	"	"
GFF4	"	"	"	"	"
GFF7 °	"	"	"	"	"
GFF7-A °	"	8.0	"	"	"
GFF7-B °	"	"	"	"	"
GFF7-C °	"	"	"	"	"
GFF9	"	4.0	"	24.0	"
GFF-10	"	"	"	"	"
GFF-11	"	"	"	"	"
GFF-12	"	"	"	"	"
GFF-13	"	"	"	"	"

Tab.1b - Main characteristics of FALSTAFF spectrum tests on flat panels. The tests indicated with (°) are those relevant to the supplementary research activity outlined in section 4.

FLAT PANELS					
					
TYPE	W mm	L mm	t mm	n. panels	
				2024-T3	7075-T6
F <sub>2</sub>	400	500	1.62	12	0

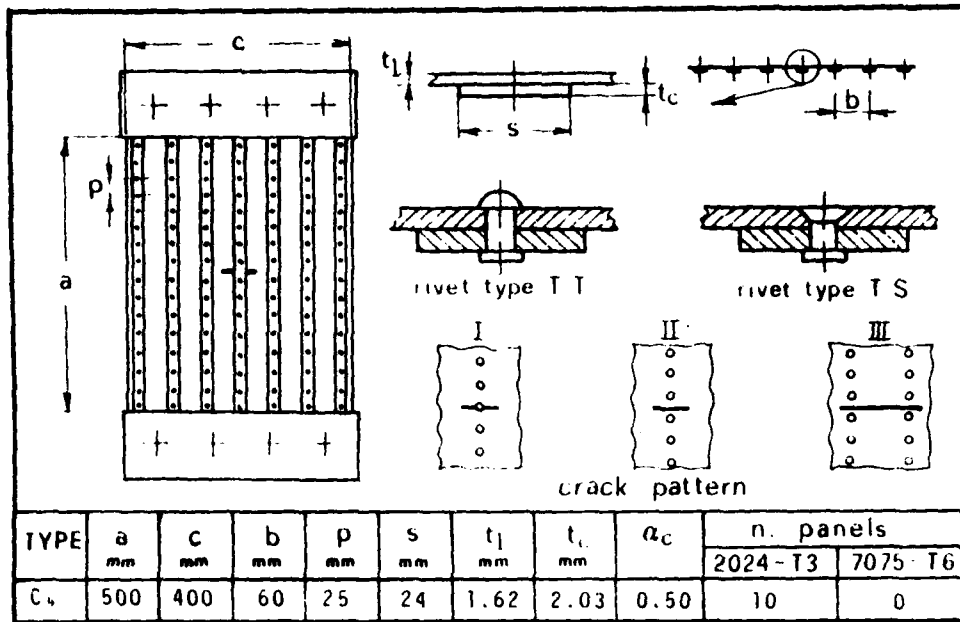
TEST	panel type	a <sub>0</sub> mm	spectrum	S <sub>ref</sub> kg/mm <sup>2</sup>	material
GFM2	F <sub>2</sub>	10.0	MINITWIST	7.0	2024-T3
GFM3	"	12.0	"	"	"
GFM4	"	11.0	"	"	"
GFM5	"	"	"	"	"
GFM6	"	"	"	"	"
GFM7	"	"	"	"	"
GFM9	"	2.7	"	10.0	"
GFM10	"	"	"	"	"
GFM11	"	"	"	"	"
GFM12	"	"	"	"	"
GFM13	"	"	"	"	"
GFM14	"	"	"	"	"

Tab.1c - Main characteristics of MINITWIST spectrum tests on flat panels.

FLAT PANELS					
					
TYPE	W mm	L mm	t mm	n. panels	
				2024-T3	7075-T6
F <sub>2</sub>	400	500	1.62	6	0

TEST	panel type	a <sub>0</sub> mm	spectrum	S <sub>ref</sub> kg/mm <sup>2</sup>	material
GFG1	F <sub>2</sub>	13.0	GAUSSIAN	2.5	2024-T3
GFG2	"	"	"	"	"
GFG4	"	"	"	"	"
GFG5	"	"	"	"	"
GFG6	"	"	"	"	"
GFG7	"	"	"	"	"

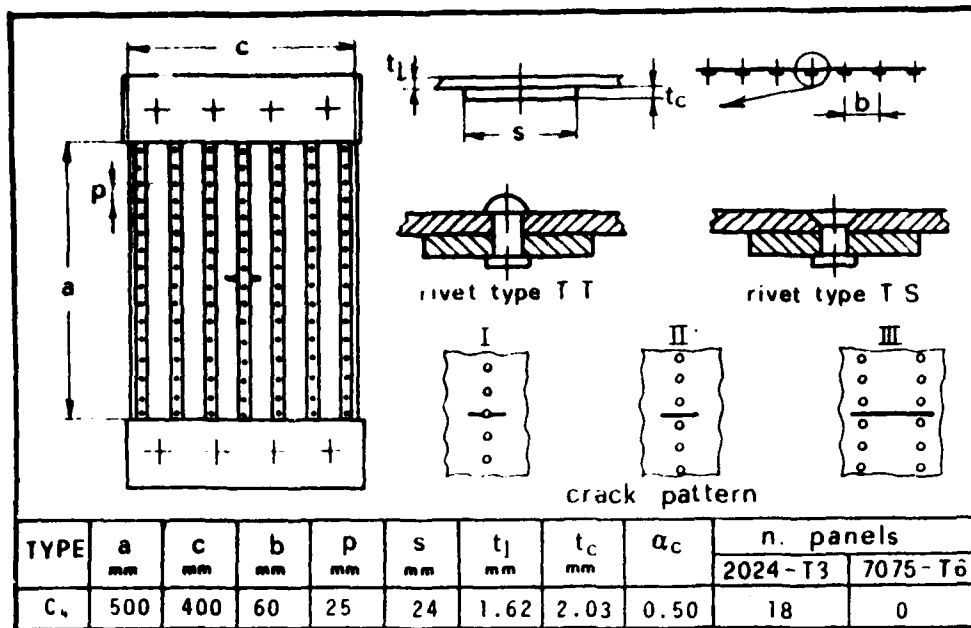
Tab.1d - Main characteristics of Gaussian random spectrum tests on sheet specimens. S<sub>ref</sub> stands for S<sub>rms</sub> and the spectrum is superposed to an average stress equal to 7.0 Kg/mm<sup>2</sup>.



$$a_c = (t_c \cdot s) / (t_1 \cdot b)$$

test	panel type	material	rivet type	crack pattern	a <sub>0</sub> mm	S <sub>max</sub> kg/mm <sup>2</sup>	R
GF1-1	C <sub>4</sub>	2024-T3	TS	II	15.0	6.0	0.2
GF1-2	"	"	"	"	20.0	"	"
GF1-3	"	"	"	"	"	"	"
GF1-4	"	"	"	"	"	"	"
GF1-5	"	"	"	"	"	"	"
GF1-6	"	"	"	"	"	"	"
GF1-7	"	"	"	"	"	"	"
GF1-8	"	"	"	"	"	"	"
GF1-9	"	"	"	"	"	"	"
GF1-10	"	"	"	"	"	"	"

Tab.1e - Main characteristics of the constant amplitude stiffened panels tests.



$$\alpha_c = (t_c \cdot s) / (t_l \cdot b)$$

test	panel type	material	rivet type	crack pattern	a <sub>0</sub> mm	S <sub>rel</sub> kg/mm <sup>2</sup>	Load spectrum
GFF1-I	C <sub>4</sub>	2024-T3	TS	II	11.0	20.0	FALSTAFF
GFF2-I	"	"	"	"	"	"	"
GFF3-I	"	"	"	"	"	"	"
GFF4-I	"	"	"	"	"	"	"
GFF5-I	"	"	"	"	"	"	"
GFF6-I	"	"	"	"	"	"	"
GFM4-I	"	"	"	"	26.0	7.0	MINITWIST
GFM5-I	"	"	"	"	26.0	"	"
GFM6-I	"	"	"	"	26.0	"	"
GFM7-I	"	"	"	"	26.0	"	"
GFM8-I	"	"	"	"	26.0	"	"
GFG1-I	"	"	"	"	14.0	2.5	GAUSSIAN
GFG2-I	"	"	"	"	13.0	"	"
GFG3-I	"	"	"	"	"	"	"
GFG4-I	"	"	"	"	"	"	"
GFG5-I	"	"	"	"	"	"	"
GFG6-I	"	"	"	"	"	"	"
GFG7-I	"	"	"	"	"	"	"

Tab.1f - Main characteristics of the variable amplitude stiffened panels tests.

Tab.1g - Dimensions of the specimens used for evaluating the yield stress and tensile strength.

Test GFL-6		Test GFL-1		Test GFL-5	
A mm	N cycles	A mm	N cycles	A mm	N cycles
5.15	8460.	5.45	10070.	6.45	3865.
5.35	10415.	5.65	13160.	6.90	54170.
5.75	14605.	5.85	15215.	7.15	19150.
6.30	19685.	6.05	17420.	7.65	25270.
6.50	21525.	6.35	21365.	7.85	28180.
7.00	25825.	6.65	25155.	8.20	32075.
7.35	28440.	6.95	27090.	9.10	42120.
7.55	30375.	7.15	29060.	9.65	47930.
7.95	33305.	7.40	31110.	9.80	49845.
8.50	37085.	7.80	35080.	10.15	54115.
8.75	39115.	8.05	37070.	10.75	61270.
9.35	43115.	8.35	39060.	10.95	63260.
9.85	46610.	8.95	43100.	11.35	66370.
10.35	48635.	9.15	45095.	11.85	70150.
10.65	51170.	9.65	49110.	12.05	72150.
11.65	55730.	10.25	53075.	12.50	76175.
12.05	57750.	10.70	55090.	13.05	80340.
12.85	61720.	11.35	59105.	13.30	82250.
13.90	65540.	11.80	61615.	13.95	86730.
14.30	67285.	12.15	63080.	14.30	88880.
15.35	71170.	12.60	65065.	15.00	93000.
15.90	72900.	12.95	67090.	15.30	94815.
16.95	76355.	13.40	68915.	15.65	96660.
17.80	78485.	14.45	73075.	16.80	103050.
18.25	79730.	15.45	77090.	17.50	106470.
18.80	81075.	15.95	79105.	18.80	112495.
19.50	82670.	17.20	83195.	19.30	114415.
20.40	84795.	17.85	85245.	19.70	116595.
21.40	86810.	18.45	87175.	20.25	118985.
23.05	90120.	19.85	91090.	21.35	122640.
24.15	92090.	20.65	93195.	23.80	130730.
25.55	94100.	22.25	97235.	25.30	135590.
26.30	95085.	23.05	99115.	25.80	136850.
28.00	97405.	23.95	101100.	26.20	138220.
28.65	98290.	25.15	103110.	26.90	140080.
29.65	99435.	26.20	105125.	27.30	141190.
32.75	102335.	27.30	107100.	28.40	144220.
34.05	103570.	29.75	111125.	28.80	145310.
37.45	106295.	34.60	117315.	29.30	146470.
40.25	108600.	36.20	119085.	32.00	152670.
42.05	109550.	40.65	123450.	34.00	157120.
44.20	110695.	42.75	125090.	35.10	159370.
46.45	111880.	45.35	127080.	36.20	161450.
48.75	112840.	48.55	129060.	36.70	162400.
52.15	114255.	51.15	130570.	37.30	163590.
56.65	115355.			38.50	165590.
58.20	116100.				

Tab.2a - Results of constant amplitude-flat specimens tests.

AD-A119 764

PISA UNIV (ITALY) INST OF AERONAUTICS

F/G 1/3

THE FATIGUE CRACK GROWTH UNDER VARIABLE AMPLITUDE LOADING IN BU---ETC(U)

APR 82 A SALVETTI, G CAVALLINI, L LAZZERI

DA-ERO-78-6-107

NL

UNCLASSIFIED

2 of 2

AD-A119 764



END

DATE

FORMED

1-82

DTIC

Test GFL-7		Test GFL-4		Test GFL-2	
A mm	N cycles	A mm	N cycles	A mm	N cycles
5.35	12910.	8.15	16170.	16.10	4835.
6.40	24440.	8.55	20100.	16.85	10175.
6.70	27655.	8.95	24230.	17.40	14295.
6.95	29845.	9.30	28120.	18.05	18385.
7.85	37210.	9.65	32620.	18.85	23910.
8.50	44525.	10.35	37660.	19.45	28585.
9.25	49690.	10.60	40195.	20.05	32135.
10.10	55565.	10.85	42615.	20.70	36895.
10.75	60495.	11.10	45085.	21.40	40175.
11.30	64080.	11.80	50120.	22.25	44300.
11.60	65865.	12.15	52670.	22.85	48330.
11.90	67655.	12.70	58150.	23.50	51580.
12.55	71100.	13.65	62680.	24.10	54500.
13.10	73955.	14.55	68600.	24.75	57655.
14.45	80735.	14.85	70300.	25.45	60470.
14.90	83030.	15.60	74410.	26.10	63520.
15.60	86160.	16.55	79240.	26.85	66430.
16.20	88525.	18.50	87730.	27.55	69435.
16.55	89885.	18.90	89395.	28.15	72095.
17.25	92495.	19.45	91420.	28.90	74585.
17.70	94020.	20.00	93455.	29.65	77330.
18.50	96625.	20.50	95335.	30.50	80305.
19.80	100500.	21.55	99220.	31.45	83755.
20.40	102280.	22.20	101395.	32.20	86255.
20.90	103610.	22.85	103315.	33.40	89885.
21.75	105860.	23.60	105450.	34.60	93035.
22.20	106890.	25.30	109980.	35.65	95915.
22.75	108105.	27.10	114220.	36.55	98265.
23.25	109460.	28.85	117875.	37.50	100715.
24.40	112015.	30.40	120920.	39.20	104965.
25.95	114980.	31.00	122010.	40.75	107820.
27.30	117455.	31.75	123160.	42.40	111150.
27.85	118385.	33.85	126395.	43.50	113180.
29.05	120400.	34.75	127770.	45.15	116310.
30.50	122535.	35.75	129170.	46.35	118155.
31.45	123675.	36.55	130215.	48.25	121075.
33.45	126175.	39.00	133290.	49.80	123115.
34.65	127495.	41.30	135870.	51.35	125075.
36.50	129500.	42.70	137100.	53.10	127125.
38.60	131525.	44.35	138610.	55.80	130140.
39.90	132650.	46.05	140050.	57.75	132075.
41.40	133725.	47.50	141090.	59.95	134095.
45.95	136930.	48.90	142095.	62.35	136140.
48.25	138240.	50.35	143070.	65.10	138105.
50.40	139280.	54.00	145210.	68.00	140080.
52.85	140435.	56.10	146330.	71.50	142130.
		58.55	147425.	75.30	144115.
		61.10	148445.	80.00	146095.
		63.80	149475.	85.75	148090.

Tab.2a - Continued.

Test GFL 10		Test GFL-13		Test GFL-12	
A mm	N cycles	A mm	N cycles	A mm	N cycles
24.50	8755.	35.30	7250.	40.40	10135.
25.05	15565.	35.85	9705.	41.30	15140.
25.50	19165.	36.30	11870.	42.55	22655.
26.05	23795.	37.00	14750.	43.05	26225.
26.70	29205.	37.50	17175.	44.45	34185.
27.10	33680.	38.00	19190.	46.20	42620.
27.50	37335.	38.70	22085.	47.85	51185.
27.90	40860.	39.30	24555.	48.25	54025.
28.40	45600.	39.95	27085.	49.40	59470.
29.00	50680.	40.65	29615.	50.85	65100.
29.45	54795.	41.20	31450.	51.60	69030.
30.05	60805.	41.80	33105.	52.95	75295.
30.70	66410.	42.25	34820.	54.20	79890.
31.10	70855.	42.90	36850.	55.75	85240.
31.50	74495.	43.65	39205.	57.40	91360.
32.30	78910.	44.25	40935.	58.35	93960.
32.70	83295.	44.90	43665.	59.10	96260.
33.50	88865.	45.60	45465.	60.25	99465.
34.00	92165.	46.45	47885.	61.65	103320.
34.55	96430.	47.20	50295.	63.50	108540.
35.15	100500.	48.00	52425.	64.05	110420.
35.95	105620.	48.80	54750.	64.95	112845.
36.50	109715.	49.70	56805.	65.80	114795.
37.35	114415.	50.90	59505.	67.05	117950.
37.95	118615.	51.65	61215.	68.00	120520.
38.50	122390.	52.65	63340.	69.25	123515.
39.40	126325.	53.05	66215.	70.45	126010.
39.90	129615.	55.50	69350.	71.45	128550.
40.55	133260.	56.75	71665.	72.80	131420.
41.40	137685.	58.35	74005.	73.75	133165.
42.20	142215.	59.75	76155.	74.95	135570.
43.20	146835.	61.45	78690.	76.85	138840.
44.70	153530.	63.10	80930.	78.40	141310.
46.20	160100.	64.95	83940.	79.40	142590.
47.45	166220.	67.00	86775.	80.35	144200.
49.05	172435.	69.05	89395.	81.60	146210.
50.65	178745.	71.40	92085.	83.10	148205.
52.45	185250.	73.50	94075.	84.40	150145.
54.05	190865.	76.50	96860.	85.90	152140.
55.85	196700.	80.00	99920.	87.05	153415.
57.70	202845.	83.50	104220.	89.30	155870.
59.75	208700.	89.90	107720.	90.70	157245.
62.25	214860.	94.70	109550.	93.00	159580.
64.55	221025.	98.00	110830.	95.25	161590.
67.00	226805.	102.00	112000.	97.25	163250.
69.90	232760.	104.20	112690.	100.35	165340.
72.95	238840.	106.30	113180.	102.55	166840.
76.55	243750.	107.80	113590.	105.65	168600.
80.85	251465.			109.15	170420.

Tab.2a - Continued.

Test GFL-11

A mm	N cycles
44.65	21535.
45.25	26820.
46.05	34190.
46.65	40000.
47.25	45705.
48.00	53055.
48.55	57825.
48.95	60930.
49.30	63450.
49.90	69100.
50.35	72445.
51.05	79070.
51.55	82565.
52.10	86905.
52.50	89055.
52.90	91095.
53.55	95990.
54.20	101405.
54.65	103675.
55.25	107885.
55.95	112755.
56.40	115930.
57.20	121410.
58.30	128310.
59.25	133095.
59.70	135615.
60.50	140910.
61.70	146380.
62.70	151620.
63.35	154590.
64.55	161430.
65.95	168040.
67.25	174875.
69.25	183195.
71.05	190605.
73.30	199125.
76.85	210900.
80.30	221075.
82.00	225965.
84.15	231645.
86.00	236585.
88.00	240945.
90.00	245320.
93.00	250830.
98.90	259050.
101.00	261970.
102.70	264300.
103.10	264750.
105.10	267650.
106.00	268950.

Tab.2a - Concluded.

Test GFF1		Test GFF7-D		Test GFF7-E	
A mm	F Flights	A mm	F Flights	A mm	F Flights
15.15	0.	15.10	0.	15.05	0.
16.65	46.	15.85	50.	15.85	50.
17.05	88.	16.20	100.	16.80	100.
17.45	132.	16.95	150.	17.05	150.
18.25	181.	17.90	200.	18.00	200.
18.75	218.	18.95	300.	18.70	250.
19.40	250.	20.20	400.	19.05	300.
19.55	300.	20.85	450.	19.70	350.
19.80	350.	21.10	511.	20.35	400.
20.35	400.	21.45	550.	21.10	450.
21.05	450.	21.95	600.	21.45	500.
21.15	500.	22.85	700.	22.05	550.
21.50	550.	23.25	750.	22.40	600.
22.00	600.	23.95	800.	23.25	650.
22.65	650.	24.65	850.	23.55	700.
22.90	700.	25.20	900.	23.85	750.
23.15	750.	25.95	1000.	24.50	800.
23.80	800.	26.95	1050.	25.20	850.
24.70	904.	27.35	1100.	25.70	900.
25.70	1010.	27.55	1150.	26.25	950.
26.65	1112.	28.70	1200.	27.00	1000.
27.75	1200.	29.70	1250.	28.20	1050.
28.85	1300.	30.15	1300.	28.60	1100.
30.35	1400.	30.80	1350.	29.20	1150.
31.75	1491.	32.10	1400.	30.20	1200.
33.10	1573.	33.60	1450.	31.55	1250.
35.05	1656.	34.15	1500.	32.50	1300.
35.80	1738.	35.00	1550.	33.50	1350.
37.95	1808.	37.00	1600.	35.60	1400.
39.85	1870.	39.20	1650.	38.10	1450.
41.10	1937.	39.60	1703.	38.70	1500.
43.95	2001.	40.80	1750.	40.05	1550.
46.65	2056.	43.40	1800.	44.10	1600.
47.70	2114.	46.90	1850.	48.60	1650.
52.10	2179.	48.00	1900.	50.40	1700.
58.30	2249.	50.20	1950.	54.40	1750.
60.45	2308.	55.40	2000.	64.40	1800.
69.45	2365.	62.50	2050.	81.90	1850.
78.50	2414.	65.50	2100.		

Tab.2b - Results of flat panels tests under FALSTAFF spectrum loading.

Test GFF7-F		Test GFF5		Test GFF3	
A mm	F Flights	A mm	F Flights	A mm	F Flights
10.95	0.	11.05	0.	11.35	0.
11.80	150.	11.75	54.	11.55	18.
12.40	204.	11.95	100.	12.10	38.
12.70	250.	12.30	150.	12.50	100.
12.85	300.	12.60	202.	12.95	151.
13.05	350.	13.00	300.	13.50	204.
13.35	400.	13.50	400.	13.95	306.
13.60	450.	13.90	500.	14.50	400.
13.80	550.	14.25	600.	15.00	500.
14.60	750.	14.60	700.	15.35	600.
14.90	800.	14.75	800.	15.85	700.
15.15	850.	15.10	900.	16.30	800.
15.40	950.	15.45	1000.	16.75	900.
15.75	1000.	15.65	1100.	17.20	1000.
16.30	1100.	16.05	1200.	17.80	1100.
16.95	1200.	16.35	1300.	18.40	1200.
17.20	1250.	16.70	1400.	19.00	1298.
17.65	1550.	16.90	1500.	19.65	1400.
18.05	1600.	17.20	1600.	20.25	1500.
18.25	1650.	17.55	1700.	20.85	1604.
18.60	1800.	17.85	1800.	21.45	1688.
18.85	1950.	18.10	1900.	22.25	1804.
19.25	2150.	18.45	2002.	22.95	1913.
20.10	2300.	18.80	2100.	23.70	2017.
20.45	2400.	19.05	2200.	24.40	2101.
21.00	2550.	19.40	2305.	25.20	2201.
21.15	2600.	19.70	2407.	26.10	2300.
21.85	2750.	20.10	2500.	27.45	2400.
22.95	2950.	20.45	2600.	28.60	2500.
23.25	3000.	20.85	2700.	30.10	2600.
23.55	3050.	21.15	2800.	31.85	2700.
23.90	3100.	21.45	2901.	34.45	2800.
24.10	3150.	21.85	3000.	37.30	2900.
24.40	3200.	22.40	3100.	41.95	3000.
25.10	3250.	22.90	3200.	47.25	3100.
25.50	3300.	23.35	3300.	58.65	3200.
25.90	3350.	24.00	3400.	72.00	3250.
26.25	3400.	24.50	3500.		
26.95	3450.	25.20	3600.		
27.25	3500.	25.90	3700.		
27.60	3550.	26.90	3800.		
28.20	3600.	27.80	3903.		
29.25	3650.	28.90	4003.		
29.45	3700.	29.85	4100.		
30.05	3750.	31.55	4200.		
31.10	3800.	32.85	4300.		
32.40	3850.	34.75	4400.		
32.80	3900.	36.75	4500.		
33.30	3950.	39.85	4600.		
34.95	4000.	43.15	4700.		

Tab.2b - Continued.

Test GFF6		Test GFF2		Test GFF4	
A mm	F Flights	A mm	F Flights	A mm	F Flights
11.20	0.	11.30	0.	11.30	0.
11.95	50.	12.00	43.	11.50	18.
12.15	100.	12.35	100.	12.15	51.
12.45	150.	13.20	200.	12.60	104.
12.75	200.	13.60	300.	12.95	150.
13.15	300.	14.10	400.	13.50	200.
13.80	400.	14.55	500.	14.15	300.
14.05	500.	15.05	618.	14.70	400.
14.50	600.	15.35	713.	15.20	500.
14.85	700.	15.70	800.	15.80	609.
15.20	800.	16.00	900.	16.30	700.
15.60	900.	16.25	1000.	16.70	800.
16.00	1000.	16.55	1100.	17.30	902.
16.30	1100.	16.95	1201.	17.80	1000.
16.65	1200.	17.30	1300.	18.40	1100.
16.95	1300.	17.60	1401.	18.95	1200.
17.20	1400.	18.00	1505.	19.50	1304.
17.75	1500.	18.40	1600.	20.25	1400.
18.05	1600.	18.75	1700.	20.85	1500.
18.60	1700.	19.20	1800.	21.55	1600.
19.05	1800.	19.60	1900.	22.35	1700.
19.30	1900.	20.05	1998.	23.25	1800.
19.95	2000.	20.35	2100.	24.25	1900.
20.35	2100.	20.80	2198.	25.40	2000.
21.05	2200.	21.25	2299.	26.60	2100.
21.50	2336.	21.65	2385.	28.50	2200.
22.15	2400.	22.20	2489.	30.15	2300.
22.75	2500.	22.70	2602.	32.40	2402.
23.35	2600.	23.15	2704.	35.15	2500.
24.10	2704.	23.75	2799.	39.40	2600.
25.05	2800.	24.25	2902.	44.20	2707.
25.85	2900.	25.00	3000.	53.90	2801.
26.90	3000.	25.70	3100.		
27.95	3103.	26.40	3200.		
29.35	3200.	26.95	3300.		
30.80	3300.	27.80	3407.		
32.80	3400.	28.90	3507.		
34.40	3500.	30.00	3600.		
37.20	3600.	31.05	3700.		
40.10	3700.	32.70	3800.		
45.30	3800.	34.35	3900.		
51.20	3900.	36.95	4000.		
		39.50	4100.		
		43.60	4200.		
		48.25	4300.		
		58.25	4400.		
		68.75	4450.		

Tab.2b - Continued.

Test GFF7		Test GFF7-A		Test GFF7-B	
A mm	F Flights	A mm	F Flights	A mm	F Flights
11.05	0.	8.35	0.	8.10	0.
12.05	50.	9.00	150.	8.30	100.
12.30	98.	9.30	200.	8.95	200.
12.65	150.	9.45	300.	9.60	350.
13.10	204.	9.75	400.	10.25	550.
13.70	300.	10.95	610.	10.70	750.
14.15	400.	11.25	800.	11.15	950.
14.55	500.	11.55	1000.	11.70	1150.
14.85	600.	11.85	1200.	11.95	1250.
15.20	700.	12.30	1400.	12.30	1350.
15.60	800.	12.85	1600.	12.65	1550.
16.00	900.	13.35	1800.	13.00	1750.
16.25	1000.	13.95	2000.	13.50	1950.
16.60	1100.	14.65	2200.	14.05	2150.
16.95	1200.	15.20	2400.	14.45	2350.
17.30	1350.	15.90	2600.	14.90	2550.
17.90	1550.	16.75	2800.	15.55	2750.
18.85	1750.	17.30	3000.	16.15	2950.
19.60	1950.	18.00	3200.	16.65	3150.
20.20	2150.	18.75	3400.	17.25	3350.
21.15	2350.	19.35	3600.	18.00	3550.
22.15	2550.	20.00	3800.	18.70	3750.
23.40	2750.	20.75	4017.	19.40	3950.
24.85	2950.	21.30	4200.	20.30	4150.
26.55	3150.	22.00	4400.	21.30	4350.
28.85	3350.	22.70	4550.	22.50	4550.
31.90	3550.	23.30	4750.	23.85	4750.
36.85	3750.	24.30	4950.	25.40	4950.
39.45	3800.	25.25	5150.	26.90	5050.
43.60	3900.	26.65	5350.	27.50	5150.
51.30	4000.	28.30	5550.	29.30	5250.
58.95	4050.	30.35	5750.	30.20	5350.
62.10	4100.	33.50	5950.	32.95	5450.
				34.25	5550.
				38.95	5652.
				41.40	5750.
				50.80	5850.

Tab.2b - Continued.

Test GFF7-C

A	F
mm	Flights
7.85	0.
8.40	100.
8.60	150.
9.20	250.
9.25	304.
9.65	400.
10.00	600.
10.45	700.
11.15	950.
11.65	1150.
12.15	1350.
12.60	1550.
12.85	1650.
13.05	1750.
13.45	1850.
13.55	1950.
14.20	2150.
14.60	2350.
15.15	2550.
15.65	2750.
16.15	2950.
16.80	3150.
17.40	3350.
18.05	3550.
18.70	3750.
19.45	3950.
20.25	4150.
21.10	4350.
22.20	4550.
23.20	4750.
23.90	4850.
24.50	4950.
25.40	5050.
25.70	5150.
26.80	5250.
27.10	5350.
28.10	5450.
28.65	5550.
31.90	5850.
32.55	5950.
34.65	6050.
35.60	6150.
40.15	6350.
45.15	6450.
46.00	6500.
51.85	6600.

Tab.2b - Continued.

Test GFF9		Test GFF10		Test GFF11	
A mm	F Flights	A mm	F Flights	A mm	F Flights
4.15	0.	4.25	0.	4.15	0.
4.25	50.	4.55	50.	4.25	50.
4.40	100.	4.70	104.	4.35	100.
4.55	150.	5.20	200.	4.55	150.
4.75	202.	5.35	250.	4.75	202.
4.95	300.	5.45	300.	4.90	312.
5.20	400.	5.60	400.	5.15	400.
5.45	501.	5.70	500.	5.35	500.
5.70	600.	5.80	600.	5.70	600.
5.90	700.	6.10	700.	6.00	700.
6.10	800.	6.35	800.	6.20	800.
6.30	900.	6.55	900.	6.60	900.
6.55	1000.	6.80	1000.	6.95	1000.
6.90	1100.	7.00	1100.	7.30	1100.
7.20	1200.	7.10	1140.	7.70	1200.
7.45	1300.	7.20	1200.	8.10	1300.
7.85	1400.	7.50	1300.	8.55	1400.
8.10	1500.	7.70	1404.	9.00	1500.
8.50	1600.	8.00	1504.	9.55	1600.
8.90	1700.	8.30	1600.	10.00	1700.
9.20	1800.	8.40	1700.	10.65	1800.
9.75	1900.	8.45	1801.	11.20	1900.
10.30	2000.	8.70	1900.	12.05	2000.
10.75	2100.	8.95	2000.	12.80	2100.
11.45	2200.	9.05	2100.	13.95	2200.
12.05	2300.	9.35	2200.	15.10	2300.
13.00	2400.	9.60	2301.	16.85	2400.
14.00	2500.	10.00	2400.	18.85	2500.
15.25	2600.	10.25	2510.	22.30	2600.
16.55	2700.	10.55	2600.	26.90	2700.
18.50	2800.	10.85	2700.	38.30	2800.
20.70	2900.	11.40	2810.		
24.85	3000.	11.75	2912.		
30.15	3100.	12.20	3000.		
		12.55	3100.		
		13.10	3200.		
		13.55	3300.		
		14.00	3400.		
		14.55	3500.		
		15.55	3600.		
		16.55	3700.		
		17.90	3801.		
		19.40	3900.		
		21.85	4000.		
		24.75	4100.		
		30.10	4200.		

Tab.2b - Continued.

Test GFF12		Test GFF13	
A	F	A	F
mm	Flights	mm	Flights
4.25	0.	4.35	0.
4.50	50.	4.50	50.
4.65	100.	4.65	100.
4.90	150.	4.80	150.
5.15	203.	5.05	200.
5.50	300.	5.40	302.
5.80	400.	5.75	400.
6.00	500.	6.05	501.
6.40	603.	6.40	611.
6.50	712.	6.80	701.
6.90	802.	7.05	800.
7.10	900.	7.55	900.
7.50	1000.	8.00	1000.
7.85	1100.	8.40	1100.
8.10	1200.	8.85	1200.
8.35	1300.	9.40	1300.
8.70	1400.	10.15	1400.
8.95	1500.	10.65	1500.
9.25	1600.	11.55	1600.
9.65	1711.	12.25	1700.
9.80	1800.	13.40	1800.
10.30	1900.	14.55	1900.
10.75	2003.	16.15	2000.
11.30	2100.	17.90	2100.
11.80	2200.	21.10	2200.
12.35	2300.	24.95	2300.
13.05	2401.	34.15	2400.
14.05	2500.		
14.95	2600.		
16.05	2700.		
17.00	2800.		
19.05	2900.		
21.80	3000.		
25.65	3100.		
35.05	3200.		

Tab.2b - Concluded.

Test GFM2		Test GFM3		Test GFM4	
A mm	F Flights	A mm	F Flights	A mm	F Flights
10.40	0.	12.20	0.	11.15	0.
11.30	560.	13.75	560.	12.30	500.
11.70	1080.	14.35	1080.	12.80	1080.
12.05	1600.	14.95	1600.	13.25	1600.
12.60	2162.	15.65	2162.	14.00	2162.
12.90	2754.	16.05	2754.	14.15	2647.
13.30	3166.	16.80	3166.	14.85	3087.
13.45	3728.	17.00	3728.	15.00	3578.
13.55	4000.	17.30	4000.	15.20	4000.
13.70	4500.	17.50	4500.	15.40	5080.
13.80	5080.	18.30	5080.	16.20	6162.
13.90	5600.	19.40	6162.	16.80	7087.
14.25	6162.	19.90	7087.	17.15	8000.
14.40	6647.	20.25	8047.	17.45	9080.
14.75	7087.	21.45	9080.	18.05	10162.
14.95	7578.	22.55	10162.	18.80	11087.
15.05	8031.	23.10	11087.	19.20	11000.
15.20	9080.	23.50	12000.	19.45	11000.
15.60	10162.	25.05	13080.	20.40	11000.
15.95	11087.	26.55	14162.	21.30	11000.
16.40	12000.	27.05	15087.	21.55	11000.
16.55	13080.	27.60	16005.	21.90	11000.
17.30	14162.	29.40	17080.	22.95	11000.
17.70	15087.	31.25	18162.	23.80	11000.
17.90	16000.	32.00	19087.	24.35	20000.
18.05	17189.	33.10	20008.	24.90	21262.
18.85	18214.	35.55	21080.	26.30	22239.
19.30	19087.	38.35	22162.	27.65	23087.
19.70	20099.	39.70	23087.	28.40	24065.
19.90	21107.	41.60	24000.	29.00	25080.
20.65	22162.	45.05	25203.	31.10	26162.
21.40	23183.	50.25	26162.	33.00	27087.
21.55	24000.	53.50	27087.	33.80	28000.
21.85	25080.	56.80	28000.	34.85	29080.
22.70	26162.	66.80	29080.	37.70	30162.
23.40	27087.			40.65	31087.
23.75	28000.			42.30	32000.
24.00	29080.			44.10	33080.
24.85	30162.			48.65	34162.
25.75	31087.			56.55	35087.
26.25	32000.			61.45	36000.
26.65	33080.				
28.20	34162.				
29.45	35087.				
30.10	36002.				
30.40	37080.				
32.40	38647.				
33.95	39087.				
34.65	40000.				
35.50	41080.				
37.75	42162.				
39.80	43087.				
40.85	44000.				

Tab.2c - Results of flat panels tests under MINITWIST spectrum loading.

Test GFMS		Test GFM6		Test GFM7	
A	F	A	F	A	F
mm	Flights	mm	Flights	mm	Flights
11.15	0.	11.25	0.	11.25	0.
12.40	500.	12.35	560.	12.25	500.
13.10	1080.	12.75	1080.	12.70	1080.
13.60	1600.	13.20	1600.	13.10	1600.
14.35	2162.	13.85	2162.	13.25	2162.
14.70	2647.	14.10	2754.	14.00	2647.
15.35	3087.	14.70	3187.	14.70	3087.
15.55	3578.	14.85	3578.	14.85	3578.
15.75	4000.	15.10	4006.	15.10	4000.
16.10	5080.	15.35	5080.	15.30	5080.
17.05	6162.	16.10	6162.	16.10	6162.
17.85	7087.	16.95	7087.	16.80	7087.
18.20	8047.	17.15	8000.	17.20	8000.
18.65	9080.	17.50	9080.	17.50	9080.
19.55	10162.	18.40	10162.	18.40	10162.
20.10	11087.	19.15	11087.	19.15	11087.
20.95	12000.	19.50	12000.	19.60	12033.
21.45	13080.	19.75	13080.	20.00	13080.
22.70	14162.	21.00	14162.	21.15	14162.
23.85	15087.	21.85	15168.	22.15	15087.
24.45	16000.	22.40	16000.	22.70	16000.
25.20	17080.	22.85	17080.	23.05	17080.
26.75	18162.	24.10	18197.	24.45	18162.
28.50	19087.	25.30	19227.	25.60	19087.
29.45	20000.	25.90	20000.	26.10	20000.
30.15	21080.	26.40	21116.	26.75	21080.
32.65	22162.	28.00	22162.	28.40	22428.
35.40	23087.	29.60	23087.	29.95	23087.
36.70	24000.	30.30	24000.	30.65	24000.
38.10	25080.	31.00	25080.	31.25	25080.
42.00	26211.	33.10	26162.	33.25	26162.
46.40	27087.	35.25	27087.	35.35	27087.
49.45	28000.	36.15	28000.	36.10	28000.
52.80	29080.	37.20	29080.	37.05	29080.
61.30	30211.	39.95	30162.	40.05	30408.
		42.85	31087.	42.40	31087.
		44.35	32000.	43.65	32000.
		45.95	33080.	45.35	33080.
		50.25	34162.	48.90	34162.
		58.75	35087.	54.15	35087.
		64.05	36000.	59.55	36000.
		70.60	37080.	65.55	37080.

Tab.2c - Continued.

Test GFM9		Test GFM10		Test GFM11	
A mm	F Flights	A mm	F Flights	A mm	F Flights
2.70	0.	2.60	0.	2.70	0.
3.00	500.	3.20	500.	3.25	500.
3.45	1080.	3.65	1080.	3.65	1080.
3.60	1600.	4.00	1600.	4.15	1600.
4.20	2162.	4.85	2162.	4.90	2162.
4.60	2650.	5.30	2650.	5.45	2650.
5.25	3080.	5.95	3080.	6.25	3080.
5.65	3580.	6.50	3580.	6.75	3580.
6.00	4000.	6.90	4000.	7.10	4000.
6.65	5080.	7.55	5080.	8.05	5080.
8.40	6162.	9.25	6162.	8.50	5600.
11.15	7087.	11.80	7080.	9.90	6162.
13.55	8000.	14.20	8000.	10.95	6650.
17.05	9080.	17.85	9080.	12.90	7080.
22.00	10162.	32.35	10162.	14.70	7580.
				17.05	8000.
				19.55	8500.
				23.75	9080.

Tab.2c - Continued.

Test GFM12		Test GFM13		Test GFM14	
A mm	F Flights	A mm	F Flights	A mm	F Flights
2.60	0.	2.70	0.	2.65	0.
3.00	618.	3.10	500.	3.20	500.
3.45	1080.	3.50	1080.	3.65	1080.
3.70	1600.	3.80	1600.	4.00	1600.
4.25	2162.	4.25	2162.	4.60	2162.
4.60	2650.	4.60	2650.	5.05	2650.
5.35	3080.	5.35	3080.	5.95	3080.
5.60	3580.	5.65	3580.	6.35	3580.
6.00	4000.	6.00	4000.	6.85	4000.
6.25	4500.	7.05	5338.	8.00	5080.
6.80	5187.	8.55	6162.	10.95	6162.
7.05	5600.	11.90	7080.	16.90	7080.
8.35	6162.	15.65	8000.		
9.10	6650.	21.35	9080.		
11.25	7080.				
12.30	7580.				
14.00	8000.				
16.15	8500.				
18.25	9080.				
21.85	9600.				

Tab.2c - Concluded.

Test GFG1		Test GFG2		Test GFG4	
A	F	A	F	A	F
mm	Flights	mm	Flights	mm	Flights
13.25	0.	13.35	0.	13.30	0.
14.00	3981.	13.95	3981.	14.05	3981.
14.45	7961.	14.45	7961.	14.50	7961.
14.80	11942.	14.90	11792.	14.95	11942.
15.40	15922.	15.30	15922.	15.25	15922.
15.80	19903.	15.85	23883.	15.75	23883.
15.95	23883.	16.45	31844.	16.40	31844.
16.30	27864.	16.90	39805.	16.95	39805.
16.60	31844.	17.40	47766.	17.35	47766.
17.10	39805.	17.85	55727.	17.70	55727.
17.75	47766.	18.40	63688.	18.25	63688.
18.20	55727.	18.85	71649.	18.50	71649.
18.75	63688.	19.40	79610.	19.15	79710.
19.30	71649.	19.85	87571.	19.60	87571.
19.80	79610.	20.50	95532.	20.20	95532.
20.40	87571.	21.00	103493.	20.45	103493.
20.95	95532.	21.65	111454.	21.10	111454.
21.45	103493.	22.05	119415.	21.55	119415.
22.00	111454.	22.75	127376.	22.10	127376.
22.45	119763.	23.10	135337.	22.70	135337.
23.35	127376.	23.70	143298.	23.30	143298.
23.80	136101.	24.25	151259.	23.70	151259.
24.60	143298.	24.90	159220.	24.50	159220.
25.15	151259.	25.45	167181.	24.85	167181.
25.90	159220.	26.20	175142.	25.50	175142.
26.50	167181.	26.75	183103.	26.05	183103.
27.35	175142.	27.45	191064.	26.90	191064.
27.90	183103.	28.05	199025.	27.45	199025.
28.95	191064.	28.85	206986.	28.15	206986.
29.50	199025.	29.50	214947.	28.75	214947.
30.45	206986.	30.40	222908.	29.65	222908.
31.20	214947.	31.15	231758.	30.25	230869.
32.25	222908.	32.05	238830.	31.15	238830.
33.15	230869.	32.90	246791.	31.70	246791.
34.55	238830.	34.00	254752.	32.85	254752.
35.55	246791.	34.80	262713.	33.45	262713.
37.15	254752.	36.05	270674.	34.70	270674.
38.25	262713.	37.20	278635.	35.60	278635.
40.40	270674.	38.85	286596.	37.05	286596.
42.30	278635.	40.15	294557.	37.80	294557.
45.70	286596.	42.55	302518.	39.75	302518.
50.40	294557.	44.55	310586.	41.45	310479.
59.70	302518.	48.55	318440.	44.25	318440.
		53.05	326401.	47.25	326401.
		64.35	334362.	53.75	334362.
		74.75	338293.		

Tab.2d - Results of flat panels tests under Gaussian random spectrum loading.

Test GFG5		Test GFG6		Test GFG7	
A mm	F Flights	A mm	F Flights	A mm	F Flights
13.20	0.	13.24	0.	13.15	0.
13.90	3981.	13.85	3981.	13.85	4258.
14.30	7941.	14.30	7941.	14.40	7961.
14.80	11942.	14.80	11942.	14.75	11942.
15.25	15922.	15.30	15922.	15.15	15922.
15.75	23883.	15.70	23883.	15.70	23883.
16.30	31844.	16.35	31844.	16.25	31844.
16.75	39805.	16.80	39805.	16.70	39805.
17.35	47766.	17.40	47766.	17.40	47766.
17.75	55727.	17.75	55727.	17.70	55727.
18.25	63688.	18.25	63688.	18.30	63688.
18.70	71649.	18.80	71649.	18.85	71649.
19.25	79610.	19.35	79610.	19.30	79610.
19.65	87571.	19.80	87571.	19.70	87571.
20.10	95532.	20.50	95532.	20.30	95532.
20.50	103493.	20.95	103493.	20.75	103493.
20.90	111454.	21.45	111454.	21.40	111454.
21.55	119415.	21.95	119415.	21.90	119415.
22.00	127376.	22.55	127376.	22.50	127376.
22.30	135337.	23.00	135337.	23.05	135337.
22.95	143298.	23.65	143298.	23.85	143298.
23.50	151259.	24.20	151259.	24.35	151259.
24.10	159220.	24.95	159220.	25.15	159220.
24.60	167181.	25.40	167181.	25.65	167181.
25.45	175142.	26.00	175142.	26.55	175142.
25.95	183103.	26.55	183103.	27.05	183103.
27.00	191064.	27.25	191064.	28.10	191064.
27.40	199025.	27.80	199025.	28.90	199025.
28.25	206986.	28.65	206986.	29.70	206986.
28.75	214947.	29.15	214947.	30.60	214947.
29.75	222908.	29.95	222908.	31.55	222908.
30.55	230869.	30.80	230869.	32.35	230869.
31.55	238830.	31.60	238830.	33.60	238830.
32.20	246791.	32.25	246791.	34.50	246791.
33.25	254752.	33.20	254752.	35.80	254752.
34.10	262713.	33.95	262713.	36.75	262713.
35.30	270674.	35.30	270674.	38.10	270674.
36.10	278635.	36.00	278635.	39.00	278635.
37.45	286596.	37.50	286596.	40.70	286596.
38.60	294557.	38.60	294557.	41.90	294557.
40.35	302515.	40.45	302515.	43.80	302515.
41.50	310479.	41.80	310479.	45.40	310479.
43.80	318440.	44.20	318440.	48.15	318440.
45.45	326401.	46.55	326401.	51.45	326401.
48.65	334362.	50.75	334362.	59.45	334362.
52.50	342323.	55.65	342323.		
62.50	350284.	60.95	346304.		
71.85	354265.	68.45	350284.		

Tab.2d - Concluded.

Test GFI-1		Test GFI-2		Test GFI-3	
A mm	N cycles	A mm	N cycles	A mm	N cycles
15.70	9195.	20.90	19735.	21.35	9470.
16.30	17300.	21.75	25150.	23.00	24300.
17.30	26070.	22.30	29980.	24.90	39780.
18.20	35690.	23.05	35555.	27.85	57590.
19.30	45705.	23.70	40820.	30.20	72005.
20.30	56225.	24.40	45470.	34.65	95460.
21.85	68570.	25.60	54765.	38.70	115625.
22.80	77695.	26.70	61555.	41.75	128410.
24.35	90090.	27.80	69225.	43.00	133770.
25.85	101675.	29.60	80600.	44.35	139060.
27.10	110115.	31.30	90945.	45.75	144180.
28.20	116580.	33.45	102360.	48.95	153750.
29.40	123695.	35.60	113265.	50.10	159815.
30.60	131590.	37.60	122725.	52.95	169630.
32.30	140725.	39.85	132310.	54.25	174345.
34.25	149960.	41.40	138200.	55.70	179255.
35.95	158600.	43.85	147405.	57.05	183925.
37.85	166655.	46.05	155070.	58.00	187740.
39.10	172860.	48.65	163740.	59.00	191730.
40.25	177740.	51.75	172715.	59.90	195100.
42.60	186800.	53.25	177860.	61.55	204940.
44.45	193215.	55.00	183415.	63.40	208350.
46.50	200670.	56.35	187305.	64.95	214410.
49.65	211710.	58.60	195290.	65.95	218830.
51.65	217680.	60.50	201910.	67.05	223830.
53.80	225050.	61.45	207440.	68.60	232190.
55.70	231650.	63.60	214905.	69.90	238560.
57.40	237210.	64.95	220180.	70.50	241745.
59.20	244715.	66.55	227555.	71.20	244300.
61.20	252340.	67.65	233190.	71.95	248165.
62.90	260150.	69.05	239350.	73.20	253300.
64.95	267450.	70.45	245390.	74.45	257365.
65.90	273740.	71.25	248835.	75.70	263745.
67.35	280525.	72.15	253235.	76.85	268385.
68.60	287300.	74.65	263305.	78.40	274530.
70.15	294175.	76.90	371560.	80.20	280675.
71.60	300670.	78.15	276410.	81.90	286785.
73.35	308910.	80.70	283590.	83.85	293010.
74.80	314975.	81.90	289715.	85.25	297325.
76.80	323295.	83.90	293770.	87.40	303495.
79.45	333190.	86.15	302195.	89.45	309155.
81.50	341055.	88.05	307540.	91.75	315580.
84.25	350465.	91.50	316390.	93.95	320570.
87.25	359710.	93.75	321835.	96.10	325805.
89.25	365650.	96.30	328155.	98.85	332735.
91.50	372025.	99.20	333970.	102.40	340010.
93.75	377715.	101.80	339045.	104.15	344430.
95.55	382185.	105.15	345160.	108.55	351705.
97.65	387060.	109.30	352550.	110.20	354750.

Tab.2e - Results of constant amplitude-stiffened panels tests.

Test GFI-4		Test GFI-5		Test GFI-6	
A mm	N cycles	A mm	N cycles	A mm	N cycles
20.50	5440.	21.15	9670.	20.80	6810.
21.65	12485.	22.95	22755.	23.10	23000.
22.90	22390.	24.90	37680.	25.15	37600.
24.60	37420.	27.35	55095.	28.25	57535.
26.65	54015.	30.15	72080.	31.05	72360.
29.25	70430.	32.85	86235.	34.10	87535.
32.80	92070.	36.05	102145.	37.00	100265.
35.75	107340.	38.20	111705.	40.75	113255.
38.45	119930.	40.05	119600.	43.70	124815.
41.30	132105.	41.55	125675.	46.10	132540.
43.85	142445.	43.00	131065.	47.25	136225.
46.20	149140.	44.65	136955.	48.40	139815.
46.90	153835.	47.25	145795.	49.60	143145.
48.50	159480.	48.60	150770.	51.00	147500.
49.60	164600.	50.20	155370.	52.15	150520.
50.60	169180.	51.85	160370.	53.25	153820.
51.60	172250.	53.30	165140.	54.80	158270.
52.70	176870.	54.25	168385.	56.10	161880.
54.10	181750.	55.45	172450.	57.10	165010.
60.55	208010.	56.60	176535.	58.15	168175.
61.45	212205.	57.65	180590.	59.45	172515.
61.90	215020.	58.95	184880.	60.45	175750.
62.55	218400.	59.80	188950.	61.65	180020.
63.65	223735.	61.85	194025.	62.55	183440.
64.60	228390.	62.25	198045.	63.55	187315.
65.45	233055.	63.05	201790.	64.45	190775.
66.50	238275.	64.25	206810.	65.45	194480.
67.20	242295.	64.85	210185.	66.45	198365.
68.10	247660.	65.75	214110.	67.40	202145.
69.20	253325.	66.65	218300.	68.60	206365.
70.15	257845.	67.75	223525.	69.55	210140.
71.20	262930.	68.95	229735.	70.35	213295.
72.15	267790.	70.30	235495.	71.90	219275.
73.50	273060.	71.20	239535.	73.05	222830.
74.15	277880.	72.00	243295.	74.25	228030.
75.60	283685.	73.05	248225.	75.00	231345.
76.75	289415.	73.95	251640.	76.35	234910.
78.30	295820.	75.05	256150.	77.65	239535.
79.85	301335.	76.20	261210.	78.65	243845.
81.10	307015.	77.40	265900.	80.40	248465.
82.15	311565.	78.75	270715.	81.95	253015.
83.80	317490.	79.80	274930.	84.60	260715.
84.85	321335.	81.45	280290.	89.25	273210.
86.45	326780.	82.65	285105.	94.60	286265.
88.40	332990.	84.70	291930.	100.10	297405.
90.20	338390.	86.25	296945.	104.30	305565.
92.00	343725.	90.20	308225.	107.25	311025.
93.90	349230.	94.00	318630.	113.85	321895.
95.85	354235.	98.45	329445.	117.60	327395.

Tab.2e - Continued.

Test GFI-7		Test GFI-8		Test GFI-9	
A mm	N cycles	A mm	N cycles	A mm	N cycles
20.95	8900.	20.60	5715.	21.25	12940.
23.05	23215.	22.75	23760.	24.15	36015.
25.60	38935.	24.80	38335.	26.15	51680.
28.20	53475.	27.50	56035.	28.95	67950.
30.95	67420.	30.80	75980.	30.85	78155.
33.75	80310.	32.60	84255.	32.10	84810.
36.85	92830.	34.75	94045.	33.20	89635.
39.80	103445.	37.10	103890.	34.20	95760.
41.90	110410.	38.70	109915.	35.35	100105.
43.35	114975.	40.40	116160.	36.80	105520.
44.30	117765.	41.20	119340.	38.10	111800.
45.90	122595.	42.05	122355.	39.40	115580.
47.10	126530.	43.05	125775.	40.45	119745.
48.30	129910.	43.95	129015.	42.75	127885.
49.65	133480.	45.40	133350.	44.15	132970.
51.35	138355.	46.55	136835.	45.60	137585.
52.95	142790.	47.50	139865.	47.35	143060.
54.65	147325.	49.55	145555.	48.35	146035.
56.00	151300.	51.50	151340.	49.70	150305.
57.10	154960.	53.45	156885.	51.25	154920.
58.10	158595.	55.05	161635.	52.80	159260.
59.10	162095.	56.65	166650.	54.25	163805.
60.05	165550.	57.95	170750.	56.60	167500.
61.40	171005.	59.75	177020.	56.95	171650.
62.30	175285.	60.75	180865.	58.25	175875.
63.45	180140.	62.05	185545.	59.45	180350.
64.50	185280.	62.90	189410.	60.50	184185.
65.50	189995.	64.00	193890.	61.80	188525.
66.85	195555.	65.05	198660.	62.80	192775.
67.90	200470.	65.90	202395.	63.75	196885.
69.10	205825.	67.05	207275.	64.80	201015.
70.10	210610.	68.25	212890.	65.70	204550.
71.25	215295.	69.45	218010.	66.70	209135.
72.30	220090.	70.85	224310.	67.80	213800.
73.30	224100.	71.90	228670.	68.90	218720.
74.30	228315.	73.00	234045.	70.00	223050.
75.45	232680.	74.30	238860.	71.10	227480.
76.70	237410.	75.50	243665.	72.25	232220.
78.00	242075.	76.90	248535.	73.80	238710.
79.15	246210.	77.95	253110.	75.20	243495.
80.50	250825.	79.45	258430.	76.50	248405.
81.90	254875.	80.60	262095.	77.95	253505.
83.60	260515.	82.40	267665.	79.50	258075.
85.25	265510.	83.75	272250.	80.95	262855.
86.85	270285.	85.15	276430.	82.45	267380.
88.25	273885.	86.30	279840.	83.90	271725.
89.60	277510.	89.55	288230.	87.25	280910.
93.40	287300.	92.70	296495.	91.80	291785.
97.40	296815.	97.65	308045.	97.30	303760.

Tab.2e - Continued.

Test GFI-10

A mm	N cycles
21.00	8960.
23.35	23205.
26.15	38620.
27.35	44975.
28.60	51550.
30.15	58555.
31.45	63890.
32.50	68390.
33.75	72500.
35.55	79780.
37.65	86220.
40.45	94785.
41.65	98610.
43.50	103385.
44.80	107290.
46.30	111460.
47.60	114670.
49.00	118480.
50.70	122380.
51.90	125440.
53.40	129170.
54.80	132570.
56.20	136930.
57.30	139950.
60.00	145370.
61.40	150850.
62.80	155130.
64.00	158660.
65.30	163540.
66.30	167220.
67.40	171430.
68.50	175070.
69.70	179370.
70.90	184210.
72.20	188260.
73.10	191950.
74.40	195670.
75.60	199560.
76.40	202960.
77.50	206060.
78.80	209520.
80.10	214140.
81.50	217750.
83.00	221790.
84.20	225420.
87.70	234210.
89.70	239240.
92.80	244230.
96.00	255210.
98.80	260700.

Tab.2e - Concluded.

Test GFF1-I		Test GFF2-I		Test GFF3-I	
A	F	F	F	A	F
mm	Flights	mm	Flights	mm	Flights
11.30	0.	11.15	0.	11.15	0.
11.45	50.	11.85	50.	11.80	55.
11.75	100.	12.05	100.	12.10	108.
11.95	150.	12.35	150.	12.30	154.
12.45	200.	12.55	200.	12.70	200.
12.70	300.	13.00	300.	13.05	300.
13.00	400.	13.35	400.	13.35	400.
13.40	500.	14.05	600.	13.85	600.
13.75	600.	14.40	800.	14.20	800.
14.15	700.	14.60	900.	15.00	1000.
14.35	800.	14.80	1000.	15.55	1200.
14.55	900.	15.30	1200.	16.05	1400.
14.90	1000.	15.70	1400.	16.45	1600.
15.10	1100.	16.15	1600.	16.85	1800.
15.35	1200.	16.70	1800.	17.20	2000.
15.60	1300.	17.05	2000.	17.65	2200.
15.80	1400.	17.30	2200.	17.95	2400.
16.30	1600.	17.85	2400.	18.35	2600.
16.85	1800.	18.30	2600.	18.85	2800.
17.15	2000.	18.75	2800.	19.45	3000.
17.70	2200.	19.25	3000.	19.55	3200.
18.10	2400.	19.70	3200.	20.20	3400.
18.70	2600.	20.20	3400.	20.60	3600.
18.95	2800.	20.90	3600.	21.25	3800.
19.55	3000.	21.40	3800.	21.80	4000.
20.25	3200.	22.20	4000.	22.40	4200.
20.85	3400.	22.85	4200.	22.70	4400.
21.30	3600.	23.55	4400.	23.30	4600.
21.70	3800.	24.30	4600.	23.75	4800.
22.65	4000.	25.10	4800.	24.25	5000.
23.30	4200.	25.90	5000.	25.00	5200.
24.15	4400.	26.75	5200.	25.65	5400.
25.00	4600.	27.75	5400.	26.40	5600.
25.80	4800.	28.85	5600.	27.00	5800.
26.70	5000.	30.05	5800.	27.75	6000.
27.70	5200.	31.40	6000.	28.30	6200.
28.90	5400.	32.80	6200.	29.20	6400.
30.05	5600.	34.60	6400.	30.00	6600.
31.90	5800.	36.60	6600.	30.90	6800.
33.95	6000.	39.00	6800.	31.85	7000.
35.85	6200.	41.95	7000.	32.80	7200.
39.65	6400.	45.65	7200.	34.25	7400.
44.15	6600.	50.40	7400.	36.00	7600.
50.35	6800.	54.85	7600.	37.80	7800.
56.05	7000.	58.25	7800.	40.30	8000.
59.95	7200.	60.60	8000.	44.10	8200.
62.70	7400.	62.60	8200.	48.65	8400.
65.55	7600.	64.45	8400.	53.70	8600.
69.80	7800.	66.50	8600.	58.80	8800.
		67.70	8700.	60.30	8827.

Tab.2f - Results of variable amplitude-stiffened panels tests.

Test GFF4-I		Test GFF5-I		Test GFF6-I	
A	F	A	F	A	F
mm	Flights	mm	Flights	mm	Flights
11.20	0.	11.15	0.	11.05	0.
11.85	50.	11.90	50.	11.75	51.
12.10	100.	12.10	110.	11.85	116.
12.35	150.	12.55	162.	12.20	150.
12.75	200.	13.00	200.	12.55	200.
13.10	300.	13.20	300.	12.85	300.
13.45	400.	13.60	400.	13.25	400.
14.05	600.	14.25	600.	13.85	600.
14.55	800.	14.80	800.	14.35	800.
15.20	1000.	15.45	1000.	14.85	1000.
15.60	1200.	15.85	1200.	15.40	1200.
16.05	1400.	16.40	1400.	15.90	1400.
16.45	1600.	16.80	1600.	16.30	1600.
16.85	1800.	17.25	1800.	16.80	1800.
17.30	2000.	17.65	2000.	17.10	2000.
17.65	2200.	18.20	2200.	17.60	2200.
18.15	2400.	18.70	2400.	17.90	2400.
18.60	2600.	19.15	2600.	18.30	2600.
19.05	2800.	19.65	2800.	18.75	2800.
19.35	3000.	20.20	3000.	19.05	3000.
19.85	3200.	20.65	3200.	19.55	3200.
20.35	3400.	21.20	3400.	20.15	3400.
20.85	3600.	21.85	3600.	20.55	3600.
21.30	3800.	22.50	3800.	21.00	3800.
21.85	4000.	23.00	4000.	21.55	4000.
22.40	4200.	23.60	4200.	22.15	4200.
22.75	4400.	24.25	4400.	22.35	4400.
23.35	4600.	24.80	4600.	22.65	4600.
24.05	4800.	25.60	4800.	23.55	4800.
24.65	5000.	26.10	5000.	23.85	5000.
25.30	5200.	26.90	5200.	24.25	5200.
25.90	5400.	27.40	5400.	24.90	5400.
26.55	5600.	28.00	5600.	25.40	5600.
27.40	5800.	28.70	5800.	25.75	5800.
28.20	6000.	29.30	6000.	26.35	6000.
29.10	6200.	30.30	6200.	27.20	6200.
30.00	6400.	31.40	6400.	27.95	6400.
31.25	6600.	32.80	6600.	28.75	6600.
32.25	6800.	34.60	6800.	29.45	6800.
33.70	7000.	36.70	7000.	30.40	7000.
35.20	7200.	39.05	7200.	31.40	7200.
37.20	7400.	42.70	7400.	32.70	7400.
39.85	7600.	46.60	7600.	34.15	7600.
43.30	7800.	51.90	7800.	35.80	7800.
47.50	8000.	56.20	8000.	37.85	8000.
52.25	8200.	60.05	8200.	40.40	8200.
56.30	8400.	61.70	8235.	43.85	8400.
59.25	8600.	64.35	8300.	48.60	8600.
		75.30	8400.	53.55	8800.
				57.15	9000.

Tab.2f - Continued.

Test GFM4-I		Test GFM5-I		Test GFM6-I	
A mm	F Flights	A mm	F Flights	A mm	F Flights
26.10	0.	26.10	0.	26.10	0.
29.55	501.	29.20	501.	29.40	501.
31.15	1124.	30.45	1080.	31.40	1600.
33.10	1665.	31.35	1600.	33.05	2162.
33.85	2290.	32.90	2162.	34.60	3087.
34.55	2675.	33.65	2675.	35.40	4000.
35.60	3087.	34.65	3087.	37.10	6162.
36.45	4000.	35.15	3578.	38.90	8000.
37.25	5080.	35.50	4102.	40.20	10162.
38.80	6162.	36.25	5093.	41.75	12000.
40.65	8021.	37.60	6162.	42.85	14162.
41.15	9080.	39.00	7174.	44.30	16000.
42.20	10285.	39.70	8000.	45.95	18162.
43.60	11087.	39.90	9080.	46.70	20000.
44.20	12000.	41.20	10162.	48.05	22162.
46.00	14162.	42.50	11087.	49.20	23137.
47.25	15087.	43.20	12000.	49.55	24000.
47.90	16000.	43.65	13080.	51.00	26162.
48.30	17080.	44.85	14162.	51.85	28000.
49.60	18162.	45.95	15087.	53.00	30162.
50.60	19087.	46.50	16000.	53.75	31087.
51.20	20000.	47.00	17080.	54.00	32000.
52.55	22162.	48.15	18162.	54.45	33080.
53.45	23087.	49.35	19087.	55.25	34162.
54.35	24000.	49.85	20000.	55.55	35087.
54.95	25080.	50.20	21107.	55.85	36000.
56.00	26162.	51.10	22162.	56.10	37080.
56.65	27087.	52.25	23087.	56.65	38162.
57.10	29080.	52.95	24000.	56.90	39087.
57.80	30162.	53.30	25080.	57.00	40000.
58.25	31087.	53.90	26162.	57.85	42739.
58.90	33080.	54.90	27087.	58.30	43087.
59.20	35087.	55.05	28000.	58.45	46162.
59.80	37080.	55.35	29080.	58.70	48000.
60.00	39087.	56.15	30162.		
60.50	42162.	56.95	31087.		
60.90	43087.	57.15	32000.		
61.10	46162.	57.60	33080.		
61.65	49080.	58.10	34221.		
61.95	52000.	58.85	35087.		
		59.25	36000.		
		59.95	39087.		
		60.20	40000.		
		60.45	41080.		
		61.00	42162.		
		61.45	44000.		
		61.95	46162.		
		62.40	48000.		
		62.55	50162.		

Tab.2f - Continued.

Test GFM7-I		Test GFM8-I	
A	F	A	F
mm	Flights	mm	Flights
26.10	0.	25.95	0.
29.65	501.	29.45	501.
31.25	1193.	31.90	1600.
33.20	1722.	33.65	2162.
34.70	2675.	34.30	2675.
35.95	3087.	35.30	3087.
36.85	4000.	36.15	4000.
38.85	6162.	36.85	5080.
40.25	7087.	37.85	6162.
41.25	9080.	39.55	7087.
42.20	10336.	40.55	9080.
43.55	11087.	41.75	10162.
44.15	12060.	42.90	11087.
45.75	14162.	43.55	12000.
46.90	15087.	44.00	13080.
47.65	16168.	44.85	14162.
48.70	18162.	46.35	15087.
49.70	19087.	47.05	17080.
50.35	21080.	47.80	18162.
51.25	22162.	49.10	19087.
52.40	23087.	49.95	21080.
52.95	25080.	50.80	22162.
53.60	26162.	51.85	23087.
54.50	27087.	52.05	24000.
55.05	29080.	52.90	26162.
55.50	30162.	53.75	27087.
56.00	31087.	54.50	29080.
56.30	33080.	54.90	30162.
56.90	34162.	55.75	32000.
57.50	35087.	56.30	34162.
57.75	37080.	57.10	36000.
58.05	38162.	57.70	38162.
58.30	39087.	58.00	39087.
58.80	42162.	58.50	41080.
59.30	43087.	59.15	43087.
59.75	46162.		
60.05	48000.		
60.60	50162.		
60.90	51087.		

Tab.2f - Continued.

Test GFG1-I		Test GFG2-I		Test GFG3-1	
A mm	F Flights	A mm	F Flights	A mm	F Flights
14.00	0.	13.20	0.	13.15	0.
15.50	15922.	15.10	15922.	14.90	15922.
16.55	31844.	16.00	31844.	16.20	31844.
17.35	47766.	17.00	47766.	17.15	47766.
18.15	63688.	17.65	63688.	18.00	63688.
19.05	79610.	18.45	79610.	18.90	79610.
19.80	95532.	19.20	95532.	19.70	95532.
20.50	111454.	20.00	111454.	20.55	111454.
21.40	127376.	20.90	127376.	21.50	127376.
22.60	143298.	21.75	143298.	22.00	135337.
23.40	159220.	23.00	159220.	22.55	143298.
24.55	175142.	23.55	175142.	23.00	151259.
25.00	183103.	24.60	191064.	23.55	159220.
25.65	191064.	25.35	206986.	23.95	167181.
26.45	201435.	26.35	222908.	24.50	175142.
27.10	207761.	27.00	230869.	25.10	183103.
27.65	214947.	27.70	238830.	25.60	191064.
28.40	222908.	28.10	246791.	26.20	199025.
29.10	231144.	28.40	254752.	26.75	206986.
30.05	238830.	29.65	262713.	27.40	214947.
30.90	246791.	30.05	270674.	27.85	222908.
32.05	254752.	30.35	278635.	28.25	230869.
32.95	262713.	30.75	286596.	29.00	238830.
34.25	270674.	31.45	294556.	29.70	246791.
35.35	278635.	32.25	302518.	30.45	254752.
37.15	286596.	32.70	310479.	31.05	262713.
38.55	294557.	33.60	318440.	31.65	270674.
40.75	302518.	34.10	326401.	32.40	278635.
42.65	310479.	34.90	334362.	33.10	286596.
45.50	318440.	35.40	342323.	33.85	294557.
48.20	326401.	36.35	350284.	34.70	302518.
51.75	334362.	37.15	358245.	35.50	310478.
55.30	342323.	38.00	366206.	36.30	318440.
56.60	350284.	38.80	374167.	37.05	326401.
57.75	358245.	39.60	382128.	37.90	334362.
58.95	366206.	40.50	390089.	38.80	342323.
59.75	374167.	41.35	398050.	40.05	350284.
60.50	382128.	42.25	406011.	40.90	358245.
61.30	390089.	43.20	413972.	42.15	366206.
61.90	398050.	44.10	421933.	43.20	374167.
62.90	406011.	45.20	429894.	44.65	382128.
63.00	413972.	46.25	437855.	46.00	390089.
63.70	421933.	47.40	445816.	48.00	398050.
64.35	429894.	48.45	453777.	49.70	406011.
65.00	437855.	50.05	461738.	52.25	413972.
65.55	445816.	51.25	469699.	54.15	421933.
66.35	453777.	52.80	477660.	56.10	429894.
67.25	461738.	53.85	485621.	57.25	437855.
67.85	469699.	54.95	493582.	62.80	453777.
68.70	477660.	56.40	509504.		

Test GFG4-I		Test GFG5-I		Test GFG6-I	
A	F	A	F	A	F
mm	Flights	mm	Flights	mm	Flights
13.10	0.	13.25	0.	13.40	0.
15.10	15922.	14.45	7961.	13.95	3981.
15.95	31844.	15.50	15922.	14.50	7961.
16.70	47766.	16.15	31844.	14.80	11942.
17.70	63688.	17.15	47766.	15.30	15922.
18.25	79610.	17.90	63688.	15.90	23883.
18.90	95532.	18.70	79610.	16.45	31844.
19.75	111454.	19.20	87571.	16.95	39805.
20.50	127376.	19.65	95532.	17.35	47766.
21.15	143298.	19.90	103493.	17.80	55727.
22.10	159220.	20.55	111454.	18.35	63688.
22.95	175142.	20.95	119415.	18.70	71979.
23.65	191064.	21.25	127376.	19.15	79610.
24.20	199025.	21.95	135337.	19.80	87571.
24.60	206986.	22.60	143298.	20.20	95703.
25.05	214947.	23.00	151259.	20.65	103493.
25.35	222908.	23.50	159220.	21.10	111454.
25.90	230869.	23.95	167181.	21.50	119512.
26.35	238830.	24.60	175142.	22.00	127376.
26.70	246791.	25.70	191064.	22.55	135337.
27.20	254752.	26.25	199025.	23.30	143298.
27.60	262713.	27.05	206986.	23.85	151259.
28.10	270674.	27.55	214947.	24.65	159220.
28.40	278635.	28.25	222908.	25.10	167181.
29.15	286596.	28.85	230896.	25.75	175142.
29.55	294557.	29.65	238830.	26.30	183103.
30.10	302518.	30.25	246791.	26.90	191064.
30.65	310478.	31.00	254752.	27.45	199025.
31.20	318440.	31.75	262713.	28.20	206986.
31.70	326401.	32.60	270674.	28.80	214947.
32.45	334362.	33.25	278635.	29.60	222908.
32.95	342329.	34.10	286596.	30.25	230869.
33.85	350284.	34.75	294557.	31.05	238830.
34.65	358245.	35.75	302518.	31.70	246791.
35.15	366206.	36.50	310479.	32.65	254752.
36.20	374166.	37.40	318440.	33.30	262713.
37.10	382128.	38.20	326401.	34.30	270674.
37.90	390089.	39.30	334408.	35.05	278635.
38.95	398050.	40.25	342323.	36.20	286596.
39.85	406011.	41.40	350284.	37.15	294557.
41.05	413972.	42.45	358246.	38.25	302518.
42.05	421933.	43.95	366208.	39.20	310479.
43.75	429894.	45.20	374167.	40.15	318440.
45.25	437855.	47.25	382172.	41.45	326401.
47.65	445816.	48.85	390089.	42.90	334362.
49.50	453777.	51.10	398050.	44.05	342323.
52.10	461738.	52.75	406011.	45.85	350284.
53.90	469699.	54.25	414071.	47.20	358245.
55.95	477660.	55.60	421933.	49.35	366206.
57.05	485621.	58.65	429894.	51.05	374167.

Tab.2f - Continued.

Test GFG7-I

A	F
mm	Flights
13.20	0.
13.90	3981.
14.40	7961.
14.80	11942.
15.15	15922.
15.70	23883.
16.35	31844.
17.20	47766.
18.15	63688.
19.15	79861.
20.00	95532.
20.95	111454.
22.10	127376.
22.90	143298.
24.00	159220.
25.35	175142.
26.50	191064.
28.10	206986.
29.40	222908.
31.65	238830.
33.55	254752.
35.50	270674.
36.50	278635.
37.75	286596.
38.75	294557.
40.25	302518.
41.25	310479.
42.95	318440.
44.10	326401.
45.80	334362.
49.60	350284.
53.65	366206.
56.65	382128.
58.50	398050.
60.00	413972.
63.15	429894.
69.30	437855.
78.75	445816.

Tab.2f - Concluded.

TEST	S <sub>y</sub>	S <sub>R</sub>
GFF5	36.5	47.9
GFF6	36.9	47.9
GFF4	36.5	48.5
GFF2	36.1	48.5
GFF1	36.9	48.2
GFF9	36.2	49.2
GFF10	36.6	49.2
GFF11	36.6	49.2
GFF12	37.7	49.2
GFF13	36.9	49.2
GFG6	37.2	49.5
GFG5	36.5	49.8
GFG4	37.2	48.8
GFG2	35.6	48.8
GFG1	36.9	49.2
GFG7	35.9	48.8

S<sub>y</sub>= yield stress (Kg/mm<sup>2</sup>)

S<sub>R</sub>= tensile strength (Kg/mm<sup>2</sup>)

Tab.2g - Some mechanical properties of  
a few flat panels utilized in  
the tests.

